

University of Alberta

Expansion and Osteogenic Differentiation of Human Umbilical Cord
Perivascular Stem Cells by Low Intensity Pulsed Ultrasound for
Dentofacial Tissue Engineering
by

Tagreed Abdullah Aldosary

A thesis submitted to the Faculty of Graduate Studies and Research
in partial fulfillment of the requirements for the degree of

Master of Science

Medical Science - Dentistry

©Tagreed Abdullah Aldosary

Fall 2009

Edmonton, Alberta

Permission is hereby granted to the University of Alberta Libraries to reproduce single copies of this thesis and to lend or sell such copies for private, scholarly or scientific research purposes only. Where the thesis is converted to, or otherwise made available in digital form, the University of Alberta will advise potential users of the thesis of these terms.

The author reserves all other publication and other rights in association with the copyright in the thesis and, except as herein before provided, neither the thesis nor any substantial portion thereof may be printed or otherwise reproduced in any material form whatsoever without the author's prior written permission.

Examining Committee

Dr. Tarek El-Bialy (Orthodontics)

Dr. Hasan Uludag (Chemical Engineering)

Dr. Micheal Doschak (Pharmacy)

Dr. Michael Eggert (Periodontics)

Dedication

I dedicate this thesis to my parents and to the spirit of my father (Abdullah) to whom I am indebted for the rest of my career, and to my husband (Yasser) for his continued support and patience

Abstract

The objective of these experiments is to explore the effect of LIPUS on the ultraexpansion and osteogenic differentiation of harvested passage-4 HUCPV-SCs. HUCPV-SCs were divided into two groups: a treatment group that received LIPUS for 10 minutes for 1, 7, and 14 days and a control group that received a sham treatment utilizing both basic and osteogenic media. The results in basic media and osteogenic media demonstrated nonsignificant differences in cell count, ALP, DNA content, and CD90. Statistically significant expression of OPN and PCNA was observed on day 14 in LIPUS treated group. Nucleostemin expression in the LIPUS-treated group was insignificant on days 1 and 7. However, a selective increase in osteogenic markers was obtained on day 7 for ALP and OCN and on day 14 for OPN. Future experiments are required to explore the effects of different application times and/or techniques of LIPUS on the behaviour of HUCPV-SCs.

Acknowledgments

I would like to offer special thanks to my supervisor *Dr. Tarek El-Bialy* for accepting me and guiding my steps in this master's program.

Special gratitude is accorded to the committee members *Dr. Hasan Uludag* and *Dr. Michael Doschak* for their valuable contributions to this research and for sharing their experiences and perspectives.

The endorsement of this research would have not been possible without the assistance of the dental, chemical engineering, pharmacy, biosciences, and medical sciences departments at the University of Alberta.

This research was generously supported by grants from the Saudi Arabian Cultural Bureau and a fund from the "*Funds for Dentistry*" at the University of Alberta.

Table of Contents

Chapter 1. Introduction and Literature Review	1
1.1 Introduction	1
1.2 Literature Review	4
1.2.1. Stem Cells and Craniofacial Tissue Engineering.....	4
1.2.2. Human Stem Cells and Tissue Engineering of the Temporomandibular Joint.....	6
1.2.3. Bone Augmentation and Repair.....	6
1.2.4. Expansion of Stem Cells for Tissue Engineering.....	7
1.2.5. Mechanical Stresses on Chondrogenic and Osteogenic Cell Differentiation	8
1.2.6. Phenotypic Characteristics of Human Umbilical Cord Perivascular Stem Cells.....	9
1.2.7. Summary	11
1.3. Objectives of the Study.....	12
1.4. Research Hypothesis.....	12
1.5. References	13
Chapter 2. Expansion of HUCPV-SC Cells in Basic Media Using LIPUS	23
2.1. Key Words	23
2.2. Introduction	23

2.3. Material and Methods	25
2.3.1. Cell Culture.....	25
2.3.2. Cell Count.....	27
2.3.3. Alkaline Phosphatase Activity Assay	27
2.3.4. Cell Proliferation and DNA Quantification Assay.....	27
2.3.5. Immunophenotyping Using Flow-Cytometry Analysis.....	28
2.3.6. Quantitative Real-Time PCR Analysis (qPCR)	29
2.3.7. Statistical Analysis.....	31
2.4. Results.....	31
2.5. Discussion.....	48
2.6. Conclusion.....	50
2.7. References	51
Appendix 1	101
Chapter 3. Differentiation of HUCPV-SC Cells in Osteogenic Media Using LIPUS.....	56
3.1. Key Words	56
3.2. Introduction	56
3.3. Material and Methods	59
3.3.1. Cell Culture.....	59
3.3.2. Cell Count.....	60

3.3.3. Alkaline Phosphatase Activity Assay	61
3.3.4. Cell Proliferation and DNA Quantification Assay	61
3.3.5. Immunophenotyping Using Flow-Cytometry Analysis.....	62
3.3.6. Quantitative Real-Time PCR Analysis (qPCR)	63
3.3.7. Statistical Analysis.....	64
3.4. Results.....	64
3.5. Discussion.....	80
3.5. Conclusion.....	81
3.5. References	82
Appendix 2	117
Chapter 4. General Discussion and Conclusion	89
4.1. Discussion.....	89
4.2. Conclusion.....	94
4.3. References	96

List of Figures

Chapter 2. Expansion of HUCPV-SC Cells in Basic Media Using LIPUS 23

Figure 2.1. Schematic diagram shows experimental LIPUS application 26

Figure 2.2. HUCPV-cell count results after application of LIPUS 10 min/day (days 1, 7, and 14) in basic media 32

Figure 2.3. HUCPV-DNA level results after application of LIPUS 10 min/day (days 1, 7, and 14) in basic media 33

Figure 2.4. HUCPV-ALP level results after application of LIPUS 10 min/day (days 1, 7, and 14) in basic media 33

Figure 2.5. HUCPV-normalization of ALP/DNA results after application of LIPUS 10 min/day (days 1, 7, and 14) in basic media..... 34

Figure 2.6. Flow cytometry analysis results on day 1 represented by histogram and charts..... 39

Figure 2.6a. Histogram..... 39

Figure 2.6b. Charts 40

Figure 2.7. Flow cytometry analysis results on day 7 represented by histogram and charts..... 41

Figure 2.7a. Histogram..... 41

Figure 2.7b. Charts 42

Figure 2.8. Flow cytometry analysis results on day 14 represented by histogram and charts 43

<u>Figure 2.8a.</u> Histogram.....	43
<u>Figure 2.8b.</u> Charts.....	44
<u>Figure 2.9.</u> qPCR results on day 1 that compare levels of nucleostemin, osteocalcin, osteopontin, and PCNA after their equalization to the endogenous control gene (GAPDH) between LIPUS (L) and control (C) in basic media	45
<u>Figure 2.10.</u> qPCR results on day 7 that compare levels of nucleostemin, osteocalcin, osteopontin, and PCNA after their equalization to the endogenous control gene (GAPDH) between LIPUS (L) and control (C) in basic media	45
<u>Figure 2.11.</u> qPCR results on day 14 that compare levels of nucleostemin, osteocalcin, osteopontin, and PCNA after their equalization to the endogenous control gene (GAPDH) between LIPUS (L) and control (C) in basic media	45
<u>Figure A1.1.</u> Unstained samples: mean differences of Isotype IgG between LIPUS (L) and control (C) in basic media on days 1, 7, and 14	101
<u>Figure A1.2.</u> CD 31: mean differences between LIPUS (L) and control (C) in basic media on days 1, 7, and 14	102
<u>Figure A1.3.</u> CD 34: mean differences between LIPUS (L) and control (C) in basic media on days 1, 7, and 14	103
<u>Figure A1.4.</u> CD 45: mean differences between LIPUS (L) and control (C) in basic media on days 1, 7, and 14	104
<u>Figure A1.5.</u> CD 90: mean differences between LIPUS (L) and control (C) in basic media on days 1, 7, and 14	105

<u>Figure A1.6.</u> MHC I: mean differences between LIPUS (L) and control (C) in basic media on days 1, 7, and 14	106
<u>Figure A1.7.</u> MHC II: mean differences between LIPUS (L) and control (C) in basic media on days 1, 7, and 14	107
<u>Figure A1.8.</u> Schematic diagram that explains the experimental design; basic media, LIPUS = low intensity pulsed ultrasound.....	108
<u>Figure A1.9.</u> qPCR comparison of levels of nucleostemin, osteocalcin, osteopontin, and PCNA after their equalization to the endogenous control gene (GAPDH) between LIPUS (L) and control (C) on days 1, 7, and 14 in basic media	110
<u>Figure A1.10.</u> Flow-cytometry of HUCPV-SC (isotype IgG, CD31, CD90, CD34, CD45, MHC I, and MHC II) treated with LIPUS 10 min/day on days 1, 7, and 14 in basic media; differences between LIPUS (L) and control (C)	111

Chapter 3. Differentiation of HUCPV-SC Cells in Osteogenic Media (OST) Using LIPUS..... 56

<u>Figure 3.1.</u> Schematic diagram shows experimental LIPUS application	60
<u>Figure 3.2.</u> HUCPV-cell count results after application of LIPUS 10 min/day (days 1, 7, and 14) in OST	65
<u>Figure 3.3.</u> HUCPV-DNA level results after application of LIPUS 10 min/day (days 1, 7, and 14) in OST	66
<u>Figure 3.4.</u> HUCPV-ALP level results after application of LIPUS 10 min/day (days 1, 7, and 14) in OST	66

<u>Figure 3.5.</u> HUcPV-normalization of ALP/DNA results after application of LIPUS 10 min/day (days 1, 7, and 14) in OST	67
<u>Figure 3.6.</u> Flow cytometry analysis results on day 1 represented by histogram and charts.....	71
<u>Figure 3.6a.</u> Histogram.....	71
<u>Figure 3.6b.</u> Charts.....	72
<u>Figure 3.7.</u> Flow cytometry analysis results on day 7 represented by histogram and charts.....	73
<u>Figure 3.7a.</u> Histogram.....	73
<u>Figure 3.7b.</u> Charts.....	74
<u>Figure 3.8.</u> Flow cytometry analysis results on day 14 represented by histogram and charts	75
<u>Figure 3.8a.</u> Histogram.....	75
<u>Figure 3.8b.</u> Charts.....	76
<u>Figure 3.9.</u> qPCR results on day 1 that compare levels of nucleostemin, osteocalcin, osteopontin, and PCNA after their equalization to the endogenous control gene (GAPDH) between LIPUS (L) and control (C) in OST.....	77
<u>Figure 3.10.</u> qPCR results on day 7 that compare levels of nucleostemin, osteocalcin, osteopontin, and PCNA after their equalization to the endogenous control gene (GAPDH) between LIPUS (L) and control (C) in OST.....	78

<u>Figure 3.11.</u> qPCR results on day 14 that compare levels of nucleostemin, osteocalcin, osteopontin, and PCNA after their equalization to the endogenous control gene (GAPDH) between LIPUS (L) and control (C) in OST.....	78
<u>Figure A2.1.</u> Unstained samples: mean differences of isotype IgG between LIPUS (L) and control (C) in OST on days 1, 7, and 14	117
<u>Figure A2.2.</u> CD 31: mean differences between LIPUS (L) and control (C) in OST on days 1, 7, and 14.....	118
<u>Figure A2.3.</u> CD 34: mean differences between LIPUS (L) and control (C) in OST on days 1, 7, and 14.....	119
<u>Figure A2.4.</u> CD 90: mean differences between LIPUS (L) and control (C) in OST on days 1, 7, and 14.....	120
<u>Figure A2.5.</u> CD 45: mean differences between LIPUS (L) and control (C) in OST on days 1, 7, and 14.....	121
<u>Figure A2.6.</u> MHCI: mean differences between LIPUS (L) and control (C) in OST on days 1, 7, and 14.....	122
<u>Figure A2.7.</u> MHCII: mean differences between LIPUS (L) and control (C) in OST on days 1, 7, and 14.....	123
<u>Figure A2.8.</u> Schematic diagram that explains the experimental design: OST, LIPUS (low intensity pulsed ultrasound)	124
<u>Figure A2.9.</u> qPCR comparison of levels of nucleostemin, osteocalcin, osteopontin, and PCNA after their equalization to the endogenous control gene (GAPDH) between LIPUS (L) and control (C) on days 1, 7, and 14 (OST).....	125

Figure A2.10. Flow-cytometry of HUCPV-SC (isotype IgG, CD31, CD90, CD34, CD45, MHC I, and MHC II) treated with LIPUS 10 min/day on days 1, 7, and 14 in OST; difference between LIPUS (L) and control (C) 126

Chapter 4. General Discussion and Conclusion 89

Figure 4.1. Exogen 2000, Smith and Nephew device (LIPUS) 90

List of Tables

Chapter 2. Expansion of HUCPV-SC Cells in Basic Media Using LIPUS 23

Table 2.1a. Immunophenotyping markers using flow-cytometry analysis..... 29

Table 2.1b. qPCR genes and gene symbols..... 30

Table 2.2. Comparison of mean \pm SD of cell count, ALP, DNA, ALP normalized to DNA levels between the LIPUS (L) and control (C) groups on days 1, 7, and 14 in basic media 35

Table 2.3. Mean \pm SD of flow-cytometry results of HUCPV-SC (isotype IgG, CD31, CD90, CD34, CD45, MHC I, and MHC II) treated with LIPUS 10 min/day on days 1, 7, and 14: difference between LIPUS (L) and control (C) in basic media..... 38

Table 2.4. qPCR comparison of mean \pm SD of nucleostemin, osteocalcin, osteopontin, and PCNA after their equalization to the endogenous control gene (GAPDH) between LIPUS (L) and control (C) on days 1, 7, and 14 in basic media 47

Table A1.1. Mean \pm SD results of t-test of mean of unstained samples: isotype IgG; differences between LIPUS (L) and control (C) in basic media on days 1, 7, and 14 101

Table A1.2. Mean \pm SD results of t-test of mean CD31 differences between LIPUS (L) and control (C) in basic media on days 1, 7, and 14 102

Table A1.3. Mean \pm SD results of t-test of mean CD34 differences between LIPUS (L) and control (C) in basic media on days 1, 7, and 14 103

Table A1.4. Mean \pm SD results of t-test of mean CD45 differences between LIPUS (L) and control (C) in basic media on days 1, 7, and 14 104

<u>Table A1.5.</u> Mean \pm SD results of t-test of mean CD90 differences between LIPUS (L) and control (C) in basic media on days 1, 7, and 14	105
<u>Table A1.6.</u> Mean \pm SD results of t-test of mean MHCI differences between LIPUS (L) and control (C) in basic media on days 1, 7, and 14	106
<u>Table A1.7.</u> Mean \pm SD results of t-test of mean MHCI differences between LIPUS (L) and control (C) in basic media on days 1, 7, and 14	107
<u>Table A1.8.</u> Comparison of the mean \pm SD of t-test of cell count, ALP, DNA, ALP normalized to DNA levels between LIPUS (L) and control (C) on days 1, 7, and 14 in basic media	109
<u>Table A1.9.</u> qPCR comparison of the mean \pm SD of nucleostemin, osteocalcin, osteopontin, and PCNA after their equalization to the endogenous control gene (GAPDH) between LIPUS (L) and control (C) on day 1 in basic media	112
<u>Table A1.10.</u> qPCR comparison of the mean \pm SD of nucleostemin, osteocalcin, osteopontin, and PCNA after their equalization to the endogenous control gene (GAPDH) between LIPUS (L) and control (C) on day 7 in basic media	112
<u>Table A1.11.</u> qPCR comparison of the mean \pm SD of nucleostemin, osteocalcin, osteopontin, and PCNA after their equalization to the endogenous control gene (GAPDH) between LIPUS (L) and control (C) on day 14 in basic media	113
<u>Table A1.12.</u> t-test of qPCR comparing the mean \pm SD of nucleostemin, osteocalcin, osteopontin, and PCNA after their equalization to the endogenous control gene (GAPDH) between LIPUS (L) and control (C) on day 1 in basic media	114

Table A1.13. t-test of qPCR comparing the mean \pm SD of nucleostemin, osteocalcin, osteopontin, and PCNA after their equalization to the endogenous control gene (GAPDH) between LIPUS (L) and control (C) on day 7 in basic media 115

Table A1.14. t-test of qPCR comparing the mean \pm SD of nucleostemin, osteocalcin, osteopontin, and PCNA after their equalization to the endogenous control gene (GAPDH) between LIPUS (L) and control (C) on day 14 in basic media 116

Chapter 3. Differentiation of HUCPV-SC Cells in Osteogenic Media (OST) Using LIPUS..... 56

Table 3.1a. Immunophenotyping markers using flow-cytometry analysis..... 63

Table 3.1b. qPCR genes and gene symbols..... 64

Table 3.2. Comparing mean \pm SD of cell count, ALP, DNA, ALP normalized to DNA levels between the LIPUS (L) and control (C) on days 1, 7, and 14 in OST 68

Table 3.3. Mean \pm SD of flow-cytometry results of HUCPV-SC (isotype IgG, CD31, CD90, CD34, CD45, MHCI, and MHCII) treated with LIPUS 10 min/day on days 1, 7, and 14 between LIPUS (L) and control (C) in OST..... 70

Table 3.4. qPCR comparison of mean \pm SD of nucleostemin, osteocalcin, osteopontin, and PCNA after their equalization to the endogenous control gene (GAPDH) between LIPUS (L) and control (C) on days 1, 7, and 14 in OST 79

Table A2.1. Mean \pm SD results of t-test of mean unstained samples isotype IgG differences between LIPUS (L) and control (C) in OST on days 1, 7, and 14..... 117

Table A2.2. Mean \pm SD results of t-test of mean CD31 differences between LIPUS (L) and control (C) in OST on days 1, 7, and 14 118

<u>Table A2.3.</u> Mean \pm SD results of t-test of mean CD34 differences between LIPUS (L) and control (C) in OST on days 1, 7, and 14	119
<u>Table A2.4.</u> Mean \pm SD results of t-test of mean CD90 differences between LIPUS (L) and control (C) in OST on days 1, 7, and 14	120
<u>Table A2.5.</u> Mean \pm SD results of t-test of mean CD45 differences between LIPUS (L) and control (C) in OST on days 1, 7, and 14	121
<u>Table A2.6.</u> Mean \pm SD results of t-test of mean MHCI differences between LIPUS (L) and control (C) in OST on days 1, 7, and 14	122
<u>Table A2.7.</u> Mean \pm SD results of t-test of mean MHCII differences between LIPUS (L) and control (C) in OST on days 1, 7, and 14	123
<u>Table A2.8.</u> Comparison of the mean \pm SD of t-test of cell count, ALP, DNA, ALP normalized to DNA levels, between LIPUS (L) and control (C) on days 1, 7, and 14 in OST	127
<u>Table A2.9.</u> qPCR comparison of the mean \pm SD of nucleostemin, osteocalcin, osteopontin, and PCNA after their equalization to the endogenous control gene (GAPDH) between LIPUS (L) and control (C) on day 1 in OST	128
<u>Table A2.10.</u> qPCR comparison of the mean \pm SD of nucleostemin, osteocalcin, osteopontin, and PCNA after their equalization to the endogenous control gene (GAPDH) between LIPUS (L) and control (C) on day 7 in OST	128
<u>Table A2.11.</u> qPCR comparison of the mean \pm SD of nucleostemin, osteocalcin, osteopontin, and PCNA after their equalization to the endogenous control gene (GAPDH) between LIPUS (L) and control (C) on day 14 in OST	129

Table A2.12. t-test of qPCR comparing the mean \pm SD of nucleostemin, osteocalcin, osteopontin, and PCNA after their equalization to the endogenous control gene (GAPDH) between LIPUS (L) and control (C) on day 1 in OST 130

Table A2.13. t-test of qPCR comparing the mean \pm SD of nucleostemin, osteocalcin, osteopontin, and PCNA after their equalization to the endogenous control gene (GAPDH) between LIPUS (L) and control (C) on day 7 in OST 131

Table A2.14. t-test of qPCR comparing the mean \pm SD of nucleostemin, osteocalcin, osteopontin, and PCNA after their equalization to the endogenous control gene (GAPDH) between LIPUS (L) and control (C) on day 14 in OST 132

List of Abbreviations

ALP	alkaline phosphatase
ANOVA	analysis of variance
BM	basic media
BMCs	bone marrow cells
C	control (sham) group
CD31	endothelial cell marker
CD34	hematopoietic cells and vascular endothelium marker
CD45	differentiated hematopoietic cell marker
CD90	stem cell marker
GAPDH	glyceraldehyde-3-phosphate dehydrogenase (human) (endogenous control)
HUCPV-SCs	human umbilical cord perivascular stem cells
LIPUS	low intensity pulsed ultrasound
MANOVA	multivariate analysis of variance
MHCI	a marker recognized during graft rejection and found on all nucleated cells
MHCII	a marker for B-lymphocytes, macrophages (initiates a primary immune response by activating lymphocytes and secreting cytokines)
MSCs	mesenchymal stem cells
NST	nucleostemin
OCN	osteocalcin
OPN	osteopontin
OST	osteogenic media
P1	cultured cells at passage 1
P4	cultured cells at passage 4
PCNA	proliferating cell nuclear antigen
qPCR	quantitative real time polymerization chain reaction
SD	standard deviation

CHAPTER 1

1. Introduction and Literature Review

1.1 Introduction

Cumulative studies from the past two decades have made it possible to conclude that stem cells are capable of self-renewal and subsequent differentiation into multiple lineages with functional outcome in vivo (1). Methodologies to isolate mesenchymal stem cells (MSCs) have been developed to allow cellular expansion ex-vivo without any apparent modification in the phenotype or loss of function. These unique inherent characteristics of MSCs are instrumental for the development of cellular-based therapies and tissue repair in regenerative medicine (2). The most common source of MSCs has been bone marrow that is obtained via direct and invasive bone marrow aspiration. Bone marrow remains a rich source for MSCs, however, it has been demonstrated that the number and the potential for differentiation of bone marrow MSCs decreases with age (2). The need to identify alternative sources for MSCs is increasing due to the limited number of bone marrow MSCs available for autologous use and the significant comorbidity at the donor site (3). The search for different sources of MSCs has been a promising avenue for research, where the focus has shifted to tissues containing cells of higher proliferative potency and differentiation capacity as well as lower risk for viral contamination and immune-rejection (2).

Sarugaser et al. (2005) postulated that human umbilical cord stem cells are competitive candidates due to their close anatomical relation to fetal vasculature, and thus to a source rich in oxygen and nutrients (4). Their rationale was that human umbilical cord perivascular (HUCPV) cells should encompass a subpopulation that is capable of exhibiting a functional mesenchymal phenotype

(4). This is an attractive option because HUCPV cells are usually discarded and they can be obtained noninvasively as is not the case for bone marrow extracts (3). “HUCPV-SCs [human umbilical cord perivascular stem cells] represent a noncontroversial source of primitive mesenchymal progenitor cells that can be harvested after birth, cryogenically stored, thawed, and expanded for therapeutic uses” (3). These cells are major histocompatibility complex class II (MHCII) negative and express both an immune privileged and an immune-modulatory phenotype. In addition, their MHC class I (MHCI) expression levels can be manipulated, making them a potential cell source for MSC-based therapies (3).

MSCs have the potential for self-renewal and differentiation into various phenotypic lineages including bone, cartilage, and fat (5). Bone marrow is not always the optimal source of these cells due to the significant drop in the cell number along with a lower proliferative/differentiation potential with age. HUCPV cells, therefore, emerge as a potential substitute for bone marrow cells (BMCs) due to the immaturity of newborn cells (5). Umbilical cord blood transplantation (UCBT) has become an established hematopoietic therapy for patients with unmatched or unrelated donors (6).

Low intensity pulsed ultrasound (LIPUS) is a noninvasive form of mechanical energy that can be transmitted as high-frequency acoustical pressure waves into biological tissues at frequencies ranging from 1.5–2 MHz and an intensity of 30 mW/cm² (7). LIPUS can provide a direct mechanical stimulation to osteoblast preparations that potentially may enhance osteoblast proliferation, endochondral ossification, in vitro mineralization, and accelerate fracture healing (7). LIPUS has been repeatedly shown to induce DNA synthesis and production of different peptides with various effects on cell membrane permeability and

repair of connective tissues such as bone, muscle, tendon, and cartilage (8). The precise mechanism by which LIPUS induces these cellular modifications has not been elucidated (8).

In vitro LIPUS applications to human osteoblasts, fibroblasts, or monocytes have been shown to induce cellular proliferation and differentiation into different mesenchymal phenotypes such as bone formation and angiogenesis (9). Direct LIPUS stimulation to bone marrow-derived MSCs has been demonstrated to affect osteogenic cells, leading to formation of mineralized nodules and enhancing chondrogenesis (9). Dimitriou and Babis have shown that application of ultrasound has accelerated the healing of bone fractures when applied during the inflammatory and early proliferative phases of bone regeneration (9). However, when applied in the late proliferative phase, it stimulated cartilage growth, suggesting that the time of application plays an integral role in the biological effect of ultrasonic energy on these tissues.

Tam et al. (2008) reported that LIPUS could stimulate a human periosteal cell model at an early period of intervention, and that different energy settings and durations might give different outcomes (10). Rutten et al. (2008) documented LIPUS-accelerated fracture healing of delayed fracture unions of the fibula by increasing osteoid thickness, mineral apposition rate, and bone volume (11). Korstjens et al. (2008) also reported LIPUS stimulated chondrocyte proliferation and matrix production in cartilaginous tissues obtained from regions with degenerating cartilage (12).

1.2. Literature Review

1.2.1. Stem Cells and Craniofacial Tissue Engineering

The active research on connective tissues inspired workers in the dental field to invest in this fertile area. Integral structures of interest to the dental field include the enamel, dentin, dental pulp, cementum, periodontal ligament, craniofacial bones, and temporomandibular joints. This includes bone, fibrocartilages and ligaments, skeletal muscles and tendons, skin and subcutaneous tissue, and salivary glands (13). All these craniofacial structures are phylogenetically derived from neural crest cells and mesenchymal cells (13). Bone marrow-derived, tooth-derived and adipose-derived stem cells belong to distinct subfamilies of MSCs (13). Postnatally, clusters of mesenchymal cells continue to reside in various tissues and are the logical sources of adult MSCs (13).

The prevalence of stem cells in the adult dental pulp has been established in different species including humans, dogs, rats, and mice (14–17). Stem cells derived from dental pulp stem cells (DPSC) have the ability to differentiate into odontoblast-like cells in both in vitro and in vivo conditions. These cells have shown plastic responses whereby they can differentiate into specialized lineages that are distinct from the original tissue (18). Gronthos et al. (2000) reported that human DPSCs could differentiate into adipocyte-like cells, which expressed adipocyte-specific transcripts. DPSCs have also revealed a potential for neurogenic commitment (14). Pierdomenico et al. (2005) found that human DPSCs derived from dental pulp stem cells showed the ability to differentiate into osteogenic and adipogenic lineages in vitro (19). Other studies have shown that stem cells from human dental pulp are able to evolve into

osteogenic, adipogenic, and myogenic phenotypes (20–22, 23). The tissue-engineered craniofacial structures to date are instrumental prototypes that require further development (23).

Newly characterized craniofacial stem cells have differentiation potential similar to bone marrow MSCs (24). The regenerative capacity of craniofacial-derived MSCs needs to be compared to that of bone marrow MSCs (23) under the effect of various mechanical stressors (25). The spectrum of craniofacial tissue engineering should signify the real corresponding developmental sequences (23, 26). Bone marrow derived MSCs became a focus of research into the repair of congenital or acquired craniofacial bone defects and the replacement of oral tissues (27). Both autografting and allografting techniques used in reconstruction of craniofacial and dental defects have numerous limitations and complications, and use of MSCs bypasses many of these disadvantages (27). The utility of stem cell-based craniofacial regeneration has been tested on experimental animal models through surgically seeding these cells onto an appropriate scaffold material (15–17, 27). Surgical approaches in craniofacial defects reconstruction implemented various methodologies ranging from autogenous bone grafts, allergenic materials, and various prostheses (23). Each strategy has its inherent advantages and drawbacks. Autogenous bone grafts require a donor site with resultant morbidity. Prosthetic materials impose the risk of loosening hardware and tissue infection (23).

1.2.2. Human Stem Cells and Tissue Engineering of the Temporomandibular Joint

Minimally invasive techniques for correction of craniofacial defects have reduced the perioperative morbidity and promoted faster recovery. Nonetheless, bone grafts or soft tissue flaps remain a source of significant donor site morbidity (28). Tissue engineering may be viewed as the hope for reproduction and recapitulation of various structures and actual organs for autogenous implantation (28).

Temporomandibular disorders (TMD) produce pain, myalgia, headaches, and other symptoms that result from degenerative joint disease (23). A severe form of temporomandibular joint (TMJ) disorder may eventually require surgical replacement of the mandibular condyle (23). Over the past few years, some studies have shown that tissue engineering can be implemented to recapitulate the actual biological dimensions of the mandibular condyle of the human temporomandibular joint (29–31).

1.2.3. Bone Augmentation and Repair

The primary target of regenerative medicine is to drive embryonic cells by the activation of progenitor cells that are capable of proliferation and differentiation to the desired end-point lineages (32). This is exemplified by the repair of long bone fractures to recapitulate the embryonic processes and ends in near-perfect repair (33). Angiogenesis precedes bone regeneration in vivo and the osteo-progenitors are perivascular cells (33). These perivascular progenitor cells are essential agents for stimulating osteoblastic differentiation in vitro (33). This has shifted the emphasis from the properties of materials to the inherent

potential of the cells and has led to new approaches in tissue engineering of osteoblastic regeneration (33).

“An estimated 1,600,000 bone grafts are performed every year to regenerate bone lost to trauma and disease, of which 6 percent (96,000) are cranio-maxillofacial in nature” (34). These procedures rely on autologous bone grafting, allogenic grafting, and natural or synthetic bony biomaterials (34). The amount of bone that can be harvested limits the extent of autologous bone grafting (34). The long-term outcome of osteoconductive biomaterials primarily depends on the ability to induce local cells to regenerate the defect that is often not enduring (34). New techniques are required to predictably restore function and form, particularly for craniofacial defects (34).

1.2.4. Expansion of Stem Cells for Tissue Engineering

Over the years, efforts have been made to expand stromal cells for tissue engineering. IL-11 or granulocyte-colony stimulating factor (G-CSF) and Flt3 ligand (FL) have been used to stimulate the growth of rat MSCs (35). Expansion of the progenitor cells by 40 fold has been achieved under the stimulatory effect of these factors within 2 weeks of incubation. Alternatively, prolactin-like protein E (PLP-E) and human thrombopoietin (TPO) have not been shown to affect the expansion of human MSCs (36). Glucocorticoids were claimed effective in recruiting rather than in stimulating cellular proliferation (37). Dickkopf homolog 1 (Dkk-1) was shown to stimulate MSC expansion (38). Conversely, culture flasks coated with heparin and N-(O-beta-(6-O-sulfogalactopyranosyl)-6-oxyhexyl)-3, 5-bis (dodecyloxy)-benzamide have been shown to expand MSCs (39). A similar

study showed that angiopoietin-like proteins expanded human MSCs 24–30 fold in 10 days (40).

Pulsed electromagnetic fields (PEMF) appear to increase proliferation of chondrocytes and osteoblast-like cells (41, 42). However, no studies have examined the effect of PEMF on HUCPV-SCs. Low intensity pulse ultrasound (LIPUS) is an intermittent pulsed electromagnetic energy. Leung et al. (2004) did not notice any periosteal cell proliferation using LIPUS for 2 and 4 days at 5, 10, and 20 minutes (43). The lack of an observable stimulatory effect could have been due to the short duration of ultrasound treatment in that experiment. Nonetheless, LIPUS was effective for fracture repair after 3 weeks of application (44). Ebisawa et al. (2004) showed that LIPUS treatment increased matrix production but not cell proliferation of human MSCs (45). The methodology of direct application of LIPUS in that study by inserting the transducer inside the culture media might explain the positive effect (45). This invasive method should be balanced against the potential for infections or other deleterious effects on the cells (45). Also, MSCs have cell-to-cell growth inhibition when they are in close proximity to each other (45). LIPUS has been shown to promote matrix production and proliferation of intervertebral disc cell culture (46). The effects of LIPUS are dose dependent and have different outcomes depending on the cells' origin, either nucleus pulposus (NP) or annulus fibrosus (AF) (46).

1.2.5. Mechanical Stresses on Chondrogenic and Osteogenic Cell Differentiation

It has been reported that the material properties of tissue-engineered cartilage constructs are measured in the range of kilopascals (KPa) which are an

order-of-magnitude lower than typical articular cartilage that are in the range of megapascals (MPa) (47–52). One of the major challenges in tissue engineered cartilage construction is the shortage of mechanical stresses (51, 52). Some recent studies reported that using bioreactors enhanced the material properties of tissue-engineered cartilage constructs (49–54). Moreover, cyclic compressive loading was demonstrated to induce phenotypic changes between cartilaginous and osseous tissues and chondrocyte differentiation (55, 56). Others documented an anabolic effect of LIPUS on osteoblasts, on chondrogenic differentiation, and on matrix production in vitro and in vivo (45, 64, 65). These results are still uncertain and parameter optimization has not been validated yet. In addition, mechanical testing machines and bioreactors have not yet been clinically applicable (57–63).

1.2.6. Phenotypic Characteristics of Human Umbilical Cord Perivascular Stem Cells

The complex composition of the human umbilical cord has necessitated multiple attempts to characterize and purify stem cell constituents. The isolation of a HUCPV-SC subpopulation remains a subjective process due to the different protocols for isolation and cultivation. Various approaches have been implemented to induce differentiation of human umbilical cord mesenchymal progenitor cells into osteogenic cells. These cultural modules have been successful in mediating the expression of more specific progenitor markers.

Multiple studies showed that HUCPV-SCs tested negative for the endothelial/hematopoietic cell markers CD34, CD45, and MHCII, but positively stained to the MSC markers, namely CD90 and MHCI (4, 66–68). These cells

demonstrated a particular trend to differentiate into osteogenic cells after 3 weeks, as well as into multiple mesenchymal lineages (66–68). Collectively, HUCPV-SCs emerged as an alternative and attractive source for bone marrow MSCs.

Kim et al. (2007) noted a potential capacity of HUCPV-SCs to differentiate into osteocyte cells after 2 weeks (69). Nevertheless, HUCPV-SCs continued to test negative to MHCII and CD31, but positive to MHCI, similar to bone marrow MSCs (69). HUCPV-SCs also demonstrated a potential for osteogenic differentiation similar to that of bone marrow stem cells (69). Furthermore, several in vitro studies revealed that HUCPV-SCs were negative to CD34, CD45, CD31, and MHCII, but persistently stained positive to CD90 (70–74). These findings have eliminated the possibility of endothelial or hematopoietic contamination and have provided a pure MSC progenitor precursor (70–73).

On the other hand, Zhang et al. (2004) reported that those cells substantially expressed osteopontin (OPN) in osteogenic differentiated media (70). Rosada et al. (2002) further documented an intense positivity of HUCPV-SCs for osteocalcin (OSC) and alkaline phosphatase (ALP) in osteogenic media (72). This was further corroborated by Gang et al. (2004) who showed a florid positivity of HUCPV-SCs for ALP and OPN (73). Interestingly, this reactivity to ALP and OPN gradually increased over 2 weeks within osteogenic media (73). Moreover, Sarugaser et al. (2005) reported a high positivity of HUCPV-SCs to ALP that reflects their metabolic activity and proliferation capacity. These cells could easily be elaborated to induce bone nodules starting at Passage 0 (4). The same group also observed that HUCPV-SCs were osteoprogenitor cells that expressed the osteogenic phenotype and provoked bone matrix in culture (4).

1.2.7. Summary

The vast majority of current dental restorative practice relies on synthetic materials rather than biological-based regenerative therapy. Synthetic dental prosthesis such as tissue grafting and metal implants retain multiple limitations; recipient immune rejection and potential viral transmission are a few examples. These inherent complications at the biologic-hardware interface invoke a tremendous need for biological-based regenerative therapy. MSCs and umbilical-cord derived stem cells that are capable of guided phenotypic differentiation paved the road for an ever-expanding regenerative technology. We have pursued a search for new, safe, and available sources of cellular lineages with lower potential for immune rejection. Our project also aimed to study the effects of the mechanical energy from LIPUS on newly characterized HUCPV-SCs. Our review of the current literature revealed that the application of LIPUS may enhance tissue regeneration. The biologic effect of LIPUS on furthering stem cell proliferation and differentiation might not be significant in vitro. Most positive results from prior research were derived from in vivo applications of the LIPUS technique. This may reflect the differences between the physiological variables of a human environment compared to that of tissue culture media. Nonetheless, this may also imply that application of LIPUS directly to living tissue can foster a more natural healing process. Further studies and clinical trials are required to define the optimal parameters of a regenerative role for LIPUS on tissue remodeling and healing in the craniofacial region.

1.3. Objectives of the Study

A. The first objective of our study is to evaluate whether LIPUS has a stimulatory effect on HUCPV-SCs; that is, whether LIPUS treatment will increase their proliferation while maintaining their stem cell characteristics.

B. The second objective is to evaluate whether LIPUS has a stimulatory effect on osteogenic differentiation of HUCPV-SCs.

1.4. Research Hypothesis

Hypothesis 1. The stimulatory effect of LIPUS on HUCPV-SC expansion is dose dependent. This hypothesis is based on previous studies that showed the positive stimulatory effect of LIPUS on MSC expansion and proliferation as reflected by increased cell count and ALP level.

Hypothesis 2. LIPUS-expanded HUCPV-SCs will maintain their stem cell and their osteogenic potentials after exposure to different LIPUS regimens. This hypothesis is based on previous research that showed that mechanical loading is stimulatory for chondrogenic and osteogenic differentiation (56).

1.5. References

- (1) Karahuseyinoglu S, Cinar O, Kilic E, Kara F, Akay GG, Demiralp DO, et al. Biology of stem cells in human umbilical cord stroma: in situ and in vitro surveys. *Stem Cells* 2007 Feb;25(2):319-331.
- (2) Kestendjieva S, Kyurkchiev D, Tsvetkova G, Mehandjiev T, Dimitrov A, Nikolov A, et al. Characterization of mesenchymal stem cells isolated from the human umbilical cord. *Cell Biol. Int.* 2008 Jul;32(7):724-732.
- (3) Baksh D, Yao R, Tuan RS. Comparison of proliferative and multilineage differentiation potential of human mesenchymal stem cells derived from umbilical cord and bone marrow. *Stem Cells* 2007 Jun;25(6):1384-1392.
- (4) Sarugaser R, Lickorish D, Baksh D, Hosseini MM, Davies JE. Human umbilical cord perivascular (HUCPV) cells: a source of mesenchymal progenitors. *Stem Cells* 2005 Feb;23(2):220-229.
- (5) Park KS, Lee YS, Kang KS. In vitro neuronal and osteogenic differentiation of mesenchymal stem cells from human umbilical cord blood. *J. Vet. Sci.* 2006 Dec;7(4):343-348.
- (6) Hofmeister CC, Zhang J, Knight KL, Le P, Stiff PJ. Ex vivo expansion of umbilical cord blood stem cells for transplantation: growing knowledge from the hematopoietic niche. *Bone Marrow Transplant.* 2007 Jan;39(1):11-23.
- (7) Qin L, Fok P, Lu H, Shi S, Leng Y, Leung K. Low intensity pulsed ultrasound increases the matrix hardness of the healing tissues at bone-tendon insertion—a partial patellectomy model in rabbits. *Clin. Biomech.* 2006 May;21(4):387-394.
- (8) Lee HJ, Choi BH, Min BH, Park SR. Low-intensity ultrasound inhibits apoptosis and enhances viability of human mesenchymal stem cells in three-

dimensional alginate culture during chondrogenic differentiation. *Tissue Eng.* 2007 May;13(5):1049-1057.

(9) Dimitriou R, Babis GC. Biomaterial osseointegration enhancement with biophysical stimulation. *J. Musculoskelet. Interact.* 2007 Jul-Sep;7(3):253-265.

(10) Tam KF, Cheung WH, Lee KM, Qin L, Leung KS. Osteogenic effects of low-intensity pulsed ultrasound, extracorporeal shockwaves and their combination—an in vitro comparative study on human periosteal cells. *Ultrasound Med. Biol.* 2008 Dec;34(12):1957-1965.

(11) Rutten S, Nolte PA, Korstjens CM, van Duin MA, Klein-Nulend J. Low-intensity pulsed ultrasound increases bone volume, osteoid thickness, and mineral apposition rate in the area of fracture healing in patients with a delayed union of the osteotomized fibula. *Bone* 2008 Aug;43(2):348-354.

(12) Korstjens CM, van der Rijt RH, Albers GH, Semeins CM, Klein-Nulend J. Low-intensity pulsed ultrasound affects human articular chondrocytes in vitro. *Med. Biol. Eng. Comput.* 2008 Dec;46(12):1263-1270.

(13) Mao JJ. Stem cells and the future of dental care. *N.Y. State Dent. J.* 2008 Mar;74(2):20-24.

(14) Gronthos S, Mankani M, Brahim J, Robey PG, Shi S. Postnatal human dental pulp stem cells (DPSCs) in vitro and in vivo. *Proc. Natl. Acad. Sci. U.S.A.* 2000 Dec 5;97(25):13625-13630.

(15) Iohara K, Nakashima M, Ito M, Ishikawa M, Nakasima A, Akamine A. Dentin regeneration by dental pulp stem cell therapy with recombinant human bone morphogenetic protein 2. *J. Dent. Res.* 2004 Aug;83(8):590-595.

- (16) Zhang W, Walboomers XF, Wolke JG, Bian Z, Fan MW, Jansen JA. Differentiation ability of rat postnatal dental pulp cells in vitro. *Tissue Eng.* 2005 Mar-Apr;11(3-4):357-368.
- (17) Mina M, Braut A. New insight into progenitor/stem cells in dental pulp using Col1a1-GFP transgenes. *Cells Tissues Organs* 2004;176(1-3):120-133.
- (18) Pittenger MF, Mackay AM, Beck SC, Jaiswal RK, Douglas R, Mosca JD, et al. Multilineage potential of adult human mesenchymal stem cells. *Science* 1999 Apr 2;284(5411):143-147.
- (19) Pierdomenico L, Bonsi L, Calvitti M, Rondelli D, Arpinati M, Chirumbolo G, et al. Multipotent mesenchymal stem cells with immunosuppressive activity can be easily isolated from dental pulp. *Transplantation* 2005 Sep 27;80(6):836-842.
- (20) Laino G, Graziano A, d'Aquino R, Pirozzi G, Lanza V, Valiante S, et al. An approachable human adult stem cell source for hard-tissue engineering. *J. Cell. Physiol.* 2006 Mar;206(3):693-701.
- (21) Graziano A, d'Aquino R, Laino G, Papaccio G. Dental pulp stem cells: a promising tool for bone regeneration.[erratum appears in *Stem Cell Rev.* 2008 Spring;4(1):65]. *Stem Cell Rev.* 2008;4(1):21-26.
- (22) Zhang W, Walboomers XF, Van Kuppevelt TH, Daamen WF, Van Damme PA, Bian Z, et al. In vivo evaluation of human dental pulp stem cells differentiated towards multiple lineages. *J. Tissue Eng. Regen. Med.* 2008 Mar-Apr;2(2-3):117-125.
- (23) Mao JJ, Giannobile WV, Helms JA, Hollister SJ, Krebsbach PH, Longaker MT, et al. Craniofacial tissue engineering by stem cells. *J. Dent. Res.* 2006 Nov;85(11):966-979.

- (24) Shi S, Bartold PM, Miura M, Seo BM, Robey PG, Gronthos S. The efficacy of mesenchymal stem cells to regenerate and repair dental structures. *Orthod. Craniofac. Res.* 2005 Aug;8(3):191-199.
- (25) Carter DR, Beaupre GS, Giori NJ, Helms JA. Mechanobiology of skeletal regeneration. *Clin. Orthop.* 1998 Oct(355 Suppl):S41-55.
- (26) Ferguson CM, Miclau T, Hu D, Alpern E, Helms JA. Common molecular pathways in skeletal morphogenesis and repair. *Ann. N.Y. Acad. Sci.* 1998 Oct 23;857:33-42.
- (27) Risbud MV, Shapiro IM. Stem cells in craniofacial and dental tissue engineering. *Orthod. Craniofac. Res.* 2005 May;8(2):54-59.
- (28) Abukawa H, Terai H, Hannouche D, Vacanti JP, Kaban LB, Troulis MJ. Formation of a mandibular condyle in vitro by tissue engineering. *J. Oral Maxillofac. Surg.* 2003 Jan;61(1):94-100.
- (29) Alhadlaq A, Mao JJ. Tissue-engineered neogenesis of human-shaped mandibular condyle from rat mesenchymal stem cells. *J. Dent. Res.* 2003 Dec;82(12):951-956.
- (30) Alhadlaq A, Elisseeff JH, Hong L, Williams CG, Caplan AI, Sharma B, et al. Adult stem cell driven genesis of human-shaped articular condyle. *Ann. Biomed. Eng.* 2004 Jul;32(7):911-923.
- (31) Alhadlaq A, Mao JJ. Tissue-engineered osteochondral constructs in the shape of an articular condyle. *J. Bone Joint Surg. Am.* 2005 May;87(5):936-944.
- (32) Ferguson MW, Whitby DJ, Shah M, Armstrong J, Siebert JW, Longaker MT. Scar formation: the spectral nature of fetal and adult wound repair. *Plast. Reconstr. Surg.* 1996 Apr;97(4):854-860.

- (33) Buxton PG, Cobourne MT. Regenerative approaches in the craniofacial region: manipulating cellular progenitors for oro-facial repair. *Oral Dis.* 2007 Sep;13(5):452-460.
- (34) Robey PG, Bianco P. The use of adult stem cells in rebuilding the human face. *J. Am. Dent. Assoc.* 2006 Jul;137(7):961-972.
- (35) Jacobsen SE, Okkenhaug C, Myklebust J, Veiby OP, Lyman SD. The FLT3 ligand potently and directly stimulates the growth and expansion of primitive murine bone marrow progenitor cells in vitro: synergistic interactions with interleukin (IL) 11, IL-12, and other hematopoietic growth factors. *J. Exp. Med.* 1995 Apr 1;181(4):1357-1363.
- (36) Lefebvre P, Lin J, Linzer DI, Cohen I. Murine prolactin-like protein E synergizes with human thrombopoietin to stimulate expansion of human megakaryocytes and their precursors. *Exp. Hematol.* 2001 Jan;29(1):51-58.
- (37) Purpura KA, Aubin JE, Zandstra PW. Sustained in vitro expansion of bone progenitors is cell density dependent. *Stem Cells* 2004;22(1):39-50.
- (38) Horwitz EM. Dkk-1-mediated expansion of adult stem cells. *Trends Biotechnol.* 2004 Aug;22(8):386-388.
- (39) Takagi M. Cell processing engineering for ex-vivo expansion of hematopoietic cells. *J. Biosci. Bioeng.* 2005 Mar;99(3):189-196.
- (40) Zhang CC, Kaba M, Ge G, Xie K, Tong W, Hug C, et al. Angiopoietin-like proteins stimulate ex vivo expansion of hematopoietic stem cells. *Nat. Med.* 2006 Feb;12(2):240-245.
- (41) De Mattei M, Caruso A, Pezzetti F, Pellati A, Stabellini G, Sollazzo V, et al. Effects of pulsed electromagnetic fields on human articular chondrocyte proliferation. *Connect Tissue Res.* 2001;42(4):269-279.

- (42) Hartig M, Joos U, Wiesmann HP. Capacitively coupled electric fields accelerate proliferation of osteoblast-like primary cells and increase bone extracellular matrix formation in vitro. *Eur. Biophys. J.* 2000;29(7):499-506.
- (43) Leung KS, Cheung WH, Zhang C, Lee KM, Lo HK. Low intensity pulsed ultrasound stimulates osteogenic activity of human periosteal cells. *Clin. Orthop.* 2004 Jan(418):253-259.
- (44) Tsai CL, Chang WH, Liu TK. Preliminary studies of duration and intensity of ultrasonic treatments on fracture repair. *Chin. J. Physiol.* 1992;35(1):21-26.
- (45) Ebisawa K, Hata K, Okada K, Kimata K, Ueda M, Torii S, et al. Ultrasound enhances transforming growth factor beta-mediated chondrocyte differentiation of human mesenchymal stem cells. *Tissue Eng.* 2004 May-Jun;10(5-6):921-929.
- (46) Iwashina T, Mochida J, Miyazaki T, Watanabe T, Iwabuchi S, Ando K, et al. Low-intensity pulsed ultrasound stimulates cell proliferation and proteoglycan production in rabbit intervertebral disc cells cultured in alginate. *Biomaterials* 2006 Jan;27(3):354-361.
- (47) Patel RV, Mao JJ. Microstructural and elastic properties of the extracellular matrices of the superficial zone of neonatal articular cartilage by atomic force microscopy. *Front. Biosci.* 2003 Jan 1;8:a18-25.
- (48) Cohen B, Chorney GS, Phillips DP, Dick HM, Buckwalter JA, Ratcliffe A, et al. The microstructural tensile properties and biochemical composition of the bovine distal femoral growth plate. *J. Orthop. Res.* 1992 Mar;10(2):263-275.
- (49) Hu K, Radhakrishnan P, Patel RV, Mao JJ. Regional structural and viscoelastic properties of fibrocartilage upon dynamic nanoindentation of the articular condyle. *J. Struct. Biol.* 2001 Oct;136(1):46-52.

- (50) Radhakrishnan P, Mao JJ. Nanomechanical properties of facial sutures and sutural mineralization front. *J. Dent. Res.* 2004 Jun;83(6):470-475.
- (51) Narmoneva DA, Wang JY, Setton LA. Nonuniform swelling-induced residual strains in articular cartilage. *J. Biomech.* 1999 Apr;32(4):401-408.
- (52) Goldstein SA. Tissue engineering: functional assessment and clinical outcome. *Ann. N.Y. Acad. Sci.* 2002 Jun;961:183-192.
- (53) Sikavitsas VI, Temenoff JS, Mikos AG. Biomaterials and bone mechanotransduction. *Biomaterials* 2001 Oct;22(19):2581-2593.
- (54) LeBaron RG, Athanasiou KA. Ex vivo synthesis of articular cartilage. *Biomaterials* 2000 Dec;21(24):2575-2587.
- (55) Elder SH, Goldstein SA, Kimura JH, Soslowsky LJ, Spengler DM. Chondrocyte differentiation is modulated by frequency and duration of cyclic compressive loading. *Ann. Biomed. Eng.* 2001 Jun;29(6):476-482.
- (56) Huang CY, Hagar KL, Frost LE, Sun Y, Cheung HS. Effects of cyclic compressive loading on chondrogenesis of rabbit bone-marrow derived mesenchymal stem cells. *Stem Cells* 2004;22(3):313-323.
- (57) Yaghoobi MM, Mowla SJ, Tiraihi T. Nucleostemin, a coordinator of self-renewal, is expressed in rat marrow stromal cells and turns off after induction of neural differentiation. *Neurosci. Lett.* 2005 Dec 23;390(2):81-86.
- (58) Segers VF, Van Riet I, Andries LJ, Lemmens K, Demolder MJ, De Becker AJ, et al. Mesenchymal stem cell adhesion to cardiac microvascular endothelium: activators and mechanisms. *Am. J. Physiol. Heart Circ. Physiol.* 2006 Apr;290(4):H1370-7.

- (59) Gao J, Dennis JE, Solchaga LA, Awadallah AS, Goldberg VM, Caplan AI. Tissue-engineered fabrication of an osteochondral composite graft using rat bone marrow-derived mesenchymal stem cells. *Tissue Eng.* 2001 Aug;7(4):363-371.
- (60) Weng JJ, Yung BY. Nucleophosmin/B23 regulates PCNA promoter through YY1. *Biochem. Biophys. Res. Commun.* 2005 Sep 30;335(3):826-831.
- (61) Wong H, Anderson WD, Cheng T, Riabowol KT. Monitoring mRNA expression by polymerase chain reaction: the "primer-dropping" method. *Anal. Biochem.* 1994 Dec;223(2):251-258.
- (62) Boerma M, Schutte-Bart CI, Wedekind LE, Beekhuizen H, Wondergem J. Effects of multiple doses of ionizing radiation on cytokine expression in rat and human cells. *Int. J. Radiat. Biol.* 2003 Nov;79(11):889-896.
- (63) Lin Y, Luo E, Chen X, Liu L, Qiao J, Yan Z, et al. Molecular and cellular characterization during chondrogenic differentiation of adipose tissue-derived stromal cells in vitro and cartilage formation in vivo. *J. Cell. Mol. Med.* 2005 Oct-Dec;9(4):929-939.
- (64) Vance J, Galley S, Liu DF, Donahue SW. Mechanical stimulation of MC3T3 osteoblastic cells in a bone tissue-engineering bioreactor enhances prostaglandin E2 release. *Tissue Eng.* 2005 Nov-Dec;11(11-12):1832-1839.
- (65) Clark PA, Rodriguez A, Sumner DR, Hussain MA, Mao JJ. Modulation of bone ingrowth of rabbit femur titanium implants by in vivo axial micromechanical loading. *J. Appl. Physiol.* 2005 May;98(5):1922-1929.
- (66) Kestendjieva S, Kyurkchiev D, Tsvetkova G, Mehandjiev T, Dimitrov A, Nikolov A, et al. Characterization of mesenchymal stem cells isolated from the human umbilical cord. *Cell Biol. Int.* 2008 Jul;32(7):724-732.

- (67) Miao Z, Jin J, Chen L, Zhu J, Huang W, Zhao J, et al. Isolation of mesenchymal stem cells from human placenta: comparison with human bone marrow mesenchymal stem cells. *Cell Biol. Int.* 2006 Sep;30(9):681-687.
- (68) Yen BL, Huang HI, Chien CC, Jui HY, Ko BS, Yao M, et al. Isolation of multipotent cells from human term placenta. *Stem Cells* 2005;23(1):3-9.
- (69) Kim J, Lee Y, Kim H, Hwang KJ, Kwon HC, Kim SK, et al. Human amniotic fluid-derived stem cells have characteristics of multipotent stem cells. *Cell Prolif.* 2007 Feb;40(1):75-90.
- (70) Zhang Y, Li C, Jiang X, Zhang S, Wu Y, Liu B, et al. Human placenta-derived mesenchymal progenitor cells support culture expansion of long-term culture-initiating cells from cord blood CD34+ cells. *Exp. Hematol.* 2004 Jul;32(7):657-664.
- (71) Musina RA, Bekchanova ES, Sukhikh GT. Comparison of mesenchymal stem cells obtained from different human tissues. *Bull. Exp. Biol. Med.* 2005 Apr;139(4):504-509.
- (72) Rosada C, Justesen J, Melsvik D, Ebbesen P, Kassem M. The human umbilical cord blood: a potential source for osteoblast progenitor cells. *Calcif. Tissue Int.* 2003 Feb;72(2):135-142.
- (73) Gang EJ, Hong SH, Jeong JA, Hwang SH, Kim SW, Yang IH, et al. In vitro mesengenic potential of human umbilical cord blood-derived mesenchymal stem cells. *Biochem. Biophys. Res. Commun.* 2004 Aug 13;321(1):102-108.

(74) Wagner W, Wein F, Seckinger A, Frankhauser M, Wirkner U, Krause U, et al. Comparative characteristics of mesenchymal stem cells from human bone marrow, adipose tissue, and umbilical cord blood. *Exp. Hematol.* 2005 Nov;33(11):1402-1416.

CHAPTER 2

Expansion of HUCPV-SCs in Basic Media Using LIPUS

2.1. Key Words: Low intensity pulsed ultrasound (LIPUS), stem cells, human umbilical cord perivascular stem cell (HUCPV-SC).

2.2. Introduction

Cumulative experience from studies over the last two decades has defined stem cells as progenitor cells capable of self-renewal and differentiation into multiple lineages (1). Mesenchymal stem cells (MSCs) have been isolated and cultured with a reasonable degree of phenotype preservation (2). The source for MSCs is primarily bone marrow where access is limited due to the significant morbidity of bone marrow aspiration (3). The invasive collection of bone marrow stem cells by direct bone marrow aspiration triggered the need to find an alternate source of stem cells (3, 4). Human umbilical cord perivascular stem cells (HUCPV-SCs) are good candidates because of their close anatomical relation to fetal vasculature, an environment rich in oxygen and essential nutrients (4). HUCPV-SCs encompass a cellular subpopulation capable of exhibiting a functional mesenchymal phenotype (4). HUCPV cells are usually discarded and their harvest does not entail any invasive procedure as is the case for bone marrow extracts (3).

Interest in MSCs as a tool for therapeutic applications has recently increased because of the relative ease of isolation and culture and the high potential for cell expansion in vitro (5). HUCPV-SCs are characterized by a low immunorejective capacity and a sizable reservoir of perivascular progenitor stem

cells (4, 6). Therapeutic application of ultrasound waves, particularly low-intensity pulsed ultrasound (LIPUS), has been shown to facilitate healing of bone fractures (7). The physiologic effects of LIPUS application has been related to an increase in the integration of calcium ions in osseous and soft tissues (8). LIPUS also appears to stimulate the expression of genes that mediate the healing process, including aggrecan and insulin-like growth factor (IGF) (8). The cellular mechanisms mediating the observed therapeutic actions of LIPUS are still poorly understood (9). The cavitation phenomenon represents the pulsation of gas or vapor-filled voids in a sound field resulting in compression of microtubules by direct ultrasonic energy (10, 11). This transmitted energy could invoke a direct effect on cell membrane permeability and on second messenger adenylate cyclase activity (10). Subsequent changes in ion channels or protein transport as a result of altered second messenger pathways could modify the intracellular signals for gene expression (10). Alternatively, the use of low-intensity ultrasound reduces the heating (compared to high intensity ultrasound) of underlying tissues and also minimizes the extent of cavitation phenomena (11).

Wang et al. (1993) reported that application of mechanical stressors to the cytoskeleton could influence cell metabolism through changes in gene expression (12). Intermittent high-frequency acoustic pressure waves are a noninvasive form of mechanical stress. LIPUS protocols are applied at frequencies ranging from 1.5–2 MHz at an intensity of 30 mW/cm² (13). LIPUS has been shown to induce synthesis of DNA and proteins with resultant changes in the permeability of cell membranes and the recovery of various connective tissues, including bone, muscle, tendon, and cartilage (14). “LIPUS application is a nonthermal and nondestructive tool because of the low-intensity of the

acoustical pressure waves” (15). The acoustic pressure of low frequency ultrasound waves does not increase the tissue temperature more than 1°C and does not significantly alter cellular activity (15).

This study investigates whether LIPUS stimulates HUCPV-SC proliferation while maintaining the stem cell character of the cells. Effects of LIPUS in vitro on cultured HUCPV-SCs was assessed in five different assays: cell count, alkaline phosphatase (ALP) level, DNA content, qPCR, and immunophenotyping of cells derived from HUCPV-SCs by flow-cytometric analysis.

2.3. Materials and Methods

2.3.1. Cell Culture

Approval for these experiments was obtained from the Health Research Ethics Board, University of Alberta, Edmonton, Canada (approval number 6431, 2006). After obtaining patient consent, HUCPV-SCs were obtained from patients undergoing full-term caesarean sections. Cells were isolated according to methods described by Sarugaser et al. (2005) and were generously provided by Dr. J. E. Davies (University of Toronto, Ontario, Canada) (4). HUCPV cells at passage 1 were thawed and seeded into three T-75 cm² tissue culture flasks (Sigma Aldrich) containing Dulbecco’s modified Eagle’s medium with low glucose (DMEM-LG) (GIBCO, Invitrogen) supplemented with 15% fetal bovine serum (FBS) and 1% antibiotic-antimycotic (Sigma Aldrich) at an initial cell density of 3.6 x 10⁶/ml. Cells were incubated at 37°C in 5% CO₂, then expanded for 10 days until P4. Media was changed every 2–3 days. When cell confluence was 80% (4.2 x 10⁶/ml), cells were harvested and trypsinized using 0.25% trypsin (GIBCO,

Invitrogen), collected in 50 ml tubes, centrifuged, then distributed into nine 6 well plates (Sigma Aldrich) at 2×10^4 /ml. 27 wells were treated for 10 min/day by 4 “Exogen LIPUS” devices with 4 transducers placed immediately below the wells and coupled to the well bases with standard ultrasound coupling gel transducers previously calibrated (Figure 2.1). The ultrasound frequency, intensity, and duration were identical to that used in the clinic for bone fracture repair (Exogen Bone Healing System, Smith and Nephew, Memphis, TN, USA); that is, each produced a 1.5-Mhz ultrasound wave composed of a 200 μ s burst with an output intensity of 30 mW/cm^2 for 1 day, 7 days, and 14 days. The other 27 wells were sham treated using the same transducers without turning the machines on. Each group was evaluated at each time point (see Figure A1.8 in Appendix 1).

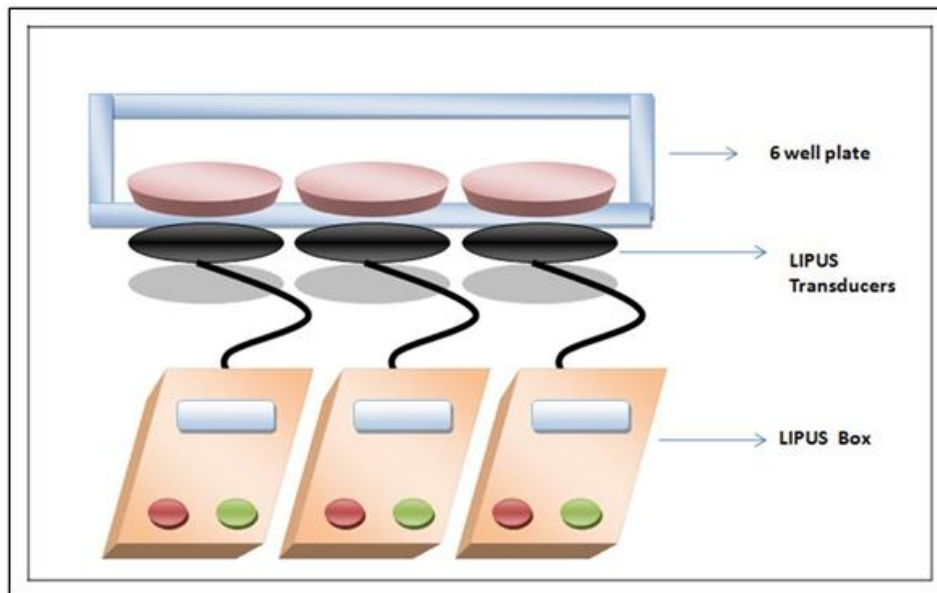


Figure 2.1 Schematic diagram shows experimental LIPUS application

2.3.2. Cell Count

Cells were washed using PBS (GIBCO, Invitrogen), then trypsinized. Cells and medium were collected in 15 ml tubes for centrifugation (6 min at 600 rpm). The supernatant was vacuumed away. Cells were counted using a Beckman Coulter counter (Faculty of Dentistry, University of Alberta, Canada).

2.3.3. Alkaline Phosphatase Activity Assay

ALP activity of HUCPV-SCs was determined by a colorimetric assay at the indicated time points (days 1, 7, and 14) (16). ALP is a biochemical marker for cell differentiation of osteogenic lineage (17, 18) Cells were washed with phosphate buffered saline (PBS) and lysed with 2 ml of ALP assay buffer per well (0.5 M 2-amino-2-methyl-1-propanol and 0.1% Triton- X-100, pH 10.5). Two hours later, after lysis, 1 ml of lysed cells was used for an ALP quantification assay. Phosphatase substrate (*p*-nitrophenyl phosphate) (Sigma) was added to the ALP assay buffer in a 1mg/ml (1:1) ratio. 100 μ l of lysed cells and 100 μ l of substrate mixture were loaded to each well of a 96 well plate to a final concentration of 1 mg/ml. The changes in optical density (absorbance, 405 nm) were determined in a multiwell plate reader at periodic intervals of 5, 10, 15, and 30 minutes.

2.3.4. Cell Proliferation and DNA Quantification Assay

1 ml of the lysed cell solution was used to measure the amount of DNA with the CyQUANT Cell Proliferation Assay Kit (Molecular Probe, Invitrogen). The CyQUANT Cell Proliferation Assay Kit measures the quantity of DNA through nucleic acid binding to a fluorescent dye (Molecular Probe, Invitrogen).

The binding of nucleic acids enhances the dye's ability to fluoresce. Thus the extent of proliferation is determined by comparing a treated cell's fluorescence, and consequently its DNA content, with the fluorescence of untreated control cells. Cells are incubated with dye for 30–60 minutes during which time lysis occurs and the dye binds to the released nucleic acids. Fluorescence is measured in a microplate reader. The assay is designed to produce a linear analytical response in a 96-well microplate (Molecular Probe, Invitrogen). A DNA standard provided with the CyQUANT kit was utilized to determine the DNA concentrations in each group of cells. According to the manufacturer's instructions, DNA was quantified using a fluorescence plate reader (excitation at 480 nm; emission at 527 nm) (Faculty of Chemical Engineering, University of Alberta).

2.3.5. Immunophenotyping Using Flow-Cytometry Analysis

Further characterization of expanded HUCPV-SCs at passage 4 using cell surface antigen phenotyping was performed on days 1, 7, and 14. The following cell-surface epitopes were labeled with antihuman antibodies: CD31 (PECAM-1) fluorescein isothiocyanate (FITC, BD Biosciences), CD34-R-phycoerythrin (R-PE, BD Biosciences), CD45-phycoerythrin (PE, BD Biosciences), CD90 (Thy1) R-phycoerythrin (R-PE, BD Biosciences), MHC I (HLA-A,B,C) R-phycoerythrin (R-PE, BD Biosciences), and MHC II (HLA-DR) fluorescein isothiocyanate (FITC, BD Biosciences) (Becton Dickinson; Beckman Coulter) (Table 2.1.a). FITC-conjugated isotype-mouse IgG_{a1} and PE-conjugated isotype-mouse IgG_{k1} served as secondary antibodies. 10,000 labeled cells were acquired and analyzed using a FACScan flow cytometer running CellQuest

software (Becton Dickinson) at the flow cytometry facility (Faculty of Medicine and Dentistry, University of Alberta). HUICPV-SCs were suspended and prepared using standard direct staining protocols (19, 20).

Markers	Description
CD90	stem cell marker
CD31	endothelial cell marker
CD34	hematopoietic cells and vascular endothelium marker
CD45	differentiated hematopoietic cell marker
MHCI	recognized during graft rejection and found on all nucleated cells
MHCII	a marker for B-lymphocytes, macrophages and dendritic cells (initiates a primary immune response by activating lymphocytes and secreting cytokines)

Table 2.1a Immunophenotyping markers using flow-cytometry analysis

2.3.6. Quantitative Real-Time PCR Analysis (qPCR)

RNA was isolated and cDNA was synthesized; total RNA was extracted from each triplicate group of both LIPUS treated and sham treated groups using the RNeasy Mini Kit (Qiagen, Mississauga, ON, Canada/Valencia, USA). RNA samples were quantified fluorometrically at 260 nm using SYBRgreen (Molecular Probes, OR, USA) as recommended by the manufacturer. Single stranded DNA (cDNA) was synthesized from 1 µg of total RNA using the Omniscript Reverse Transcription Kit (Qiagen, Mississauga, ON, Canada).

Primers for real-time PCR were designed with Primer Express 2.0 software from Applied Biosystems (ABI) (Foster City, CA). Real-time PCR reactions were performed using TaqMan®Gene Expression Assays (Applied Biosystems AB) and TaqMan®Gene Expression Assays protocol (Applied

Biosystems AB). The TaqMan®MGB probes and primers were premixed to concentrations of 18 µM for each primer and 5 µM for the probe. Amplifications were carried out in a final reaction volume of 10 µl. IDs for gene assays and gene symbols are explained in Table 2.1b; the reaction mixtures were aliquoted into 96 well ABI reaction plates. The plates were placed in an ABI Prism 7500 fast system V 1.4.0 Applied Biosystems qPCR machine under the following conditions: stage 1 consisted of 95°C for 10 min; stage 2 consisted of 40 cycles of 95°C for 15 s, followed by 60°C for 1 min. The qPCR data were analyzed with SDS 7500 Fast system V.2.01 software (ABI).

Gene Name	Gene Symbol	Assay ID
Endogenous control: human glyceraldehyde 3-phosphate dehydrogenase (GAPDH)	GAPDH	4333764F
Osteocalcin (OCN)	BGLAP	Hs00609452_g1
Osteopontin (OPN)	SPP1	Hs00959009_m1
Proliferating cell nuclear antigen (PCNA)	PCNA	Hs99999177_g1
Nucleostemin (NST)	GNL3	Hs00205071_m1

Table 2.1b qPCR genes and gene symbols

2.3.7. Statistical Analysis

Data are presented as mean and standard deviation. MANOVA was applied to all acquired data to compare the expansion capacities of the treated (LIPUS) group and the control (sham) group. A two-way ANOVA was used to analyze the flow-cytometry data and qPCR data. Differences were considered significant at $P < 0.05$. The SPSS software package (version 16.0; SPSS Inc.) was used for the statistical tests.

2.4. Results

The HUCPV-SCs were observed on days 1, 7, and 14 after the application of LIPUS. Spindle-shaped monolayer cells appeared at the bottom of the culture plates. They grew as swirls into fibroblast-like cells. The cell count showed a nonsignificant increase ($P < 0.9$) in the LIPUS treated group compared to the sham treated group (Figure 2.2). The cell count was less in the LIPUS treated group on day 1. However, the overall cell count on days 1, 7, and 14 in the LIPUS treated group was comparable to the sham group with no significant difference. Nonetheless, LIPUS may promote HUCPV-SC proliferation capacity if applied for 2–3 days (21).

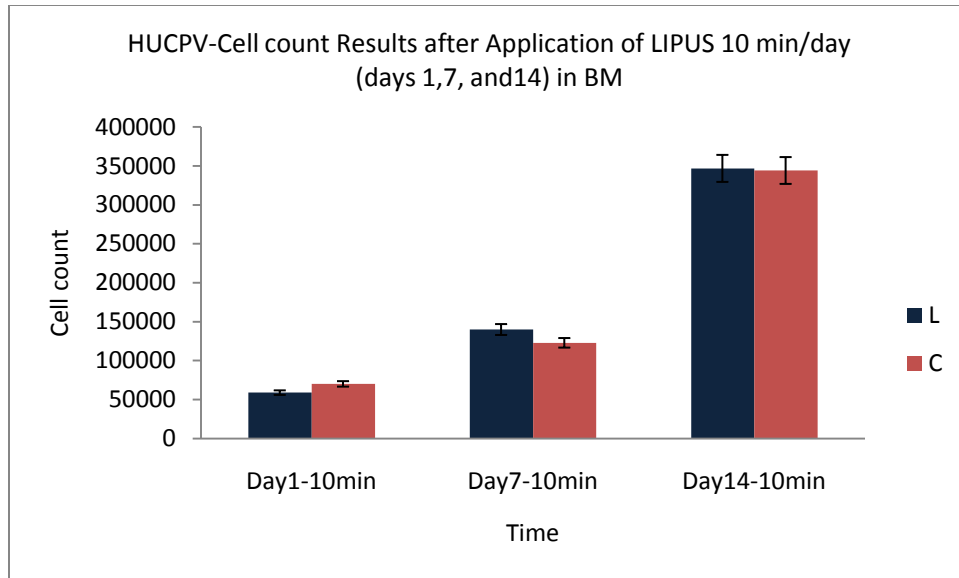


Figure 2.2. HUCPV-cell count results after application of LIPUS 10 min/day (days 1, 7, and 14) in basic media, L = LIPUS, C = Control, BM = basic medium.

The cell proliferation assay exhibited a nonsignificant increase in DNA synthesis when equilized with the ALP level in the LIPUS treated group ($P < 0.9$). The DNA content (Figures 2.3 and 2.5) on day 1 was not significantly different from the control. In addition, we did not detect a significant difference in DNA content between samples treated with LIPUS for 10 minutes per day versus control samples on days 1, 7, and 14. DNA content was quantitatively slightly higher on day 7 in the LIPUS treated group compared to the control group, and on day 14 compared with the sham treated group (see Appendix 1 and Table 2.2).

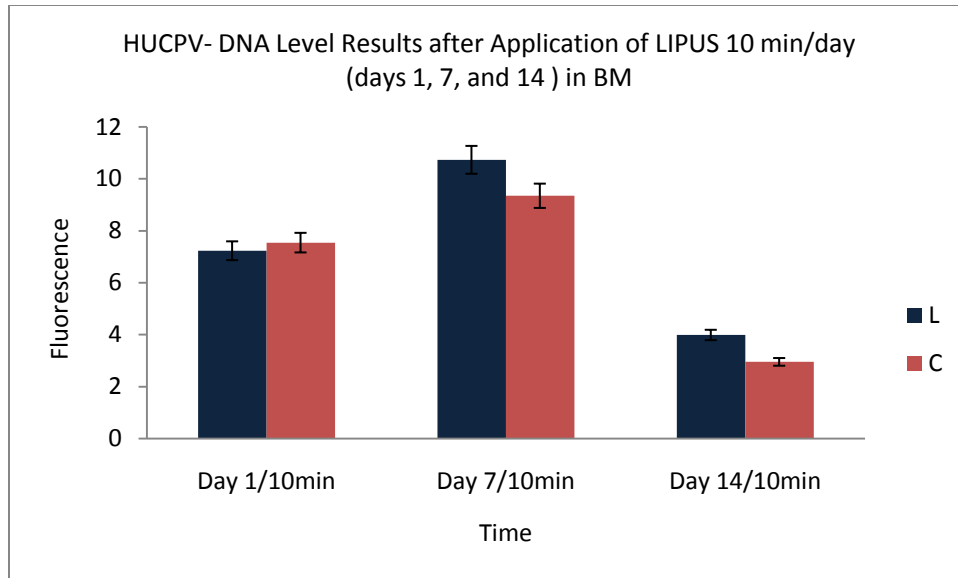


Figure 2.3. HUCPV-DNA level results after application of LIPUS 10 min/day (days 1, 7, and 14) in basic media, L = LIPUS, C = control, BM = basic medium

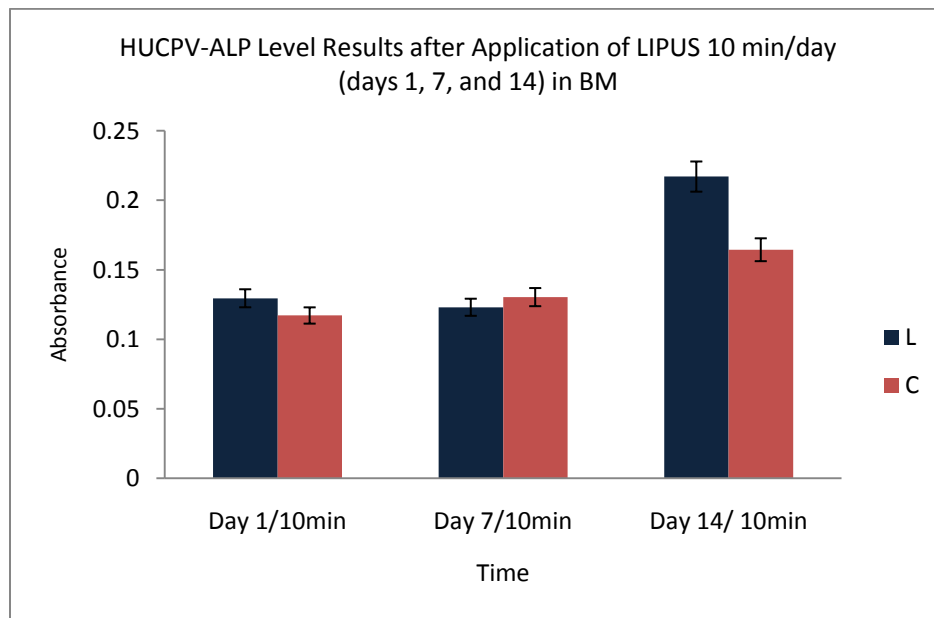


Figure 2.4. HUCPV-ALP level results after application of LIPUS 10 min/day (days 1, 7, and 14) in basic media, L = LIPUS, C = control, BM = basic medium

ALP activity was increased on day 1 in the LIPUS treated group compared to the control group (difference 0.018 ± 0.004). ALP activity, however, was less on day 7 in the LIPUS treated group compared to the sham treated group (difference = 0.012 ± 0.005). ALP activity increased significantly on day 14 in the LIPUS treated group compared to the control group (difference = 0.020 ± 0.010) (Figure 2.5 and Table 2.2).

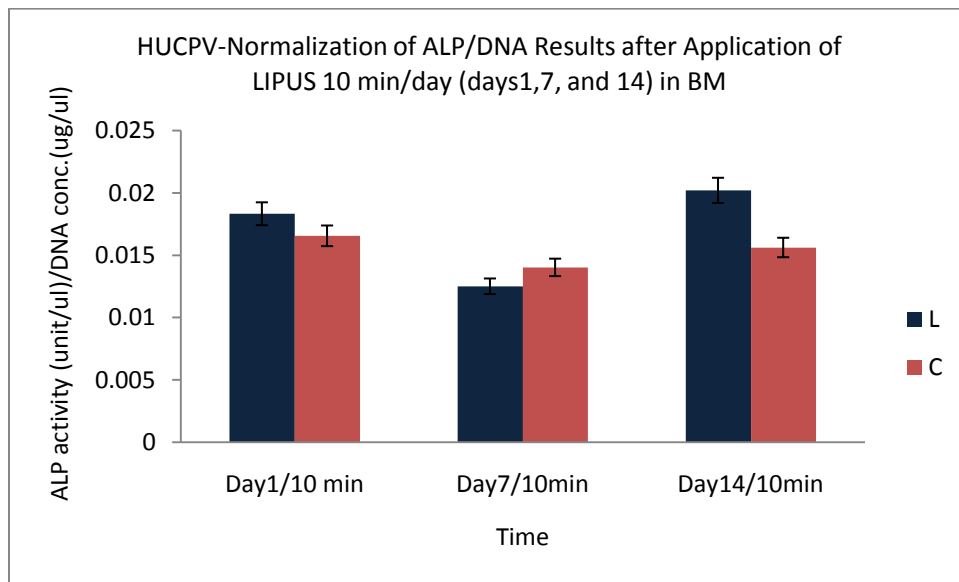


Figure 2.5. HUCPV-normalization of ALP/DNA results after application of LIPUS 10 min/day (days 1, 7, and 14) in basic media, L = LIPUS, C = control, BM = basic medium

Variables/ BM	Day 1			Day 7			Day 14		
	L Mean \pm SD	C Mean \pm SD	P-Value	L Mean \pm SD	C Mean \pm SD	P-Value	L Mean \pm SD	C Mean \pm SD	P-Value
	Cell count	58916.7 \pm 48341.1	70161. 3 \pm 36247. 8	0.9	139986 \pm 63343	122913. 3 \pm 66881.7	0.9	346834 \pm 365337. 8	344140. 7 \pm 257946. 5
DNA	7.2 \pm .96	7.5 \pm 2.2	0.7	10.7 \pm 2.9	9.3 \pm 1.8	0.9	12 \pm 3.9	11 \pm 2.9	0.9
ALP	0.129 \pm 0.016	0.117 \pm 0.012	0.1	0.123 \pm 0.017	0.130 \pm 0.036	0.05	0.217 \pm 0.025	0.164 \pm 0.024	0.05
ALP/ DNA	0.018 \pm 0.004	0.016 \pm 0.005	0.7	0.012 \pm 0.005	0.014 \pm 0.003	0.4	0.020 \pm 0.010	0.015 \pm 0.004	0.4

Table 2.2. Comparison of mean \pm SD of cell count, ALP, DNA, ALP normalized to DNA levels between the LIPUS (L) and control (C) groups on days 1, 7, and 14 in basic media

Immunophenotyping by fluorescent activated cell sorting (FACS) was used to analyze cell surface markers on HUCPV-SCs at passage 4. Cells were gated according to size and expressed surface markers. HUCPV-SCs were negative for CD31 (found on endothelial cells, platelets, macrophages) and MHCII (HLA-DR) (Figures 2.6, 2.7, and 2.8). The marker MHCII is a cell surface antigen that mediates graft-versus-host disease and is responsible for the

rejection of tissue transplants in human leukocyte antigen (HLA) mismatched donors.

HUCPV-SCs were negative for CD34 (a hematopoietic stem cell marker) and CD45 (a leukocyte common antigen). Conversely, they were strongly positive for CD90 (mesenchymal progenitor-specific markers) and moderately positive for MHC I (HLA-A,B,C) (recognized during graft rejection, found in all nucleated cells in the body). LIPUS treated HUCPV-SCs expressed a high level of CD90 on day 14 compared with the sham treated group (Table 2.3).

The data from this experiment may confirm part of our hypothesis that LIPUS has the ability to maintain the stem cell characteristics after one day of treatment. We further investigated this hypothesis by testing the expression of nucleostemin after LIPUS treatment. Nucleostemin was reported as a marker of undifferentiated human mesenchymal stromal stem cells and appeared to be involved in regulation of their proliferation (5, 22). In addition, we studied the expression of the proliferating cell nuclear antigen (PCNA), osteocalcin (OCN), and osteopontin (OPN) after equalizing them to the endogenous control gene GAPDH. HUCPV-SCs expressed significantly higher levels of OPN and PCNA in the LIPUS treated group ($P < 0.01$) on day 14. However, no difference in nucleostemin expression on days 1, 7, and 14 was observed. The level of PCNA was significantly higher in the LIPUS treated group ($P < 0.01$) on day 14. This is supported by the findings of Yoon et al. (2009) and may further validate our hypothesis that the LIPUS can increase PCNA (the proliferation gene of HUCPV-SCs) while maintaining their stem cell characteristics after 14 days of treatment (21).

We also examined the effects of LIPUS on levels of OPN and OCN expression in HUCPV-SCs. The results showed that the level of OCN was almost 0.25 fold higher in the LIPUS treated group than in the control group on days 1 and 14, but was 0.25 fold less on day 7. We further investigated the difference in OSP expression. OSP expression was 1.25 fold higher in the LIPUS treated group on day 14 ($P < 0.01$) and 0.25 fold higher on day 1, but was comparable to the control group on day 7 (Figures 2.9, 2.10, 2.11, and Table 2.4).

Markers / BM	Day 1			Day 7			Day 14		
	L	C	P-	L	C	P-	L	C	P-
	Mean	Mean	Value	Mean	Mean	Value	Mean	Mean	Value
	± SD	± SD		± SD	± SD		± SD	± SD	
Isotype IgG	3 ± 0.9	8.3 ± 4	0.2	27.3 ± 9.7	25.4 ± 8.1	0.8	9.9 ± 2.5	6.5 ± 2.9	0.8
CD31	16.3 ± 8.8	19.8 ± 13.5	0.8	41.6 ± 12.5	38.9 ± 10.9	0.2	13.7 ± 1.7	8.9 ± 1.3	0.2
CD90	2211.9 ± 1644.4	3204 ± 689.6	0.3	3896.9 ± 953.6	4394.2 ± 2033.9	0.4	1383.2 ± 1403.9	534.8± 471.3	0.4
CD34	12.8 ± 5.7	22.5± 20.6	0.5	45 ± 20.8	47.3 ± 30.2	0.8	10.8 ± 2.1	6.8 ± 2.9	0.8
CD45	25.9 ± 27.9	14.5±7	0.8	67.6 ± 61.3	43.7 ± 24.7	0.6	11.5 ± 1.3	6.9 ± 2.7	0.6
MHCI	346.2 ± 59.2	241.5 ± 38.9	0.07	217.9 ± 69.1	219.9 ± 7.5	0.8	44.9 ± 6.9	35.1 ± 5.8	0.8
MHCII	13.9 ± 4.6	22.8 ± 19.8	0.4	41.1 ± 13.6	46 ± 27.5	0.6	14.3 ± 3.7	8.5 ± 1.2	0.6

Table 2.3 . Mean ± SD of flow-cytometry results of HUcPV-SC (isotype IgG, CD31, CD90, CD34, CD45, MHC I, and MHC II) treated with LIPUS 10 min/day on days 1, 7, and 14: difference between LIPUS (L) and control (C) in basic media

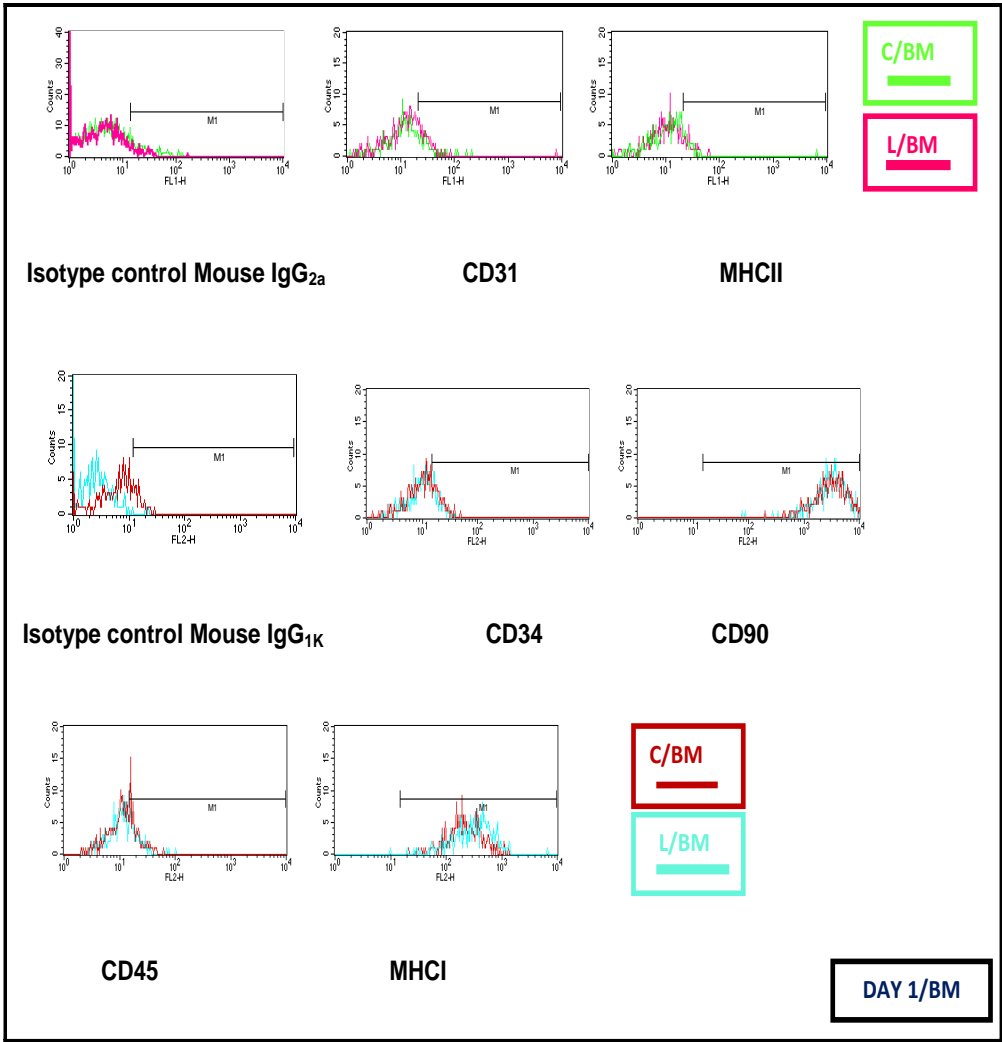


Figure 2.6a. Flow cytometry analysis results on day 1 represented by histogram, LIPUS (L), control(C), basic media (BM)

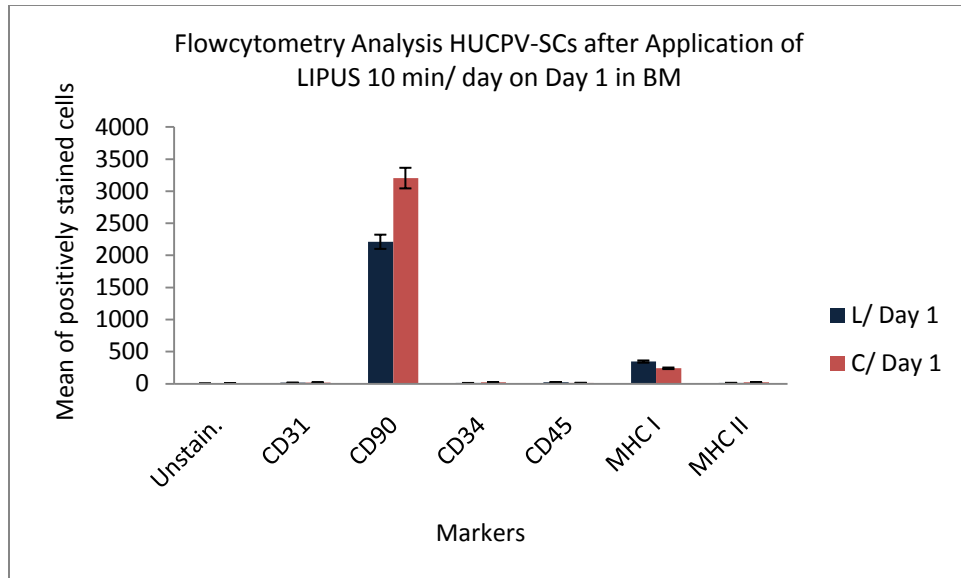


Figure 2.6b. Flow cytometry analysis results on day 1 represented by charts, LIPUS (L), control (C), basic media (BM)

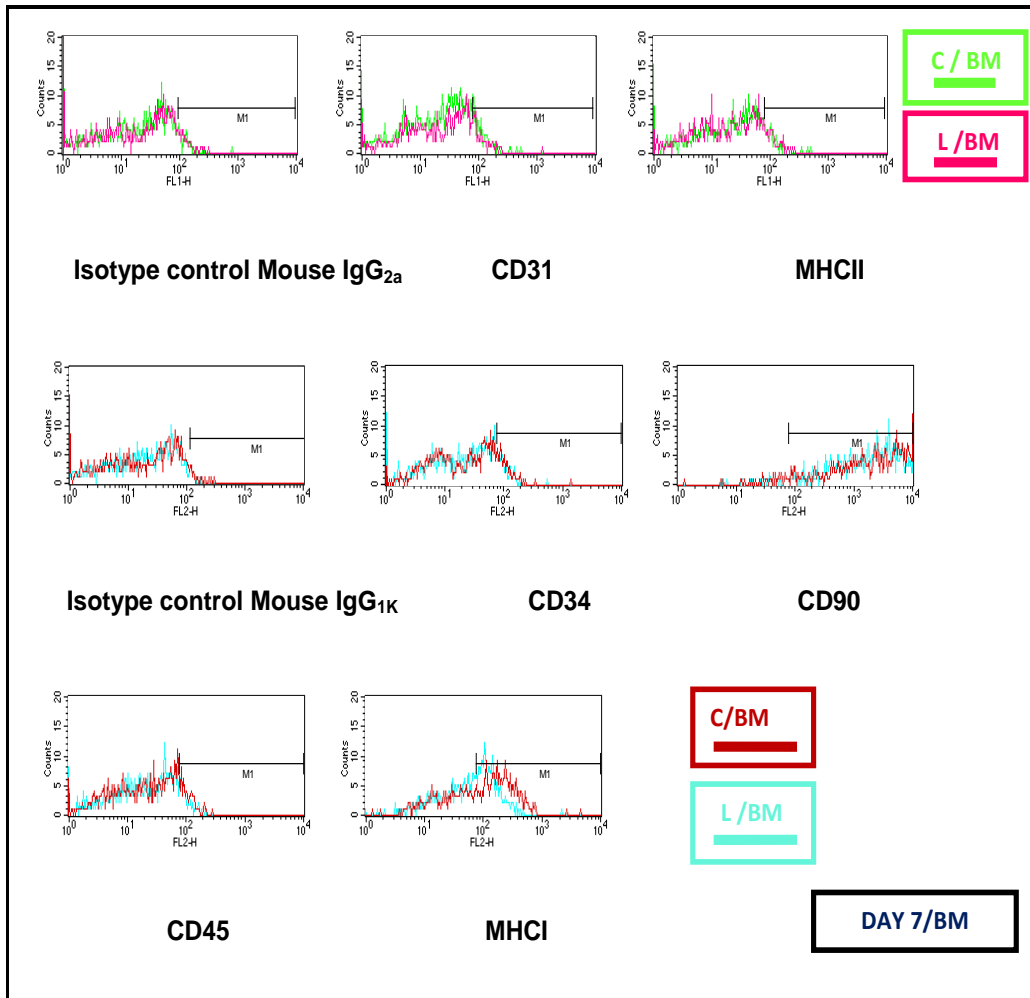


Figure 2.7a. Flow cytometry analysis results on day 7 represented by histogram, LIPUS (L), control (C), basic media (BM)

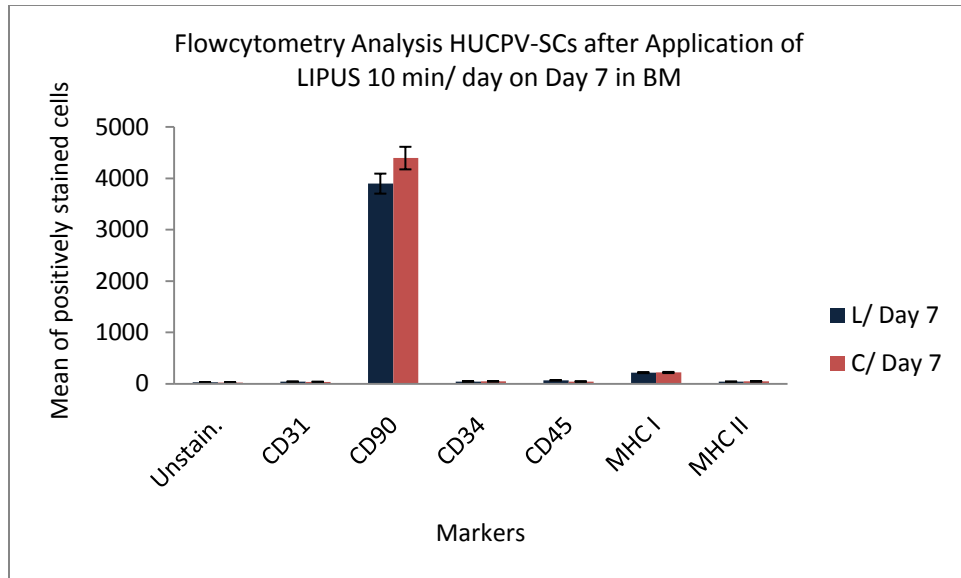


Figure 2.7b. Flow cytometry analysis results on day 7 represented by charts, LIPUS (L), control (C), basic media (BM)

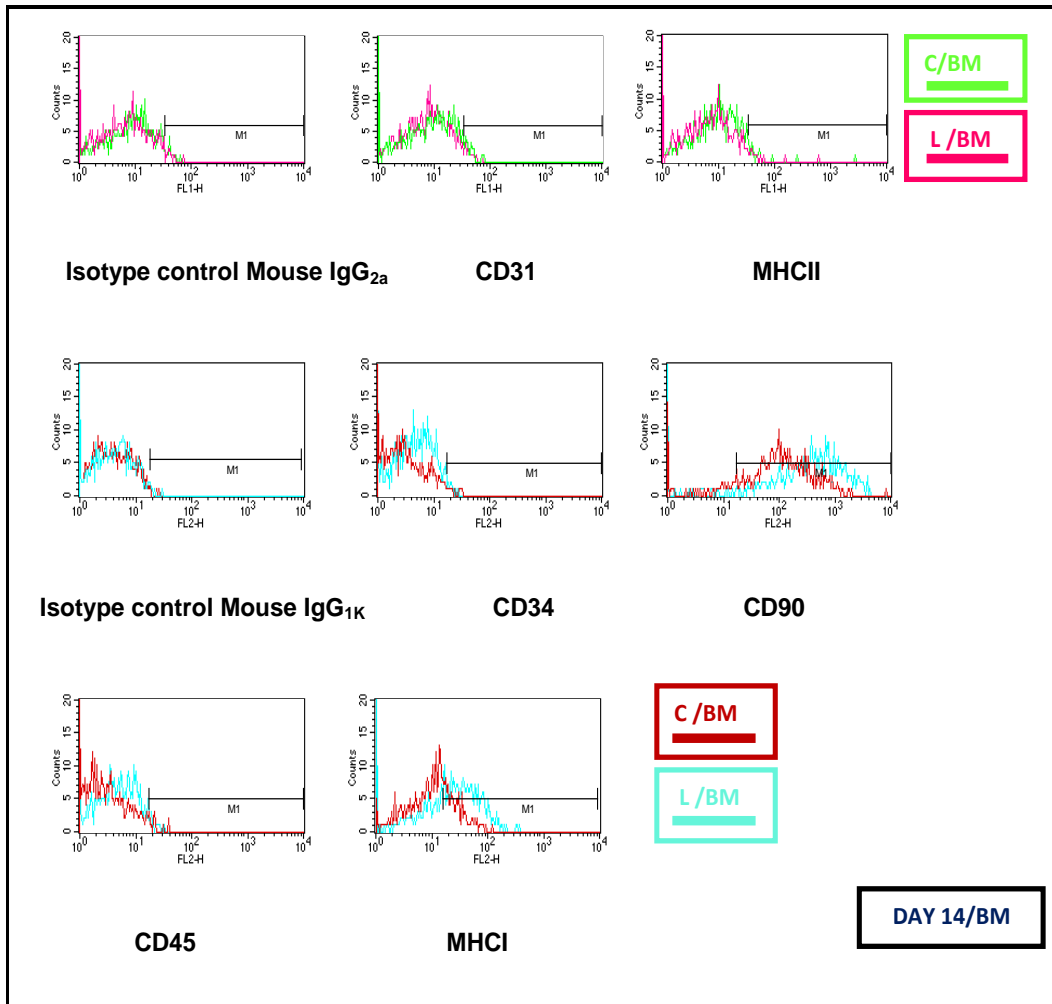


Figure 2.8a. Flow cytometry analysis results on day 14 represented by histogram, LIPUS (L), control (C), basic media (BM)

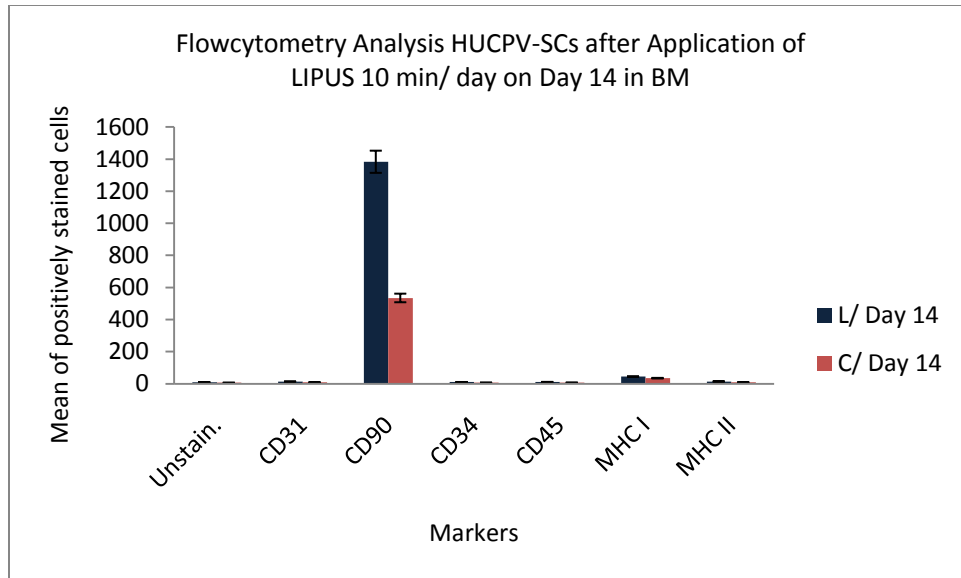


Figure 2.8b. Flow cytometry analysis results on day 14 represented by charts, LIPUS (L), control (C), basic media (BM)

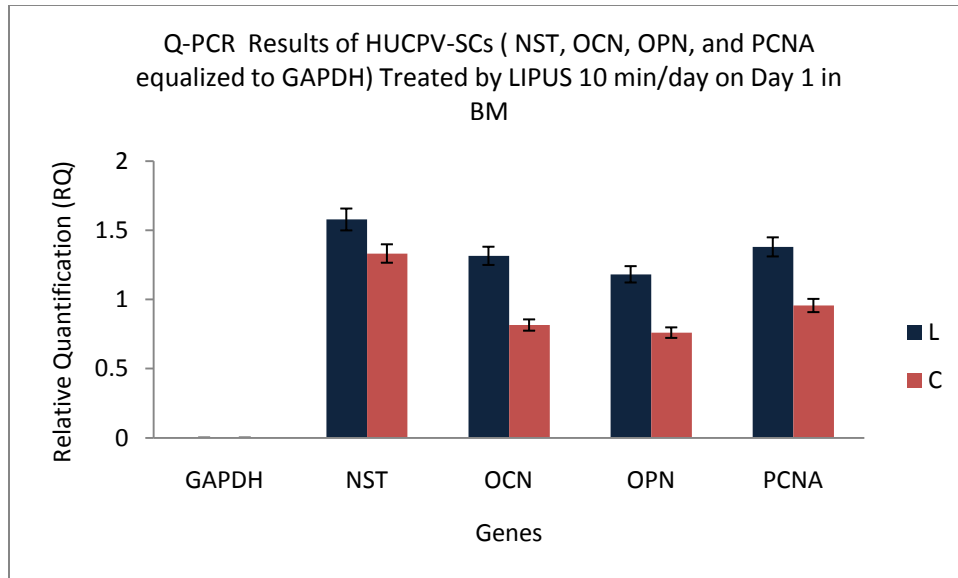


Figure 2.9. qPCR results on day 1 that compare levels of nucleostemin, osteocalcin, osteopontin, and PCNA after their equalization to the endogenous control gene (GAPDH) between LIPUS (L) and control (C) in basic media

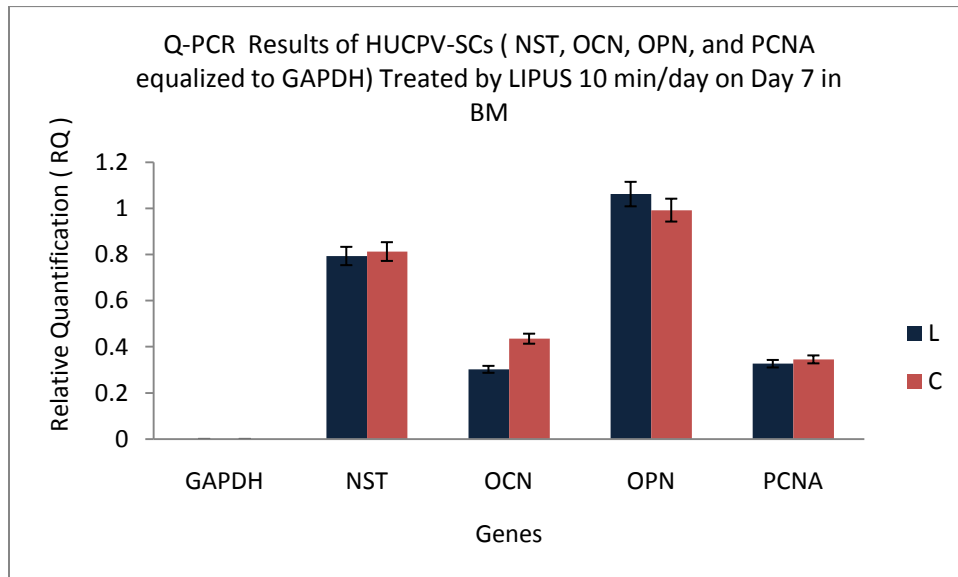


Figure 2.10. qPCR results on day 7 that compare levels of nucleostemin, osteocalcin, osteopontin, and PCNA after their equalization to the endogenous control gene (GAPDH) between LIPUS (L) and control (C) in basic media

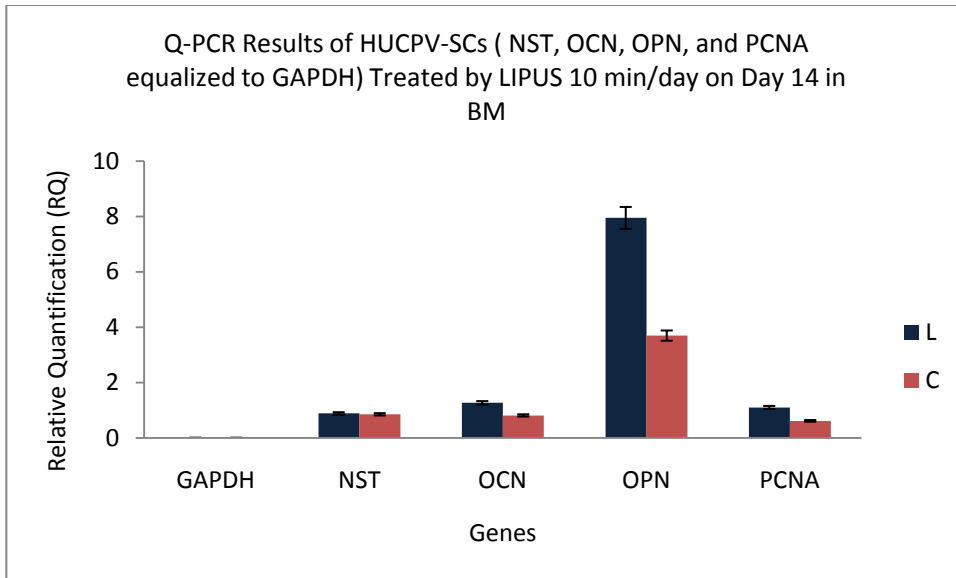


Figure 2.11. qPCR results on day 14 that compare levels of nucleostemin, osteocalcin, osteopontin, and PCNA after their equalization to the endogenous control gene (GAPDH) between LIPUS (L) and control (C) in basic media

Genes / B M	Day 1			Day 7			Day 14		
	L Mean ± SD	C Mean ± SD	P- Value	L Mean ± SD	C Mean ± SD	P- Value	L Mean ± SD	C Mean ± SD	P- Value
GAPDH	.00 ± .00	.00 ± .00	0.03	.00 ± .00	.00 ± .00	0.9	.00 ± .00	.00± .00	0.7
NST	1.58 ± .44	1.33 ± .32	0.4	.79 ± .03	.81 ± .15	0.9	.88 ± .16	.85± .16	0.7
OCN	1.32 ± .27	.82 ± .33	0.7	.30 ± .04	.43 ± .11	0.3	1.26 ± .29	.81± .22	0.9
OPN	1.18 ± .37	.76 ± .21	0.9	1.06 ± .12	.99 ± .48	0.5	7.95 ± 6.20	3.69± 2.26	0.01
PCNA	1.38 ± .24	.96 ± .28	0.9	.33 ± .09	.35 ± .17	0.5	1.09 ± .49	.61± .29	0.01

Table 2.4 qPCR comparison of mean ± SD of nucleostemin, osteocalcin, osteopontin, and PCNA after their equalization to the endogenous control gene (GAPDH) between LIPUS (L) and control (C) on days 1, 7, and 14 in basic media

2.5. Discussion

In this study, we investigated the effects of LIPUS on the characteristics and proliferation capacity of HUCPV-SCs. The 10 minute LIPUS application was based on a previous study by Zhou et al. (2004) (23) that showed that LIPUS exerted its optimum stimulatory effect on skin fibroblasts when applied at 10 minutes per day for 7 days. Our results showed that LIPUS did not significantly increase HUCPV-SC cell counts after 10 minute daily applications on days 1, 7, and 14. This is in disagreement with previous studies that showed that LIPUS had a stimulatory effect on a variety of cell lines such as osteoblasts, chondrocytes, and marrow-derived stromal cells (24, 25, 26).

Conversely, other studies demonstrated that continuous mechanical stress may decrease cellular activities as reflected by DNA content, ALP levels, and calcium content (27). Others reported that persistent mechanical stress reduced the activation of mechanosensitive cation channels in osteoblast-like cells (28). Parvizi et al. (1999) did not detect any effects of LIPUS on the expression of transforming growth factor- β , osteocalcin, ALP, or α (I)-procollagen genes in cultured osteoblasts (29). They noted that cell proliferation is not stimulated by ultrasound at 4, 6, or 8 days at intensities of 20 and 50 mW/cm².

LIPUS cavitation is the pulsation of gas or vapor-filled voids in a sound field that results in compression of microtubules (29). This potentially changes the permeability of cell membranes and calcium channels (29). Some of these findings were confirmed in our study where no significant differences in cell count, DNA content, or ALP levels existed between the LIPUS treated group and the control, except that there was increased ALP on day 14 in the LIPUS treated

group. These data indicate that the potential stimulatory effect of LIPUS on these cells may occur at and beyond 14 days.

Some increase in the expression of CD90, PCNA, and OPN was detected in the LIPUS treated group compared to the sham treated group on day 14. PCNA, OCN, and OPN increased 0.25 fold and nucleostemin (NST) increased 0.2 fold on day 1. The increments in the expression of these genes may relate to enhancement of intracellular metabolic activities by LIPUS. The rise in PCNA ($P < 0.01$) was not associated with a measurable increase in cell count in the LIPUS treated group, probably due to the short time of LIPUS treatment in our study. Experiments with longer duration of LIPUS application may further our understanding of the biological behaviors of HUCPV-SCs.

The LIPUS induced increase in ALP, OPN, and OCN on day 14 may indicate that LIPUS may have an anabolic effect on HUCPV-SCs. This agrees with a previous report that LIPUS enhanced osteogenic differentiation of human gingival fibroblasts (37). The increased NST expression induced by LIPUS may signify that LIPUS maintains the stem cell characteristics of HUCPV-SC stimulated cells. Supportive studies suggested that application of LIPUS on different types of cells could result in nonsignificant differences in cell proliferation (25, 30–36) and differentiation (21, 25, 36). Our findings were consistent with literature reports of MSCs (31–33) and chondrocytes (25, 33, 34, 36) that postulated that the mechanical stress of LIPUS may direct cell efforts toward maintenance rather than proliferation and differentiation.

2.6. Conclusion

The optimum application of LIPUS has not been unequivocally established. Our study suggests that LIPUS may induce HUCPV-SC proliferation while maintaining the phenotypic stem cell characteristics of these cells. This may prove true if we could apply an alternative methodology of LIPUS treatment. Furthermore, our findings signify that a short duration of LIPUS treatment may not enhance HUCPV-SCs sufficiently to overcome the conventional limitations of bone marrow mesenchymal stromal progenitor cells. In addition, our experiments suggest that direct contact of LIPUS transducers within the media may enhance the expansion and proliferation of HUCPV-SCs as assessed using various biological markers. Future investigations are required to test the effect of LIPUS on the differentiation capacity of HUCPV-SCs into multiple lineages, including osteogenic and neurogenic differentiation capability.

2.7. References

- (1) Karahuseyinoglu S, Cinar O, Kilic E, Kara F, Akay GG, Demiralp DO, et al. Biology of stem cells in human umbilical cord stroma: in situ and in vitro surveys. *Stem Cells* 2007 Feb;25(2):319-331.
- (2) Kestendjieva S, Kyurkchiev D, Tsvetkova G, Mehandjiev T, Dimitrov A, Nikolov A, et al. Characterization of mesenchymal stem cells isolated from the human umbilical cord. *Cell Biol. Int.* 2008 Jul;32(7):724-732.
- (3) Baksh D, Yao R, Tuan RS. Comparison of proliferative and multilineage differentiation potential of human mesenchymal stem cells derived from umbilical cord and bone marrow. *Stem Cells* 2007 Jun;25(6):1384-1392.
- (4) Sarugaser R, Lickorish D, Baksh D, Hosseini MM, Davies JE. Human umbilical cord perivascular (HUCPV) cells: a source of mesenchymal progenitors. *Stem Cells* 2005 Feb;23(2):220-229.
- (5) Qiao C, Xu W, Zhu W, Hu J, Qian H, Yin Q, et al. Human mesenchymal stem cells isolated from the umbilical cord. *Cell Biol. Int.* 2008 Jan;32(1):8-15.
- (6) Bieback K, Kern S, Kluter H, Eichler H. Critical parameters for the isolation of mesenchymal stem cells from umbilical cord blood. *Stem Cells* 2004;22(4):625-634.
- (7) Duarte LR. The stimulation of bone growth by ultrasound. *Arch. Orthop. Trauma. Surg.* 1983;101(3):153-159.
- (8) Childs SG. Stimulators of bone healing. Biologic and biomechanical. *Orthopaedic Nursing* 2003 Nov-Dec;22(6):421-428.
- (9) Doan N, Reher P, Meghji S, Harris M. In vitro effects of therapeutic ultrasound on cell proliferation, protein synthesis, and cytokine production by human

fibroblasts, osteoblasts, and monocytes. *J. Oral Maxillofac. Surg.* 1999 discussion 420; Apr;57(4):409-419.

(10) Ryaby JT. Clinical effects of electromagnetic and electric fields on fracture healing. *Clin. Orthop.* 1998 Oct(355 Suppl):S205-15.

(11) Webster DF, Harvey W, Dyson M, Pond JB. The role of ultrasound-induced cavitation in the 'in vitro' stimulation of collagen synthesis in human fibroblasts. *Ultrasonics* 1980 Jan;18(1):33-37.

(12) Wang N, Butler JP, Ingber DE. Mechanotransduction across the cell surface and through the cytoskeleton. *Science* 1993 May 21;260(5111):1124-1127.

(13) Qin L, Fok P, Lu H, Shi S, Leng Y, Leung K. Low intensity pulsed ultrasound increases the matrix hardness of the healing tissues at bone-tendon insertion—a partial patellectomy model in rabbits. *Clin. Biomech.* 2006;21(4):387-394.

(14) Min BH, Woo JI, Cho HS, Choi BH, Park SJ, Choi MJ, et al. Effects of low-intensity ultrasound (LIUS) stimulation on human cartilage explants. *Scand. J. Rheumatol.* 2006 Jul-Aug;35(4):305-311.

(15) Korstjens CM, Nolte PA, Burger EH, Albers GH, Semeins CM, Aartman IH, et al. Stimulation of bone cell differentiation by low-intensity ultrasound—a histomorphometric in vitro study. *J. Orthop. Res.* 2004 May;22(3):495-500.

(16) Leung KS, Cheung WH, Zhang C, Lee KM, Lo HK. Low intensity pulsed ultrasound stimulates osteogenic activity of human periosteal cells. *Clin. Orthop.* 2004 Jan(418):253-259.

(17) Martini L, Giavaresi G, Fini M, Torricelli P, de Pretto M, Schaden W, et al. Effect of extracorporeal shock wave therapy on osteoblastlike cells. *Clin. Orthop.* 2003 Aug(413):269-280.

- (18) Owen TA, Aronow M, Shalhoub V, Barone LM, Wilming L, Tassinari MS, et al. Progressive development of the rat osteoblast phenotype in vitro: reciprocal relationships in expression of genes associated with osteoblast proliferation and differentiation during formation of the bone extracellular matrix. *J. Cell. Physiol.* 1990 Jun;143(3):420-430.
- (19) Holmes K, Lantz LM, Fowlkes BJ, Schmid I, Giorgi JV. Preparation of cells and reagents for flow cytometry. *Curr. Protoc. Immunol.* 2001 Nov;Chapter 5:Unit 5.3.
- (20) Malley A, Stewart CC, Stewart SJ, Waldbeser L, Bradley LM, Shiigi SM. Flow cytometric analysis of I-J expression on murine bone marrow-derived macrophages. *J. Leukoc. Biol.* 1988 Jun;43(6):557-565.
- (21) Yoon JH, Roh EY, Shin S, Jung NH, Song EY, Lee DS, et al. Introducing pulsed low-intensity ultrasound to culturing human umbilical cord-derived mesenchymal stem cells. *Biotechnol. Lett.* 2009 Mar;31(3):329-335.
- (22) Kafienah W, Mistry S, Williams C, Hollander AP. Nucleostemin is a marker of proliferating stromal stem cells in adult human bone marrow. *Stem Cells* 2006 Apr;24(4):1113-1120.
- (23) Zhou S, Schmelz A, Seufferlein T, Li Y, Zhao J, Bachem MG. Molecular mechanisms of low intensity pulsed ultrasound in human skin fibroblasts. *J. Biol. Chem.* 2004 Dec 24;279(52):54463-54469.
- (24) Sun JS, Hong RC, Chang WH, Chen LT, Lin FH, Liu HC. In vitro effects of low-intensity ultrasound stimulation on the bone cells. *J. Biomed. Mater. Res.* 2001 Dec 5;57(3):449-456.

- (25) Zhang ZJ, Huckle J, Francomano CA, Spencer RG. The effects of pulsed low-intensity ultrasound on chondrocyte viability, proliferation, gene expression, and matrix production. *Ultrasound Med. Biol.* 2003 Nov;29(11):1645-1651.
- (26) Naruse K, Mikuni-Takagaki Y, Azuma Y, Ito M, Oota T, Kameyama K, et al. Anabolic response of mouse bone-marrow-derived stromal cell clone ST2 cells to low-intensity pulsed ultrasound. *Biochem. Biophys. Res. Commun.* 2000 Feb 5;268(1):216-220.
- (27) Winter LC, Walboomers XF, Bumgardner JD, Jansen JA. Intermittent versus continuous stretching effects on osteoblast-like cells in vitro. *J. Biomed. Mater. Res. A.* 2003 Dec 15;67(4):1269-1275.
- (28) Duncan RL, Hruska KA. Chronic, intermittent loading alters mechanosensitive channel characteristics in osteoblast-like cells. *Am. J. Physiol.* 1994 Dec;267(6 Pt 2):F909-16.
- (29) Parvizi J, Wu CC, Lewallen DG, Greenleaf JF, Bolander ME. Low-intensity ultrasound stimulates proteoglycan synthesis in rat chondrocytes by increasing aggrecan gene expression. *J. Orthop. Res.* 1999 Jul;17(4):488-494.
- (30) Inubushi T, Tanaka E, Rego EB, Kitagawa M, Kawazoe A, Ohta A, et al. Effects of ultrasound on the proliferation and differentiation of cementoblast lineage cells. *J. Periodontol.* 2008 Oct;79(10):1984-1990.
- (31) Angele P, Schumann D, Angele M, Kinner B, Englert C, Hente R, et al. Cyclic, mechanical compression enhances chondrogenesis of mesenchymal progenitor cells in tissue engineering scaffolds. *Biorheology* 2004;41(3-4):335-346.

- (32) Ebisawa K, Hata K, Okada K, Kimata K, Ueda M, Torii S, et al. Ultrasound enhances transforming growth factor beta-mediated chondrocyte differentiation of human mesenchymal stem cells. *Tissue Eng.* 2004 May-Jun;10(5-6):921-929.
- (33) Schumann D, Kujat R, Zellner J, Angele MK, Nerlich M, Mayr E, et al. Treatment of human mesenchymal stem cells with pulsed low intensity ultrasound enhances the chondrogenic phenotype in vitro. *Biorheology* 2006;43(3-4):431-443.
- (34) Torzilli PA, Grigiene R, Huang C, Friedman SM, Doty SB, Boskey AL, et al. Characterization of cartilage metabolic response to static and dynamic stress using a mechanical explant test system. *J. Biomech.* 1997 Jan;30(1):1-9.
- (35) Toyoda T, Seedhom BB, Kirkham J, Bonass WA. Upregulation of aggrecan and type II collagen mRNA expression in bovine chondrocytes by the application of hydrostatic pressure. *Biorheology* 2003;40(1-3):79-85.
- (36) Park SR, Choi BH, Min BH. Low-intensity ultrasound (LIUS) as an innovative tool for chondrogenesis of mesenchymal stem cells (MSCs). *Organog.* 2007 Oct;3(2):74-78.
- (37) Mostafa NZ, Uludag H, Dederich, DN, Doschak MR, El-Bialy TH. Anabolic effects of low intensity pulsed ultrasound on gingival fibroblasts. *Archives of Oral Biology* (in press).

CHAPTER 3

Differentiation of HUCPV-SCs in Osteogenic Media Using LIPUS

3.1. Key Words: LIPUS (low intensity pulse ultrasound), stem cells, human umbilical cord perivascular stem cells (HUCPV-SCs), osteogenic differentiation (OST).

3.2. Introduction

The capacity for self renewal and the capacity for multilineage differentiation are intrinsic features of mesenchymal stem cells (MSCs) that allow them to evolve into mesodermal, ectodermal, and endodermal cells (1, 2). The limited accessibility for bone marrow stem cells and the effect of the donor's age have narrowed the widespread use of bone marrow specimens for progenitor stem cells (6). The harvest of bone marrow is a highly invasive procedure and the number, differentiation potential, and maximal life span of MSCs from bone marrow decline with increasing age. Therefore, alternative sources from which to isolate MSCs are subject to intensive investigation (9). Umbilical cord blood has been increasingly used as an alternative source for hematopoietic stem cells (HSC) for allogenic stem cell transplants (3–7). However, the lack of common standards for initial cell preparation remains an obstacle for standardization of research methodology and the clinical application of MSCs (8).

MSCs (stromal cells) have been isolated from both human umbilical cord blood and bone marrow preparations (10, 11). "Mesenchymal stem cells derived from the umbilical cord vein are functionally similar to bone marrow MSCs" (12). Isolation of umbilical cord MSCs is less invasive than bone marrow derivations,

and because of the fetal origin of MSCs, their proliferative and differentiation potential could be better than that of MSCs from other sources (12). In a comparative study, Baksh et al. (2007) documented that human umbilical cord perivascular stem cells (HUCPV-SCs) have higher capacity to differentiate and to proliferate than bone marrow MSCs (13). In addition, HUCPV-SCs were shown to have a faster rate of osteogenic differentiation compared to bone marrow MSCs (13). Cells with MSC characteristics can be harvested from multiple organs and tissues including brain, heart, spleen, liver, kidney, lung, bone marrow, muscle, thymus, and pancreas (14). Umbilical cord sources provide a pool of cells of vast abundance, and with the advantage of less donor site morbidity.

Umbilical cord MSCs during the neonatal stage are less mature than MSCs from the adult stage and do not possess a potent immune rejection in unrelated donor transplantation (15). An umbilical cord blood graft can tolerate 1–2 mismatches between unmatched human leukocyte antigen (HLA) subtypes, which significantly expands the available donor pool (15). Human umbilical cord stromal cells have the character of mesenchymal stem cell lineages (16,17). Wang et al. (2004) induced the differentiation of umbilical cord stromal cells into mesenchymal cell lineages; osteogenic, adipogenic, cardiomyogenic, and chondrogenic types have been accomplished (16, 18). In addition, Sarugaser et al. (2005) demonstrated techniques for harvesting and culturing HUCPV-SCs and their achieved osteogenic nodules, and described their differentiation behavior (18). In general, the blood that remains inside the human umbilical cord is usually considered a valid source of hematopoietic stem cells (19, 20). Current clinical applications of mesenchymal progenitor stem cells (MPCs), including treatment of osteogenesis imperfecta, demonstrated impressive histologic changes of

trabecular bones with new dense bone formation (21). The stromal cell population in bone marrow has shown a capacity for expansion and differentiation into various phenotypic cellular lineages such as bone, cartilage, muscle, stroma, neural, and fat cells (22).

Heckman (1994), Kristiansen (1997), Mayr (2000), Nolte (2001), Leung (2004), Tsumaki (2004), Gebauer (2005), Gold (2005), Ricardo (2006), and Schmelz (2006) (23-32) confirmed that LIPUS enhances bone remodelling and bone formation and decreases healing time significantly. Mechanical stresses have been reported to enhance activities of osteoclasts and osteoblasts leading to increases bone remodeling and bone regeneration, respectively (33). Different forms of mechanical stress such as LIPUS have been clinically tested for their ability to enhance new bone formation (34).

Acceleration of fracture healing by LIPUS was attributed to the recurrent pressure waves that trigger a complex series of biochemical and molecular events at the cellular level (35). An increase in alkaline phosphatase (ALP) activity was detected in human osteoblast cultures after continuous exposure to the low intensity pressure waves of LIPUS (36).

This experimental study investigated whether LIPUS has a stimulatory effect on osteogenic differentiated HUCPV-SCs that can potentially increase the differentiation capacity of these stem cells during certain periods of time. We studied the effect of LIPUS in vitro on cultured HUCPV-SCs. The influence of LIPUS was assessed using different methods including cell count, ALP assay, DNA assay, real-time PCR, and immunophenotyping of cells derived from HUCPV-SCs by flow-cytometry analysis.

3.3. Materials and Methods

3.3.1. Cell Culture

Ethical approval was obtained from the Health Research Ethics Board, University of Alberta, Edmonton, Canada (approval number 6431, 2006). After obtaining patient consent, HUCPV-SCs were obtained from patients undergoing full-term caesarean sections. Cells were isolated according to methods described by Sarugaser et al. (2005) and were generously provided by Dr. J. E. Davies (University of Toronto, Ontario, Canada) (18). HUCPV cells at passage 1 were thawed and seeded into three T-75 cm² tissue culture flasks (Sigma Aldrich). Cell culture osteogenic media contained Dulbecco's modified Eagle's medium with low glucose (DMEM-LG) (GIBCO, Invitrogen) supplemented with 15% fetal bovine serum (FBS), 1% antibiotic-antimycotic (Sigma Aldrich), 10⁻⁸ M dexamethasone (Sigma Aldrich), 5 mM β-glycerophosphate (Sigma Aldrich), and 50 μg/ml L-ascorbic acid (Sigma Aldrich) (18). Initial cell density used was 3.6 × 10⁶/ml. Cells were incubated at 37°C in 5% CO₂. HUCPV cells were expanded for 10 days until P4 and media was changed every 2–3 days. When their confluence reached 80% (4.2 × 10⁶/ml), cells were harvested and trypsinized using 0.25% trypsin (GIBCO, Invitrogen), collected in 50 ml tubes, centrifuged, then plated into nine 6 well plates (Sigma Aldrich) at 2 × 10⁴/ml. As shown in Figure 3.1, 27 wells were treated for 10 min/day by 4 "Exogen LIPUS" devices with 4 transducers placed immediately below the wells and coupled to the well bases with standard ultrasound coupling gel transducers previously calibrated. The ultrasound frequency, intensity, and duration were identical to that used in the clinic for bone fracture repair (Exogen Bone Healing System, Smith and Nephew, Memphis, TN, USA). Each produces a 1.5 Mhz ultrasound wave composed of a 200 μs burst

with an output intensity of 30 mW/cm² for 1 day, 7 days, and 14 days. The other 27 wells were sham treated using the same transducers without turning the machines on. Each group was evaluated at each time point (see Figure A2.8 in the Appendix 2).

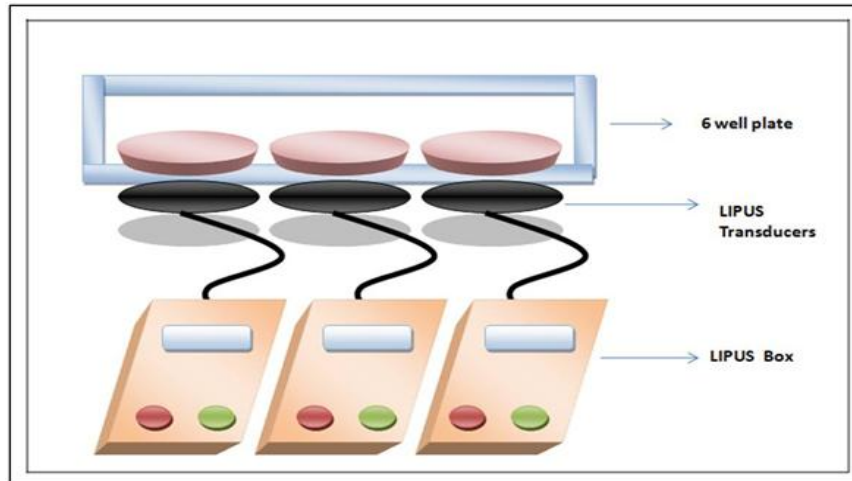


Figure 3.1 Schematic diagram shows experimental LIPUS application

3.3.2. Cell Count

Cells were washed using PBS (GIBCO, Invitrogen) then trypsinized, Cells were watched for de-attachment under the microscope. Basic medium was added to stop the trypsin reaction. Cells and medium were collected in 15 ml tubes for centrifugation (6 min at 600 rpm). The supernatant was vacuumed away. Cells were counted using a Beckman Coulter counter (Faculty of Dentistry, University of Alberta, Canada).

3.3.3. Alkaline Phosphatase (ALP) Activity Assay

ALP activity of HUCPV-SCs was determined by a colorimetric assay at the indicated time points (on days 1,7 and 14) (37). ALP is a biochemical marker for cell differentiation of osteogenic lineage (38, 39). Cells were washed with PBS and lysed with 2 ml of ALP buffer/well (0.5 M 2-amino-2-methyl-1-propanol and 0.1% Triton X-100, pH 10.5). Two hours later, after lysis, 1 ml of lysed cells was taken for an ALP activity assay. Phosphatase substrate (p-nitrophenyl phosphate) (Sigma) was added to the ALP buffer in a 1 mg/ml (1:1) ratio. 100 µl of lysed cells and 100 µl of substrate mixture were loaded to each well of a 96 well plate to a final concentration of 1 mg/ml. The changes in optical density (absorbance, 405 nm) were determined in a multiwell plate reader at periodic intervals 5, 10, 15, 30 minutes.

3.3.4. Cell Proliferation and DNA Quantification Assay

1 ml of the lysed cell solution was used to measure the amount of DNA with the CyQUANT Cell Proliferation Kit (Molecular Probe, Invitrogen). The CyQUANT cell proliferation kit assay measures the quantity of DNA through the enhancement of fluorescence of a dye when it is bound to nucleic acids (Molecular Probe, Invitrogen). Lysed cells were incubated with the dye for 30–60 minutes, then fluorescence was measured in a microplate reader. The assay is designed to produce a linear analytical response in a 96-well microplate (Molecular Probe, Invitrogen). DNA standard provided with the CyQUANT kit was utilized to determine the DNA concentrations in each group of cells. According to the manufacturer's instructions, DNA was quantified using a fluorescence plate reader (excitation at 480 nm; emission at 527 nm).

3.3.5. Immunophenotyping Using Flow-Cytometry Analysis

Further characterization of expanded HUCPV-SCs at passage 4 using cell surface antigen phenotyping was performed on days 1, 7, and 14. The following cell-surface epitopes were labeled with antihuman antibodies: CD31(PECAM-1) fluorescein isothiocyanate (FITC, BD Biosciences), CD34-R-phycoerythrin (R-PE, BD Biosciences), CD45-phycoerythrin (PE, BD Biosciences), CD90 (Thy1) R-phycoerythrin (R-PE, BD Biosciences), MHC I (HLA-A,B,C) R- phycoerythrin (R-PE, BD Biosciences), and MHCII (HLA-DR) fluorescein isothiocyanate (FITC, BD Biosciences) (Becton Dickinson; Beckman Coulter), FITC (fluorescein isothiocyanate)-conjugated isotype-mouse IgG_{a1} and PE-conjugated isotype-mouse IgG_{k1} served as secondary antibodies (Table 3.1a). 10,000 labelled cells were acquired and analyzed using a FACScan (fluorescence activated cell sorting) flow cytometer running CellQuest software (Becton Dickinson) at the flow cytometry facility (Faculty of Medicine and Dentistry, University of Alberta). HUCPV-SCs were suspended and prepared using standard direct staining protocols (40, 41).

Markers	Description
CD90	stem cell marker
CD31	endothelial cell marker
CD34	hematopoietic cells and vascular endothelium marker
CD45	differentiated hematopoietic cell marker
MHC I	recognized during graft rejection and found on all nucleated cells
MHCII	a marker for B-lymphocytes, macrophages and dendritic cells (initiates a primary immune response by activating lymphocytes and secreting cytokines)

Table 3.1a. Immunophenotyping markers using flow-cytometry analysis

3.3.6. Quantitative Real-Time PCR Analysis (qPCR)

RNA was isolated and cDNA was synthesized. Total RNA was extracted from each triplicate group of both LIPUS treated and sham treated groups using the RNeasy Mini Kit (Qiagen, Mississauga, ON, Canada/Valencia, USA). RNA samples were quantified fluorometrically at 260 nm using SYBRgreen (Molecular Probes, OR, USA) as recommended by the manufacturer. Single stranded DNA (cDNA) was synthesized from 1 µg of total RNA using the Omniscript Reverse Transcription Kit (Qiagen, Mississauga, ON, Canada).

Primers for real-time PCR were designed with Primer Express 2.0 software from Applied Biosystems (ABI) (Foster City, CA). Real-time PCR reactions were performed using TaqMan®Gene Expression Assays (Applied Biosystems AB) and TaqMan®Gene Expression Assays protocol (Applied Biosystems AB). The TaqMan®MGB probes and primers had been premixed to concentrations of 18 µM for each primer and 5 µM for the probe. Amplifications were carried out in a final reaction volume of 10 µl. IDs for gene assays and gene symbols are listed in Table 3.1b; the reaction mixtures were aliquoted into 96 well ABI reaction plates. The plates were treated in an ABI Prism 7500 fast system V

1.4.0 Applied Biosystems qPCR machine under the following conditions: stage 1 consisted of 95°C for 10 min; stage 2 consisted of 40 cycles of 95°C for 15 s, followed by 60°C for 1 min. The qPCR data were analyzed with SDS 7500 Fast system V.2.01 software (ABI).

Gene Name	Gene Symbol	Assay ID
Endogenous control human glyceraldehyde 3 – phosphate dehydrogenase (GAPDH)	GAPDH	4333764F
Osteocalcin (OCN)	BGLAP	Hs00609452_g1
Osteopontin (OPN)	SPP1	Hs00959009_m1
Proliferating cell nuclear antigen (PCNA)	PCNA	Hs99999177_g1
Nucleostemin (NST)	GNL3	Hs00205071_m1

Table 3.1b. qPCR genes and gene symbols

3.3.7. Statistical Analysis

Data are presented as mean \pm standard deviation. MANOVA was applied to all acquired data to compare the expansion and the proliferation capacities of the treated (LIPUS) group and the control (sham) group. A two-way ANOVA was used to analyze the flow cytometry data. Differences were considered significant at $P < 0.05$. The SPSS software package (version 16.0; SPSS Inc., Chicago, USA) was used for the statistical tests.

3.4. Results

The HUCPV-SCs were observed on days 1, 7, and 14 after application of LIPUS and sham treatments. The cell count in the LIPUS treated group was nonsignificantly reduced on days 1 and 14 despite an increase noted on day 7 that was also statistically nonsignificant (Figure 3.2 and Table 3.2).

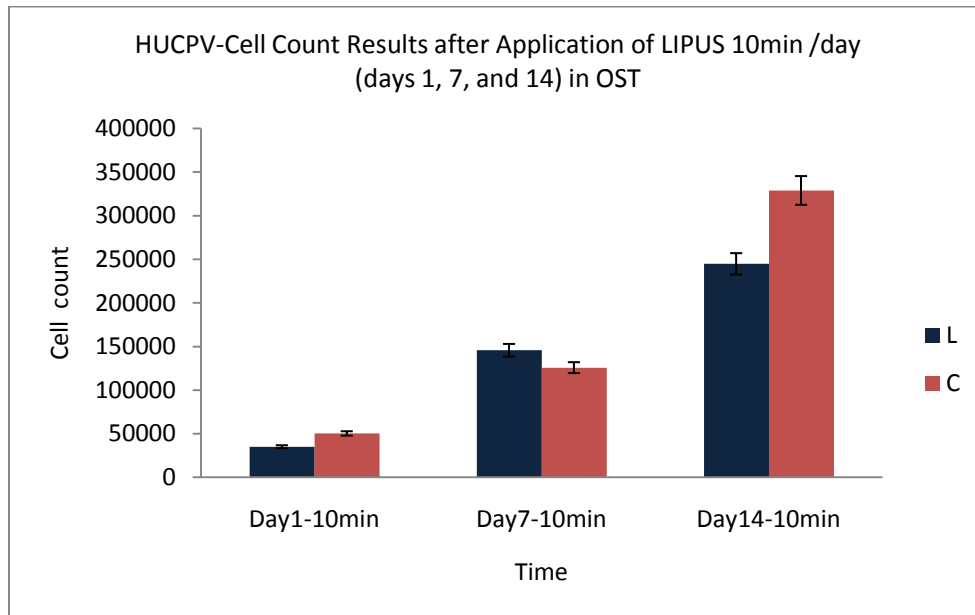


Figure 3.2. HUCPV-cell count results after application of LIPUS 10 min/day (days 1, 7, and 14) in OST, L = LIPUS, C = control, OST = osteogenic media

The cell proliferation assay as reflected by DNA content did not change after equalization with ALP level in the LIPUS treated group ($P < 0.9$). The DNA content in the LIPUS treated group was nonsignificantly lower on day 1 ($P < 0.7$). During osteogenic differentiation, no significant differences in DNA content could be detected between samples treated with LIPUS for 10 minutes per day and the untreated sham group (Figures 3.3 and 3.4; Table 3.2). DNA content was 0.5 fold higher on day 7 in the LIPUS treated group (0.018 ± 0.003), whereas it was lower on day 14 in the LIPUS treated group (0.015 ± 0.006) compared with the sham group (Table 3.2).

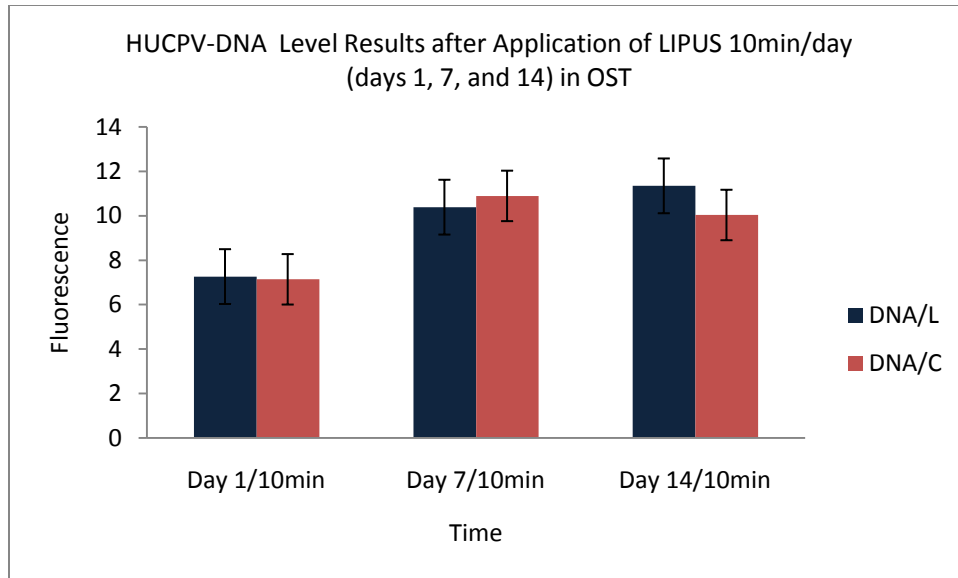


Figure 3.3. HUCPV-DNA level results after application of LIPUS 10 min/day (days 1, 7, and 14) in OST, L = LIPUS, C = control, OST = osteogenic media

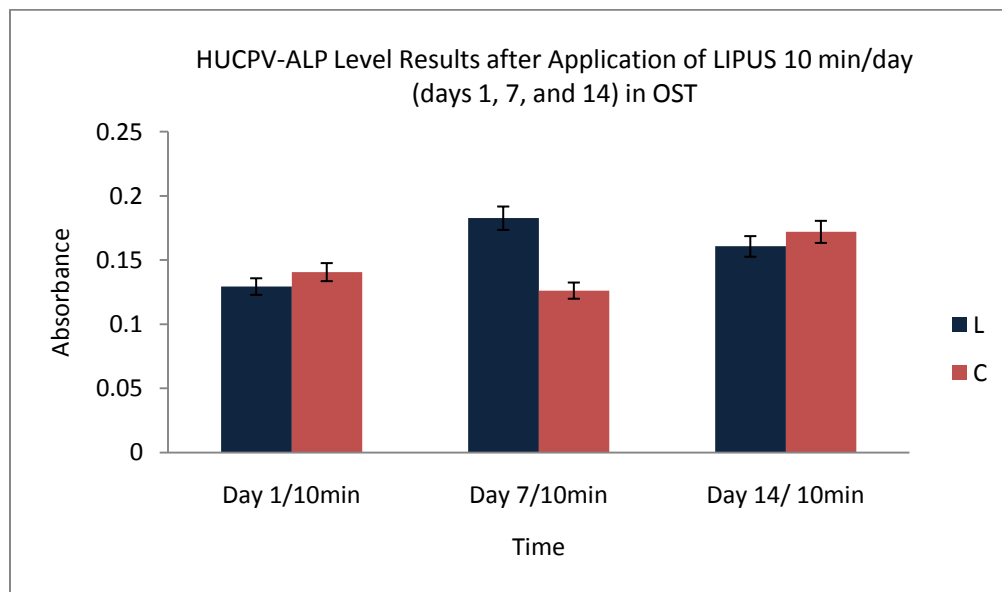


Figure 3.4. HUCPV-ALP level results after application of LIPUS 10 min/day (days 1, 7, and 14) in OST, L = LIPUS, C = control, OST = osteogenic media

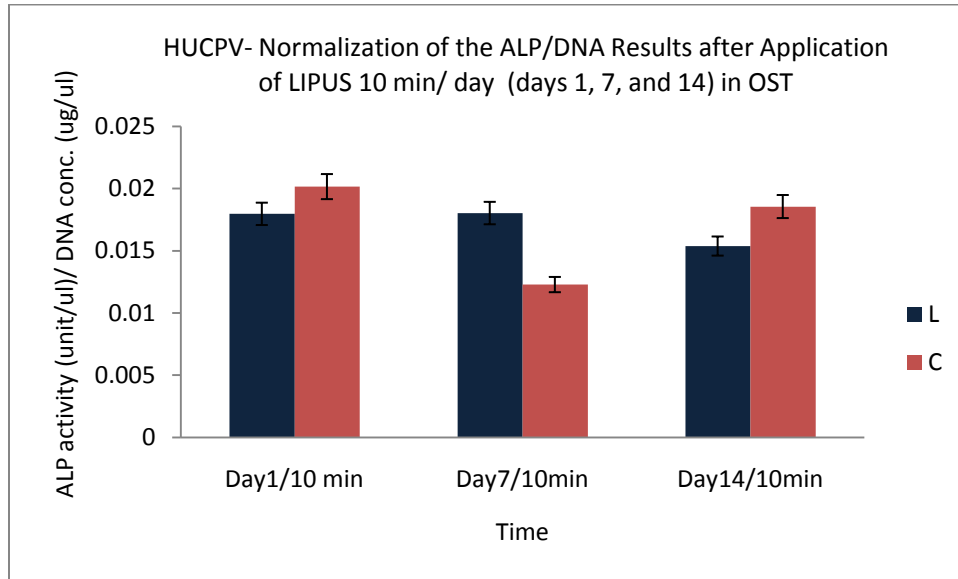


Figure 3.5. HUCPV-normalization of ALP/DNA results after application of LIPUS 10 min/day (days 1, 7, and 14) in OST, L = LIPUS, C = control, OST = osteogenic media

HUCPV-SCs expressed a nonsignificant increase of ALP activity in the LIPUS treated group compared to the sham group ($P < 0.9$). ALP activity was slightly reduced on day 1 (0.018 ± 0.006), higher on day 7 (0.018 ± 0.003), and slightly lower on day 14 (0.015 ± 0.006) in the LIPUS treated group compared to the control (Figure 3.5, Table 3.2).

Variables / OST	Day 1			Day 7			Day 14		
	L Mean ± SD	C Mean ± SD	P-Value	L Mean± SD	C Mean ± SD	P-Value	L Mean ± SD	C Mean ± SD	P-Value
Cell count	35013. 3± 15617. 3	50298. 0 ± 30519. 4	0.7	145642. 0 ± 23730.5	125711. 3 ± 10938.5	0.6	244756. 7± 177275. 6	328923. 3± 305838. 9	0.6
DNA	7.3 ± 0.9	7.1 ± 1.4	0.7	10.4 ± 3.7	10.9 ± 3.2	0.6	11.3 ± 3.6	10 ± 2.7	0.6
ALP	0.129± 0.043	0.140± 0.03	0.9	0.183 ± 0.051	0.126 ± 0.011	0.08	0.161 ± 0.012	0.172 ± 0.021	0.08
ALP/DNA	0.018± 0.006	0.020± 0.005	0.9	0.018 ± 0.003	0.012 ± 0.004	0.2	0.015 ± 0.006	0.019 ± 0.006	0.2

Table 3.2. Comparing mean ± SD of cell count, ALP, DNA, ALP normalized to DNA levels between the LIPUS (L) and control (C) on days 1, 7, and 14 in OST

Immunophenotyping (FACS) was performed to analyze cell surface markers on HUCPV-SCs at passage 4. Cells were gated according to size and expressed surface markers. HUCPV-SCs were negative for CD31 (found on endothelial cells, platelets, macrophages) and MHCII [HLA-DR] (Figures 3.6, 3.7, and 3.8). MHCII antigens are cell surface markers involved in graft-versus-host disease and the rejection of tissue transplants in HLA mismatched donors.

HUCPV-SCs were also negative for CD34 (a hematopoietic stem cell marker) and CD45 (leukocyte common antigen). Conversely, HUCPV-SCs were strongly positive for CD90 (a mesenchymal progenitor-specific marker) and moderately positive for MHC I [HLA-A,B,C] (recognized during graft rejection, found in all nucleated cells). HUCPV-SCs in the LIPUS treated group expressed a high level of CD90 on day 14 compared with control (Table 3.3).

We further investigated our original hypothesis, that LIPUS-expanded HUCPV-SCs will maintain their osteogenic differentiation potential, by assessing the expression of nucleostemin, PCNA, OCN, and OPN after equalization to the endogenous control gene GAPDH. Nucleostemin is a marker of undifferentiated human mesenchymal stromal stem cells and is involved in regulation of MSC proliferation (42). HUCPV-SCs expressed lower levels of nucleostemin in the LIPUS treated group on days 1 and 7 compared to the control, with a nonsignificant higher expression on day 14 (Table 3.4). Alternatively, the level of PCNA was significantly higher in the LIPUS treated group on day 14 ($P < 0.001$).

The levels of OCN expression were approximately 0.2 fold lower in the LIPUS treated group on day 1, 1.5 fold higher on day 7, and 0.5 fold higher on day 14. These responses were, however, statistically nonsignificant. The level of OPN was 1 fold higher on day 14 ($P < 0.001$), whereas it was 0.2 fold lower on day 1 and almost comparable to the control group on day 7. These findings suggest that LIPUS treatment for 10 min/day may enhance osteogenic differentiation of HUCPV-SCs on day 14 and beyond (Figures 3.9, 3.10, and 3.11; Tables 3.4) (see Appendix 2 Figure A2.9).

Markers / OST	Day 1			Day 7			Day 14		
	L	C	P- Value	L	C	P- Value	L	C	P- Value
	Mean ± SD	Mean ± SD		Mean ± SD	Mean ± SD		Mean ± SD	Mean ± SD	
Isotype	9.3±	8.4±2.	0.5	18.5±	16.7±	0.6	10.1±	4.5±2	0.6
IgG	2.9	5		4.6	9.3		9.6	.5	
CD31	11.6±	14±1.	0.3	19±2.	22±14.	0.3	14.1±	7.3±2	0.3
	3.4	8		5	4		8.2	.2	
CD90	2766.7	2854.	0.7	1731.	1601.1	0.9	516.7±	370.7	0.9
	±	5±		3±	±		292.5	±	
	156.9	549.4		732.9	771.5			162.5	
CD34	11.5±	9.4±	0.9	21.6±	19.8±	0.9	7±4.9	4.6±1	0.9
	6.2	1.5		10.9	12.4			.6	
CD45	9.5±3.	19.4±	0.3	24.4±	30.5±	0.9	7.6±5.	4.5±1	0.9
	6	15.1		14.6	30		4	.1	
MHC I	211.5±	294.5	0.7	170.3	155.9±	0.9	43.6±	42.7±	0.9
	66.5	±		±	157.7		24.8	22.7	
		177.6		164.7					
MHC II	40.1±	34.4±	0.7	26.5±	21.9±	0.8	13.9±7	14.9±	0.8
	25.5	27.2		3.4	16.2			8.7	

Table 3.3 . Mean ± SD of flow-cytometry results of HUcPV-SC (isotype IgG, CD31, CD90, CD34, CD45, MHC I, and MHC II) treated with LIPUS 10 min/day on days 1, 7, and 14 between LIPUS (L) and control (C) in OST

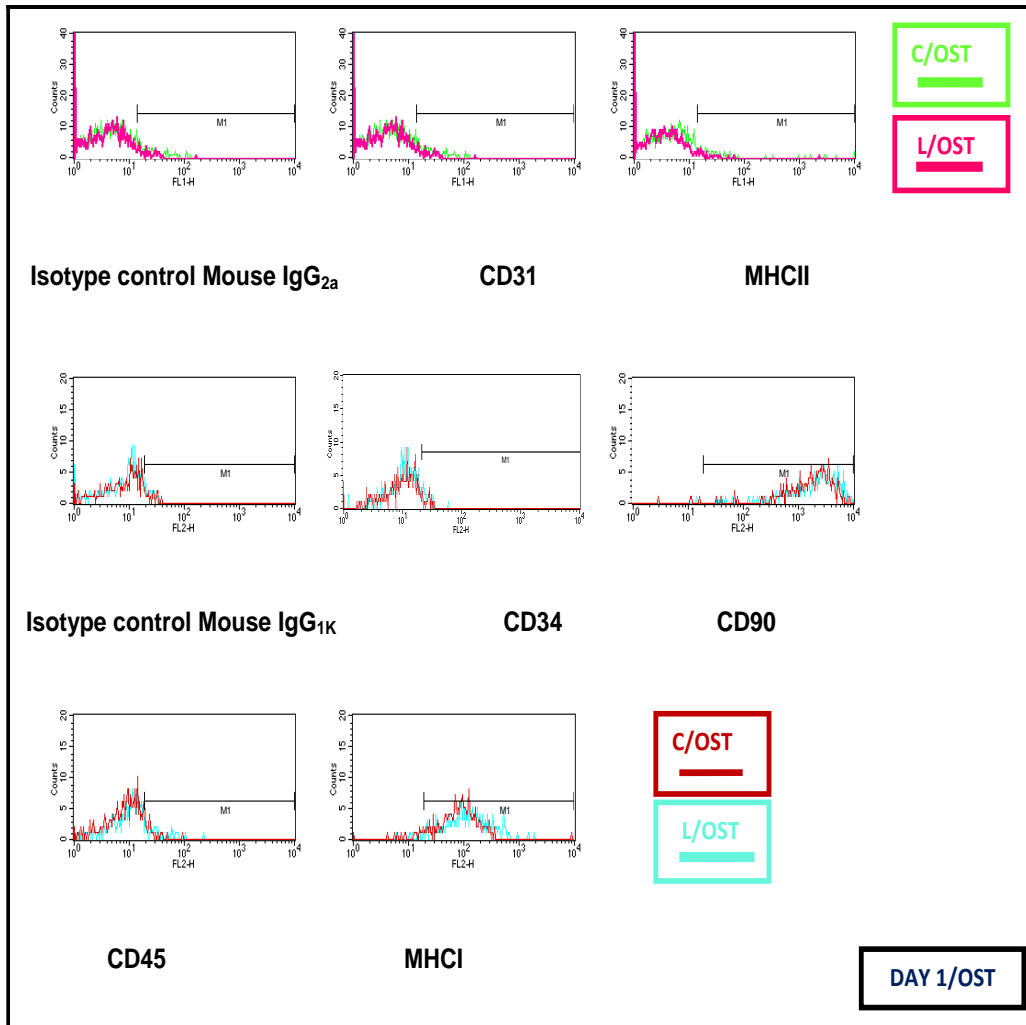


Figure 3.6a. Flow cytometry analysis results on day 1 represented by histogram, LIPUS(L), control (C), osteogenic media (OST)

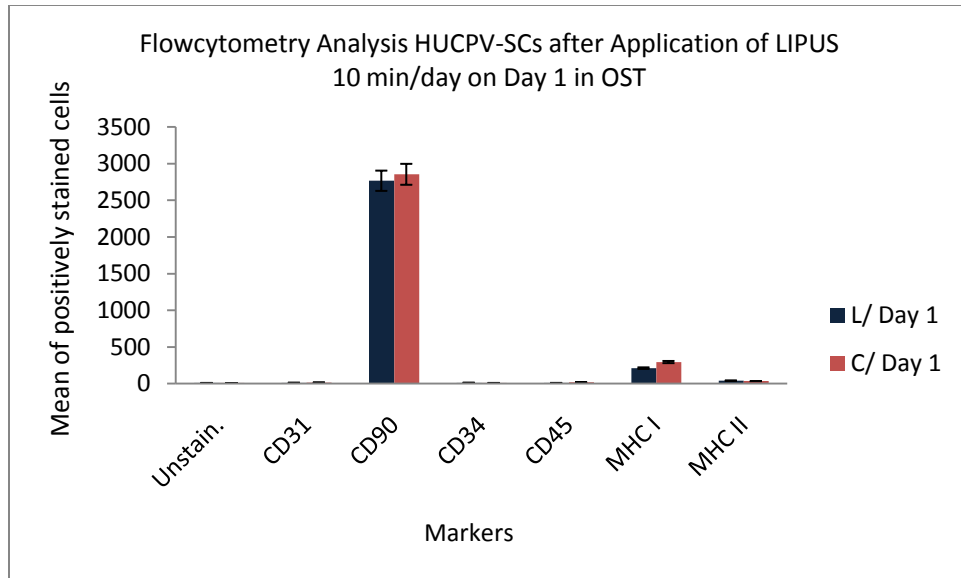


Figure 3.6b. Flow cytometry analysis results on day 1 represented by charts, LIPUS(L), control (C), osteogenic media (OST)

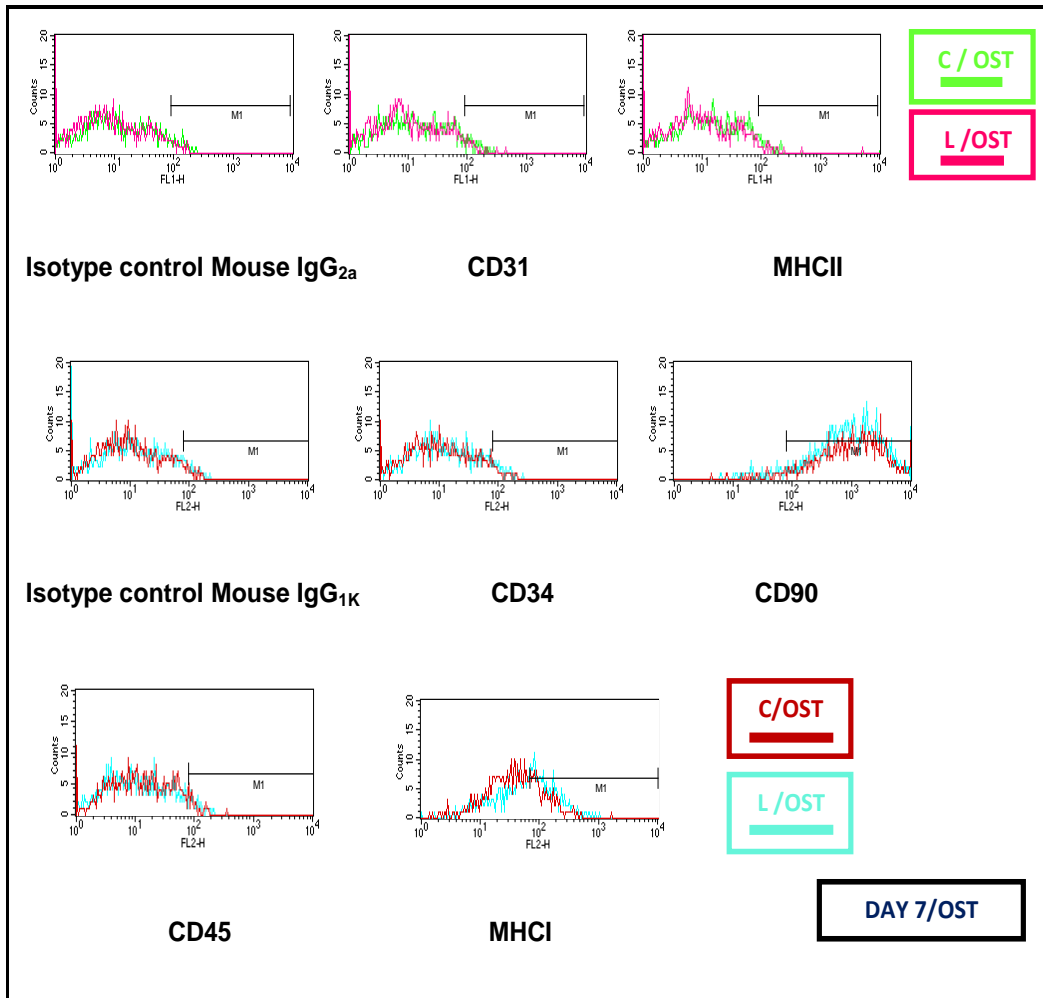


Figure 3.7a. Flow cytometry analysis results on day 7 represented by histogram, LIPUS (L), control (C), osteogenic media (OST)

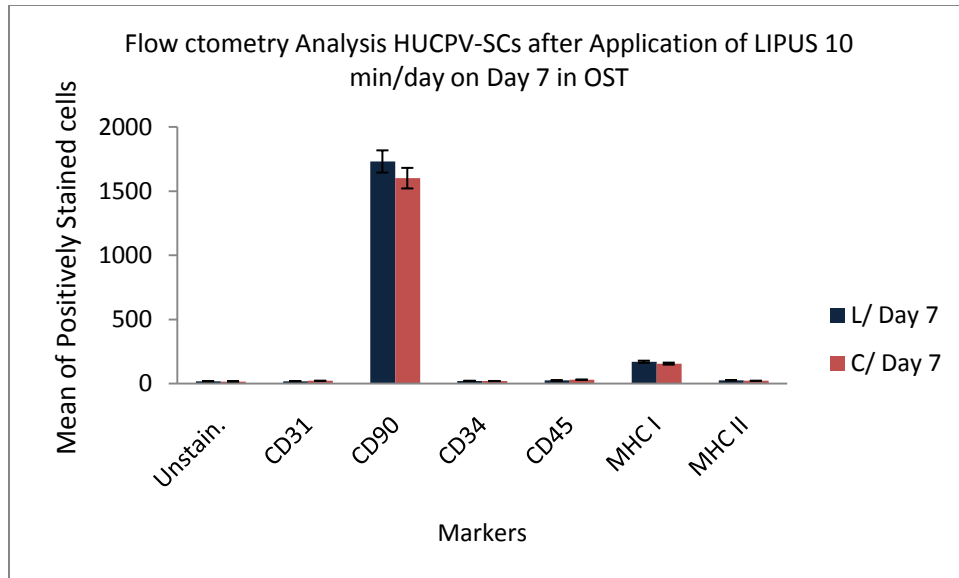


Figure 3.7b. Flow cytometry analysis results on day 7 represented by charts, LIPUS (L), control (C), osteogenic media (OST)

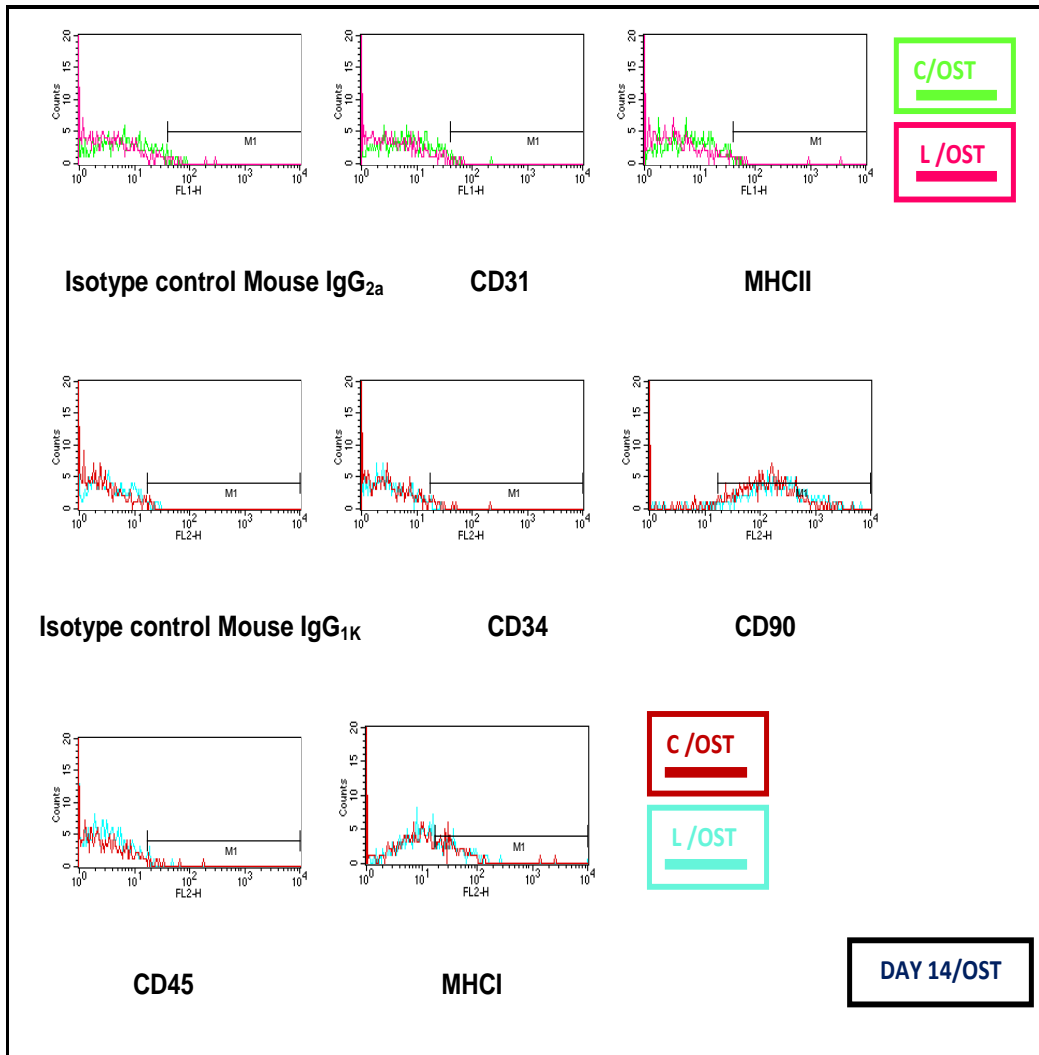


Figure 3.8a. Flow cytometry analysis results on day 14 represented by histogram, LIPUS (L), control (C), osteogenic media (OST)

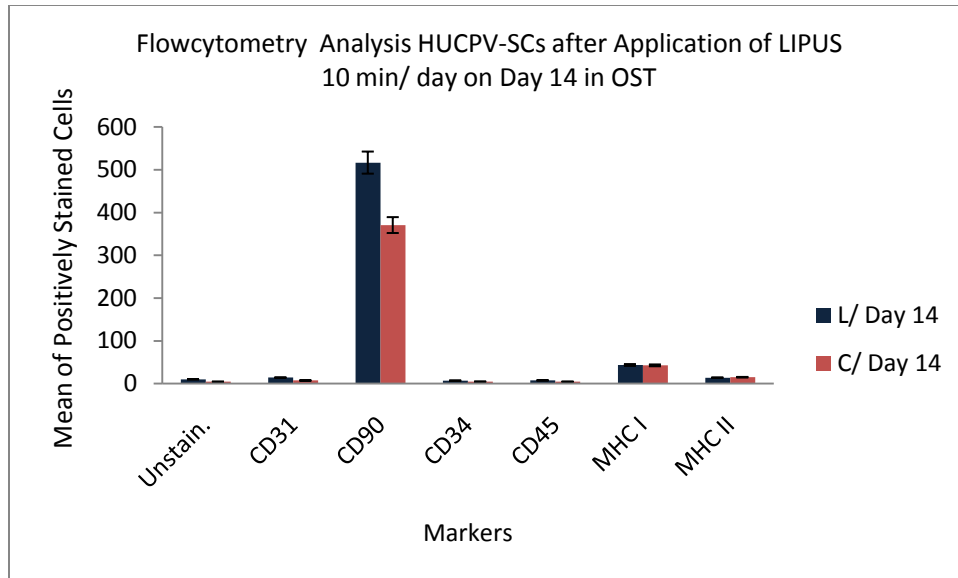


Figure 3.8b. Flow cytometry analysis results on day 14 represented by charts, LIPUS (L), control (C), osteogenic media (OST)

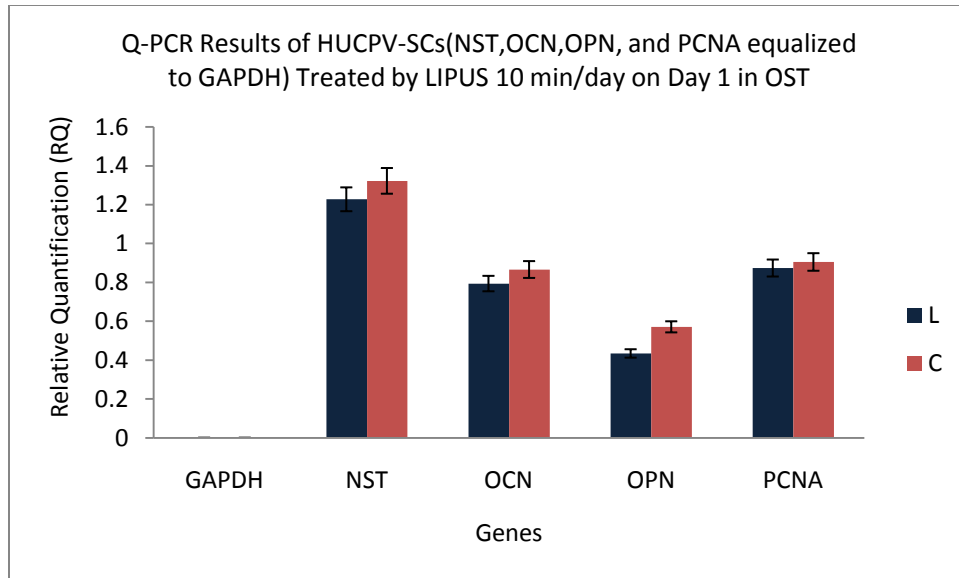


Figure 3.9. qPCR results on day 1 that compare levels of nucleostemin, osteocalcin, osteopontin, and PCNA after their equalization to the endogenous control gene (GAPDH) between LIPUS (L) and control (C) in OST

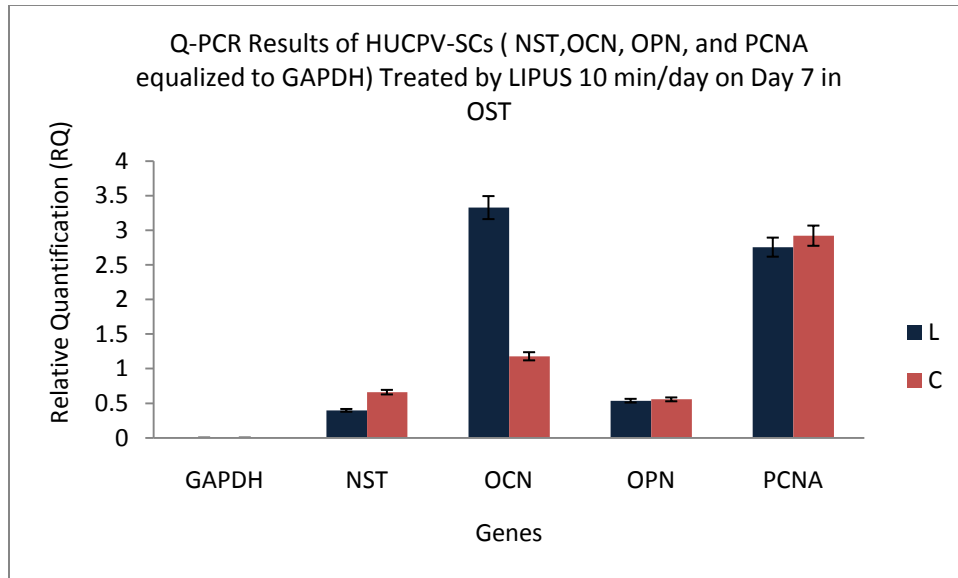


Figure 3.10. qPCR results on day 7 that compare levels of nucleostemin, osteocalcin, osteopontin, and PCNA after their equalization to the endogenous control gene (GAPDH) between LIPUS (L) and control (C) in OST

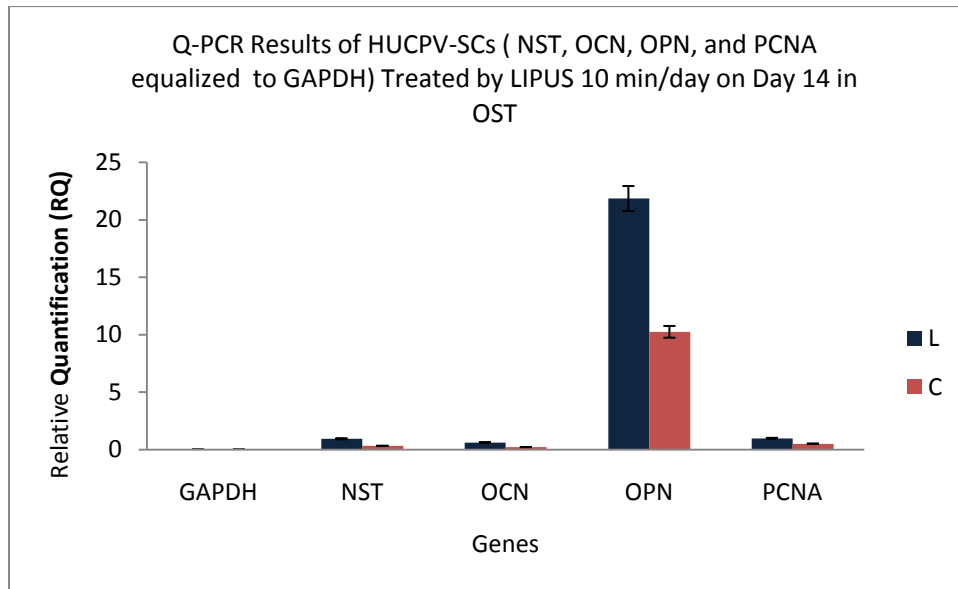


Figure 3.11. qPCR results on day 14 that compare levels of nucleostemin, osteocalcin, osteopontin, and PCNA after their equalization to the endogenous control gene (GAPDH) between LIPUS (L) and control (C) in OST

Genes / OST	Day 1			Day 7			Day 14		
	L Mean ± SD	C Mean ± SD	P- Value	L Mean ± SD	C Mean ± SD	P- Value	L Mean ± SD	C Mean ± SD	P- Value
GAPDH	0.00 ± 0.00	0.00 ± 0.00	0.8	0.00 ± 0.00	0.00 ± 0.00	0.9	0.00 ± 0.00	0.00± 0.00	0.9
NST	1.23 ± 0.16	1.32 ± 0.19	0.6	0.39 ± 0.42	0.66 ± 0.57	0.9	0.95 ± 0.10	0.33 ± 0.05	0.9
OCN	0.79 ± 0.19	0.87 ± 0.12	0.7	3.33 ± 3.54	1.18 ± 1.39	0.08	0.62 ± 0.29	0.22 ± 0.07	0.9
OPN	0.43 ± 0.21	0.57 ± 0.42	0.4	0.54 ± 0.40	0.56 ± 0.65	0.9	21.84 ± 15.64	10.25 ± 3.61	0.001
PCNA	0.87 ± 0.15	0.91 ± 0.04	0.4	2.76 ± 2.01	2.92 ± 3.62	0.9	0.98 ± 0.10	0.51 ± 0.05	0.001

Table 3.4. qPCR comparison of mean ± SD of nucleostemin, osteocalcin, osteopontin, and PCNA after their equalization to the endogenous control gene (GAPDH) between LIPUS (L) and control (C) on days 1, 7, and 14 in OST

3.5. Discussion

MSCs have been shown to be suitable for osteoblastic lineage (16, 18, 49). Osteogenic differentiation of MSCs was established in culture media containing ascorbic acid, β -glycerophosphate, and dexamethasone. The HUCPV-SCs that we used in our experiments were shown in other studies to be capable of osteogenic differentiation in vitro after incubation in osteogenic media for 5, 21, and 28 days (16, 18, 49). The stimulatory properties of LIPUS has been documented in many studies using a variety of cell lineages such as osteoblasts, chondrocytes, and marrow-derived stromal cells (43–46).

Our experiments measured the osteogenic differentiation capacity of HUCPV-SCs after a 10 minute/day application of LIPUS. Our results showed a nonsignificant increase in HUCPV-SC osteogenic differentiation capacity after 1 day of LIPUS treatment. On day 7 of LIPUS treatment, increases in some osteogenic markers, namely OCN and ALP, were evident, and there was a measurable rise in OPN on day 14. No quantitative differences in cell count, DNA content, or immunophenotypic characteristics were detected between the LIPUS treated preparation and a sham treated control.

DNA content, ALP activity, and calcium content were used as surrogate measures for cellular activities in some experimental studies. These markers were found to decline in response to various forms of mechanical stress, such as stretching and loading (47). Similarly, intermittent loading mechanical stress also appeared to reduce the activation of mechanosensitive cation channels on osteoblast-like cells (48). Intermittent cyclic loading has been used as a form of applied mechanical stress (47, 48). Some of these findings were consistent with

our results; that is, we observed downregulation of some cellular markers after exposure to LIPUS.

Nonsignificant increases of CD90 and nucleostemin on day 14 were noted in the LIPUS treated group. In the LIPUS treated group, nonsignificant changes in levels of OCN were observed: OCN was approximately 0.2 fold lower on day 1, 1.5 fold higher on day 7, and 0.5 fold higher on day 14. Statistically significant higher expression of PCNA and OPN in the LIPUS treated group compared to the control was observed on day 14. These findings suggest that the stimulatory effect of LIPUS takes 14 days and beyond to upregulate OPN gene expression in HUCPV-SCs.

3.6. Conclusion

The results of our study suggest that LIPUS can induce osteogenic differentiation of HUCPV-SCs at or beyond 14 days if applied daily for 10 minutes in osteogenic media. LIPUS treated HUCPV-SCs may retain their original phenotype in culture without spontaneous differentiation. Intermittent daily treatment of LIPUS may maintain the multipotent stem cell properties of HUCPV-SCs if LIPUS treatment is continued for a minimum of 14 days. The differences between our results and the findings of Leung et al. (2004) may be related to the LIPUS application technique or to the machine used in our study (27).

Effects of LIPUS methodology have not been conclusively established, therefore, different LIPUS techniques might be used in future experiments on HUCPV-SCs, including direct application of LIPUS within the tissue culture medium. The effects of LIPUS on human umbilical cord stem cell differentiation need to be explored, particularly for chondrogenic and neurogenic lineages.

3.7. References

- (1) Reyes M, Lund T, Lenvik T, Aguiar D, Koodie L, Verfaillie CM. Purification and ex vivo expansion of postnatal human marrow mesodermal progenitor cells. *Blood* 2001 Nov 1;98(9):2615-2625.
- (2) Lee OK, Kuo TK, Chen WM, Lee KD, Hsieh SL, Chen TH. Isolation of multipotent mesenchymal stem cells from umbilical cord blood. *Blood* 2004 Mar 1;103(5):1669-1675.
- (3) in 't Anker PS, Noort WA, Kruisselbrink AB, Scherjon SA, Beekhuizen W, Willemze R, et al. Nonexpanded primary lung and bone marrow-derived mesenchymal cells promote the engraftment of umbilical cord blood-derived CD34(+) cells in NOD/SCID mice. *Exp. Hematol.* 2003 Oct;31(10):881-889.
- (4) Broxmeyer HE, Douglas GW, Hangoc G, Cooper S, Bard J, English D, et al. Human umbilical cord blood as a potential source of transplantable hematopoietic stem/progenitor cells. *Proc. Natl. Acad. Sci. U.S.A.* 1989 May;86(10):3828-3832.
- (5) Gluckman E, Broxmeyer HA, Auerbach AD, Friedman HS, Douglas GW, Devergie A, et al. Hematopoietic reconstitution in a patient with Fanconi's anemia by means of umbilical-cord blood from an HLA-identical sibling. *N. Engl. J. Med.* 1989 Oct 26;321(17):1174-1178.
- (6) Wagner JE, Rosenthal J, Sweetman R, Shu XO, Davies SM, Ramsay NK, et al. Successful transplantation of HLA-matched and HLA-mismatched umbilical cord blood from unrelated donors: analysis of engraftment and acute graft-versus-host disease. *Blood* 1996 Aug 1;88(3):795-802.
- (7) Jin HJ, Park SK, Oh W, Yang YS, Kim SW, Choi SJ. Down-regulation of CD105 is associated with multi-lineage differentiation in human umbilical cord

blood-derived mesenchymal stem cells. *Biochem. Biophys. Res. Commun.* 2009 Apr 17;381(4):676-681.

(8) Wagner W, Wein F, Seckinger A, Frankhauser M, Wirkner U, Krause U, et al. Comparative characteristics of mesenchymal stem cells from human bone marrow, adipose tissue, and umbilical cord blood. *Exp. Hematol.* 2005 Nov;33(11):1402-1416.

(9) Kern S, Eichler H, Stoeve J, Kluter H, Bieback K. Comparative analysis of mesenchymal stem cells from bone marrow, umbilical cord blood, or adipose tissue. *Stem Cells* 2006 May;24(5):1294-1301.

(10) Erices A, Conget P, Minguell JJ. Mesenchymal progenitor cells in human umbilical cord blood. *Br. J. Haematol.* 2000 Apr;109(1):235-242.

(11) Lee MW, Choi J, Yang MS, Moon YJ, Park JS, Kim HC, et al. Mesenchymal stem cells from cryopreserved human umbilical cord blood. *Biochem. Biophys. Res. Commun.* 2004 Jul 16;320(1):273-278.

(12) Kestendjieva S, Kyurkchiev D, Tsvetkova G, Mehandjiev T, Dimitrov A, Nikolov A, et al. Characterization of mesenchymal stem cells isolated from the human umbilical cord. *Cell Biol. Int.* 2008 Jul;32(7):724-732.

(13) Baksh D, Yao R, Tuan RS. Comparison of proliferative and multilineage differentiation potential of human mesenchymal stem cells derived from umbilical cord and bone marrow. *Stem Cells* 2007 Jun;25(6):1384-1392.

(14) Qiao C, Xu W, Zhu W, Hu J, Qian H, Yin Q, et al. Human mesenchymal stem cells isolated from the umbilical cord. *Cell Biol. Int.* 2008 Jan;32(1):8-15.

(15) Gang EJ, Hong SH, Jeong JA, Hwang SH, Kim SW, Yang IH, et al. In vitro mesengenic potential of human umbilical cord blood-derived mesenchymal stem cells. *Biochem. Biophys. Res. Commun.* 2004 Aug 13;321(1):102-108.

- (16) Wang HS, Hung SC, Peng ST, Huang CC, Wei HM, Guo YJ, et al. Mesenchymal stem cells in the Wharton's jelly of the human umbilical cord. *Stem Cells* 2004;22(7):1330-1337.
- (17) Weiss ML, Medicetty S, Bledsoe AR, Rachakatla RS, Choi M, Merchav S, et al. Human umbilical cord matrix stem cells: preliminary characterization and effect of transplantation in a rodent model of Parkinson's disease. *Stem Cells* 2006 Mar;24(3):781-792.
- (18) Sarugaser R, Lickorish D, Baksh D, Hosseini MM, Davies JE. Human umbilical cord perivascular (HUCPV) cells: a source of mesenchymal progenitors. *Stem Cells* 2005 Feb;23(2):220-229.
- (19) Gluckman E, Rocha V, Boyer-Chammard A, Locatelli F, Arcese W, Pasquini R, et al. Outcome of cord-blood transplantation from related and unrelated donors. Eurocord Transplant Group and the European Blood and Marrow Transplantation Group. *N. Engl. J. Med.* 1997 Aug 7;337(6):373-381.
- (20) Han IS, Ra JS, Kim MW, Lee EA, Jun HY, Park SK, et al. Differentiation of CD34+ cells from human cord blood and murine bone marrow is suppressed by C6 beta-chemokines. *Mol. Cells* 2003 Apr 30;15(2):176-180.
- (21) Kim JW, Kim SY, Park SY, Kim YM, Kim JM, Lee MH, et al. Mesenchymal progenitor cells in the human umbilical cord. *Ann. Hematol.* 2004 Dec;83(12):733-738.
- (22) Goodwin HS, Bicknese AR, Chien SN, Bogucki BD, Quinn CO, Wall DA. Multilineage differentiation activity by cells isolated from umbilical cord blood: expression of bone, fat, and neural markers. *Biol. Blood Marrow Transplant.* 2001;7(11):581-588.

- (23) Heckman JD, Ryaby JP, McCabe J, Frey JJ, Kilcoyne RF. Acceleration of tibial fracture-healing by non-invasive, low-intensity pulsed ultrasound. *Journal of Bone & Joint Surgery—American Volume* 1994 Jan;76(1):26-34.
- (24) Kristiansen TK, Ryaby JP, McCabe J, Frey JJ, Roe LR. Accelerated healing of distal radial fractures with the use of specific, low-intensity ultrasound. A multicenter, prospective, randomized, double-blind, placebo-controlled study. *Journal of Bone & Joint Surgery—American Volume* 1997 Jul;79(7):961-973.
- (25) Mayr E, Rudzki MM, Rudzki M, Borchardt B, Hausser H, Ruter A. Does low intensity, pulsed ultrasound speed healing of scaphoid fractures? *Handchirurgie, Mikrochirurgie, Plastische Chirurgie* 2000 Mar;32(2):115-122.
- (26) Nolte PA, van der Krans A, Patka P, Janssen IM, Ryaby JP, Albers GH. Low-intensity pulsed ultrasound in the treatment of nonunions. *Journal of Trauma-Injury Infection & Critical Care* 2001 discussion 702-3; Oct;51(4):693-702.
- (27) Leung KS, Lee WS, Cheung WH, Qin L. Lack of efficacy of low-intensity pulsed ultrasound on prevention of postmenopausal bone loss evaluated at the distal radius in older Chinese women. *Clinical Orthopaedics & Related Research* 2004 Oct(427):234-240.
- (28) Tsumaki N, Kakiuchi M, Sasaki J, Ochi T, Yoshikawa H. Low-intensity pulsed ultrasound accelerates maturation of callus in patients treated with opening-wedge high tibial osteotomy by hemicallotaxis. *Journal of Bone & Joint Surgery—American Volume* 2004 Nov;86-A(11):2399-2405.
- (29) Gebauer D, Mayr E, Orthner E, Ryaby JP. Low-intensity pulsed ultrasound: effects on nonunions. *Ultrasound Med. Biol.* 2005 Oct;31(10):1391-1402.

- (30) Gold SM, Wasserman R. Preliminary results of tibial bone transports with pulsed low intensity ultrasound (Exogen). *J. Orthop. Trauma* 2005 Jan;19(1):10-16.
- (31) Ricardo M. The effect of ultrasound on the healing of muscle-pediculated bone graft in scaphoid non-union. *Int. Orthop.* 2006 Apr;30(2):123-127.
- (32) Schmelz A, Friedrich A, Kinzl L, Einsiedel T. Low intensity pulsed ultrasound (LIPUS) is shortening healing time following callus distraction for bony defects of the tibia. *Aktuelle Traumatol.* 2006;36(4):149-158.
- (33) Nomura S, Takano-Yamamoto T. Molecular events caused by mechanical stress in bone. *Matrix Biol.* 2000 May;19(2):91-96.
- (34) Bandow K, Nishikawa Y, Ohnishi T, Kakimoto K, Soejima K, Iwabuchi S, et al. Low-intensity pulsed ultrasound (LIPUS) induces RANKL, MCP-1, and MIP-1beta expression in osteoblasts through the angiotensin II type 1 receptor. *J. Cell. Physiol.* 2007 May;211(2):392-398.
- (35) Ikai H, Tamura T, Watanabe T, Itou M, Sugaya A, Iwabuchi S, et al. Low-intensity pulsed ultrasound accelerates periodontal wound healing after flap surgery. *J. Periodontal. Res.* 2008 Apr;43(2):212-216.
- (36) Ebersson CP, Hogan KA, Moore DC, Ehrlich MG. Effect of low-intensity ultrasound stimulation on consolidation of the regenerate zone in a rat model of distraction osteogenesis. *J. Pediatr. Orthop.* 2003 Jan-Feb;23(1):46-51.
- (37) Leung KS, Cheung WH, Zhang C, Lee KM, Lo HK. Low intensity pulsed ultrasound stimulates osteogenic activity of human periosteal cells. *Clin. Orthop.* 2004 Jan(418):253-259.

- (38) Martini L, Giavaresi G, Fini M, Torricelli P, de Pretto M, Schaden W, et al. Effect of extracorporeal shock wave therapy on osteoblastlike cells. *Clin. Orthop.* 2003 Aug(413):269-280.
- (39) Owen TA, Aronow M, Shalhoub V, Barone LM, Wilming L, Tassinari MS, et al. Progressive development of the rat osteoblast phenotype in vitro: reciprocal relationships in expression of genes associated with osteoblast proliferation and differentiation during formation of the bone extracellular matrix. *J. Cell. Physiol.* 1990 Jun;143(3):420-430.
- (40) Holmes K, Lantz LM, Fowlkes BJ, Schmid I, Giorgi JV. Preparation of cells and reagents for flow cytometry. *Curr. Protoc. Immunol.* 2001 Nov;Chapter 5:Unit 5.3.
- (41) Malley A, Stewart CC, Stewart SJ, Waldbeser L, Bradley LM, Shiigi SM. Flow cytometric analysis of I-J expression on murine bone marrow-derived macrophages. *J. Leukoc. Biol.* 1988 Jun;43(6):557-565.
- (42) Kafienah W, Mistry S, Williams C, Hollander AP. Nucleostemin is a marker of proliferating stromal stem cells in adult human bone marrow. *Stem Cells* 2006 Apr;24(4):1113-1120.
- (43) Sun JS, Hong RC, Chang WH, Chen LT, Lin FH, Liu HC. In vitro effects of low-intensity ultrasound stimulation on the bone cells. *J. Biomed. Mater. Res.* 2001 Dec 5;57(3):449-456.
- (44) Parvizi J, Wu CC, Lewallen DG, Greenleaf JF, Bolander ME. Low-intensity ultrasound stimulates proteoglycan synthesis in rat chondrocytes by increasing aggrecan gene expression. *J. Orthop. Res.* 1999 Jul;17(4):488-494.

- (45) Zhang ZJ, Huckle J, Francomano CA, Spencer RG. The effects of pulsed low-intensity ultrasound on chondrocyte viability, proliferation, gene expression, and matrix production. *Ultrasound Med. Biol.* 2003 Nov;29(11):1645-1651.
- (46) Naruse K, Mikuni-Takagaki Y, Azuma Y, Ito M, Oota T, Kameyama K, et al. Anabolic response of mouse bone-marrow-derived stromal cell clone ST2 cells to low-intensity pulsed ultrasound. *Biochem. Biophys. Res. Commun.* 2000 Feb 5;268(1):216-220.
- (47) Winter LC, Walboomers XF, Bumgardner JD, Jansen JA. Intermittent versus continuous stretching effects on osteoblast-like cells in vitro. *J. Biomed. Mater. Res. A.* 2003 Dec 15;67(4):1269-1275.
- (48) Duncan RL, Hruska KA. Chronic, intermittent loading alters mechanosensitive channel characteristics in osteoblast-like cells. *Am. J. Physiol.* 1994 Dec;267(6 Pt 2):F909-16.
- (49) Karahuseyinoglu S, Cinar O, Kilic E, Kara F, Akay GG, Demiralp DO, et al. Biology of stem cells in human umbilical cord stroma: in situ and in vitro surveys. *Stem Cells* 2007 Feb;25(2):319-331.

CHAPTER 4

General Discussion and Conclusion

4.1. Discussion

Duarte et al. (1983) was the first to develop and clinically use a biophysical profile utilizing LIPUS treatment to stimulate bone osteogenesis (1). The LIPUS signal used by Duarte consisted of a 200 ms burst of 1.5 MHz sine waves at a frequency of 1 kHz delivered at 30 mW/cm² spatial and temporal averaged (SATA) intensity (2). In a double-blind clinical trial, Pilla et al. (1990) reported a significant recovery of bilateral fibular osteotomies in rabbits after LIPUS application for 20 min/day (3). Subsequently, several researchers confirmed the potential of LIPUS to accelerate fracture healing in various animal models (2–5). Some studies reported that LIPUS increased the activity of intervertebral disc cells by stimulating expression of various receptors, promoting collagen synthesis, and enhancing sensitivity to growth factors (6–8). They theorized that this involved a direct effect of mechanical stress and an indirect effect of vibration on the extracellular matrix (6–8). Other studies reported that direct application of LIPUS for 20 min/day at 30 mW/cm² intensity through cell culture media significantly increased the expression of BMP-2 mRNA of rat osteoblast cells on days 5–14, with a peak on day 7 (9, 21). In addition, they demonstrated that the optimal stimulatory effect of LIPUS on skin fibroblasts was achieved at 10 min/day for 7 days (9, 21).



Figure 4.1. Exogen 2000, Smith and Nephew device (LIPUS)

Based on these reports, we investigated the effect of LIPUS on HUCPV-SC monolayers in tissue cultures to evaluate the effect of LIPUS on their proliferation capacity and on their potential for osteogenic differentiation. The results of our experiments showed an unusually differential response of HUCPV-SCs after LIPUS treatment. In order to assess the experimental findings, we carried out previously accepted methodologies in testing this type of cells. Levels of CD90 and nucleostemin, validated stem cell markers (16, 17, 20), were measured. We also estimated levels of ALP, OCN, and OPN as they were previously validated markers for osteogenic differentiation (15, 18, 19). We found that HUCPV-SCs tend to maintain their phenotypic stem cell characteristics and their osteogenic differentiation capacity after LIPUS treatment (Figure 4.1). These two characteristics increased in response to 10 minutes of daily LIPUS application for 1, 7, and 14 days. However, some markers of these two characteristics appeared not statistically significant, such as cell proliferation, DNA content, and ALP levels. The differential effect of LIPUS on various markers may be related to the LIPUS application method in this study.

More potent stimulatory effects were obtained by direct application of LIPUS to tissue culture media in other experimental studies (9, 10, 30–32). The accurate direct application methods and the application time seemed to be crucial factors for successful ultrasound treatment (9, 10, 30–32). In our study, LIPUS application directly to the culture medium resulted in multiple occasions of fungal outgrowth despite strict sterile conditions. We therefore shifted the application method to project from beneath the tissue flasks instead of direct insertional application. LIPUS application outside the tissue container might account for the variable responses of some markers, as the thickness and homogeneity of the flask materials are likely variable and thus power dissipation would have been inconsistent. HUCPV-SCs from the LIPUS treated group expressed a high level of CD90 on day 14 compared with cells in the sham treated group in both basic and osteogenic media (Tables 2.3, 3.3).

Some studies reported evidence that continuous mechanical stress may decrease cellular activities in terms of DNA quantity, ALP activity, and calcium content (13, 22, 24). Persistent mechanical stress was shown also to reduce the activation of mechanosensitive cation channels in osteoblast-like cells (13, 14, 22, 24). Our results correlated with some of these findings as there were no significant differences between the LIPUS treated group and the sham treated group in terms of cell proliferation, quantitative DNA measures, and ALP levels in basic media or in osteogenic media.

In basic media, higher expressions of CD90, PCNA, and OPN were observed in the LIPUS treated group compared to the sham group. HUCPV-SCs expressed significantly higher levels of OPN and PCNA in the LIPUS treated group compared to the sham group on day 14 ($P < 0.01$). This suggests that

LIPUS may enhance osteogenic phenotypic differentiation of HUCPV-SCs in basic media after 14 days. This result was consistent with Mostafa et al. (in press) that showed LIPUS-enhanced osteogenic differentiation of human gingival fibroblasts in basic media (33). Nevertheless, there was no difference in nucleostemin expression on days 1, 7, and 14. The level of PCNA was significantly higher in the LIPUS treated group on day 14; this result is supported by the findings of Yoon et al. (2009) (12). The findings from Yoon et al. (2009) and Mostafa et al. (in press) appear to validate part of our hypothesis—that LIPUS can increase PCNA (the proliferation gene of HUCPV-SCs) while maintaining the stem cell characteristics of the cells after 14 days of treatment in basic media.

We also examined the effects of LIPUS on OCN and OPN expression of HUCPV-SCs after osteogenic induction using dexamethasone and β -glycerophosphate. The level of OCN expression was almost 0.2 fold lower in the LIPUS treated group on day 1, but it was 1.5 fold higher on day 7. It was almost comparable to the sham treated group on day 14 (Figures 3.9, 3.10, and 3.11). In osteogenic media on day 14, LIPUS treated HUCPV-SCs expressed a high level of OPN, almost 1.5 fold greater than the sham treated group ($P < 0.001$) (Figure 3.11). However, OPN expression was almost comparable on day 7 in both groups. These findings suggest that LIPUS might have a selective and time-dependent stimulatory effect on the osteogenic differentiation of HUCPV-SCs. Interestingly, LIPUS treated HUCPV-SCs in osteogenic media expressed a high level of CD90 on day 14 compared with the sham treated group (Table 3.4). These data support further investigation of the effects of LIPUS on stem cell markers and osteogenic differentiation.

These observations appear consistent with the hypothesis that LIPUS has selective and time-dependent effects on the osteogenic differentiation of HUCPV-SCs. This is further supported by the notable increases in CD90 and nucleostemin on day 14 in osteogenic inducing media in the LIPUS treated group. Based on these findings, LIPUS appears to have unpredictable effects on the osteogenic differentiation of HUCPV-SCs after 14 days.

Supportive studies suggest that application of LIPUS on different types of cells could result in variable but nonsignificant differences in cell proliferation (10, 22–28) and differentiation (12, 27, 28). Our results are consistent with studies of MSCs (22–24) and chondrocytes (25–28) that postulated that the mechanical stress of LIPUS may push cells toward maintenance rather than proliferation and differentiation. Another study reported a nonsignificant outcome in LIPUS treated HUCPV-SCs in terms of cell proliferation and differentiation (12). One study reported LIPUS stimulation of nucleus pulposus (NP) cells after adding the growth factor TGF- β (6). The growth factor treated NP cells yielded a significant difference in TGF- β type I receptor gene expression when exposed to LIPUS for 20 min/day on days 3 and 4 (6). This finding suggested that LIPUS enhanced the sensitivity of NP cells to TGF- β 1 despite a nonsignificant difference in cell proliferation (6). Another experiment demonstrated that LIPUS treatments of 15 min/day at 30 mW/cm² intensity for 6 days applied through a water bath placed underneath the culture flask had no significant effect on immature cementoblast cell proliferation (10). In addition, bone sialo-protein (BSP), osteocalcin (OCN) and osteopontin (OPN) were not detected with or without LIPUS exposure (10).

One investigator stated that LIPUS had a positive osteogenic differentiation effect on human periosteal cells only on day 6 of treatment (11). A

similar study reported that LIPUS application for 50 seconds/day at an intensity of 30 mW/cm^2 significantly increased the HUCPV-SC count after 3 days of application ($n = 3$). They noted that different time periods of applications—1.7 min, 5 min, and 10 min—yielded different results (12). There was a 3.3 fold increase in cell proliferation numbers at a LIPUS regimen of 1.7 min/day, while LIPUS exposure for 5 min/day and 10 min/day induced less cell proliferation than observed in relative control groups (12). However, they reported an unlikely adverse effect of LIPUS on the differentiation potential for these timed applications (12). Inconsistent results were also shown in previous studies that evaluated the effects of LIPUS on different types of cell line (27, 29). Another study showed that LIPUS stimulated aggrecan m-RNA expression and proteoglycan synthesis, but did not influence cell proliferation of rat chondrocytes in vitro (29). Nevertheless, some authors stated that LIPUS could enhance cell proliferation in an intensity dependant manner with no significant difference in cell proliferation at 30 mW/cm^2 and significant differences at 2 mW/cm^2 (27). However, LIPUS was not associated with increased expression or synthesis of aggrecan and type II collagen of chick embryo chondrocytes in vitro (27).

4.2. Conclusion

LIPUS appears to have a selective and time-dependent stimulatory effect on the osteogenic differentiation of HUCPV-SCs. The effect of LIPUS on cellular proliferation could be improved by changing the LIPUS application technique. Our results suggest that LIPUS may have a more anabolic effect on HUCPV-SCs if the LIPUS transducer were introduced directly inside the media. Additionally, the presented results suggest that LIPUS may enhance the osteogenic

differentiation of HUCPV-SCs after 7 days of application. Future studies might further our understanding of the biological behaviour of HUCPV-SCs by exploring the following factors:

1. The effects of LIPUS on the osteogenic differentiation of HUCPV-SCs beyond a 14 day treatment.
2. The effects of LIPUS treatment on chondrogenic and neurogenic differentiation of HUCPV-SCs.
3. Comparisons of LIPUS effects on HUCPV-SCs using different treatment duration protocols.

4.3. References

- (1) Duarte LR. The stimulation of bone growth by ultrasound. Arch. Orthop. Trauma. Surg. 1983;101(3):153-159.
- (2) Romano CL, Romano D, Logoluso N. Low-intensity pulsed ultrasound for the treatment of bone delayed union or nonunion: a review. Ultrasound Med. Biol. 2009 Apr;35(4):529-536.
- (3) Pilla AA, Mont MA, Nasser PR, Khan SA, Figueiredo M, Kaufman JJ, et al. Non-invasive low-intensity pulsed ultrasound accelerates bone healing in the rabbit. J. Orthop. Trauma 1990;4(3):246-253.
- (4) Wang SJ, Lewallen DG, Bolander ME, Chao EY, Ilstrup DM, Greenleaf JF. Low intensity ultrasound treatment increases strength in a rat femoral fracture model. J. Orthop. Res. 1994 Jan;12(1):40-47.
- (5) Yang KH, Parvizi J, Wang SJ, Lewallen DG, Kinnick RR, Greenleaf JF, et al. Exposure to low-intensity ultrasound increases aggrecan gene expression in a rat femur fracture model. J. Orthop. Res. 1996 Sep;14(5):802-809.
- (6) Hiyama A, Mochida J, Iwashina T, Omi H, Watanabe T, Serigano K, et al. Synergistic effect of low-intensity pulsed ultrasound on growth factor stimulation of nucleus pulposus cells. J. Orthop. Res. 2007 Dec;25(12):1574-1581.
- (7) Matsumoto T, Kawakami M, Kuribayashi K, Takenaka T, Tamaki T. Cyclic mechanical stretch stress increases the growth rate and collagen synthesis of nucleus pulposus cells in vitro. Spine 1999 Feb 15;24(4):315-319.
- (8) Hutton WC, Elmer WA, Boden SD, Hyon S, Toribatake Y, Tomita K, et al. The effect of hydrostatic pressure on intervertebral disc metabolism. Spine 1999 Aug 1;24(15):1507-1515.

- (9) Suzuki A, Takayama T, Suzuki N, Sato M, Fukuda T, Ito K. Daily low-intensity pulsed ultrasound-mediated osteogenic differentiation in rat osteoblasts. *Acta Biochim. Biophys. Sin. (Shanghai)* 2009 Feb;41(2):108-115.
- (10) Inubushi T, Tanaka E, Rego EB, Kitagawa M, Kawazoe A, Ohta A, et al. Effects of ultrasound on the proliferation and differentiation of cementoblast lineage cells. *J. Periodontol.* 2008 Oct;79(10):1984-1990.
- (11) Tam KF, Cheung WH, Lee KM, Qin L, Leung KS. Osteogenic effects of low-intensity pulsed ultrasound, extracorporeal shockwaves and their combination—an in vitro comparative study on human periosteal cells. *Ultrasound Med. Biol.* 2008 Dec;34(12):1957-1965.
- (12) Yoon JH, Roh EY, Shin S, Jung NH, Song EY, Lee DS, et al. Introducing pulsed low-intensity ultrasound to culturing human umbilical cord-derived mesenchymal stem cells. *Biotechnol. Lett.* 2009 Mar;31(3):329-335.
- (13) Winter LC, Walboomers XF, Bumgardner JD, Jansen JA. Intermittent versus continuous stretching effects on osteoblast-like cells in vitro. *J. Biomed. Mater. Res. A.* 2003 Dec 15;67(4):1269-1275.
- (14) Duncan RL, Hruska KA. Chronic, intermittent loading alters mechanosensitive channel characteristics in osteoblast-like cells. *Am. J. Physiol.* 1994 Dec;267(6 Pt 2):F909-16.
- (15) Chipoy C, Berreur M, Couillaud S, Pradal G, Vallette F, Colombeix C, et al. Downregulation of osteoblast markers and induction of the glial fibrillary acidic protein by oncostatin M in osteosarcoma cells require PKC delta and STAT3. *J. Bone Miner. Res.* 2004 Nov;19(11):1850-1861.

- (16) Kafienah W, Mistry S, Williams C, Hollander AP. Nucleostemin is a marker of proliferating stromal stem cells in adult human bone marrow. *Stem Cells* 2006 Apr;24(4):1113-1120.
- (17) Nakamura Y, Muguruma Y, Yahata T, Miyatake H, Sakai D, Mochida J, et al. Expression of CD90 on keratinocyte stem/progenitor cells. *Br. J. Dermatol.* 2006 Jun;154(6):1062-1070.
- (18) Sun H, Ye F, Wang J, Shi Y, Tu Z, Bao J, et al. The upregulation of osteoblast marker genes in mesenchymal stem cells prove the osteoinductivity of hydroxyapatite/tricalcium phosphate biomaterial. *Transplant. Proc.* 2008 Oct;40(8):2645-2648.
- (19) Wenstrup RJ, Fowlkes JL, Witte DP, Florer JB. Discordant expression of osteoblast markers in MC3T3-E1 cells that synthesize a high turnover matrix. *J. Biol. Chem.* 1996 Apr 26;271(17):10271-10276.
- (20) Wiesmann A, Buhring HJ, Mentrup C, Wiesmann HP. Decreased CD90 expression in human mesenchymal stem cells by applying mechanical stimulation. *Head Face Med.* 2006;2:8.
- (21) Zhou S, Schmelz A, Seufferlein T, Li Y, Zhao J, Bachem MG. Molecular mechanisms of low intensity pulsed ultrasound in human skin fibroblasts. *J. Biol. Chem.* 2004 Dec 24;279(52):54463-54469.
- (22) Angele P, Schumann D, Angele M, Kinner B, Englert C, Hente R, et al. Cyclic, mechanical compression enhances chondrogenesis of mesenchymal progenitor cells in tissue engineering scaffolds. *Biorheology* 2004;41(3-4):335-346.

- (23) Ebisawa K, Hata K, Okada K, Kimata K, Ueda M, Torii S, et al. Ultrasound enhances transforming growth factor beta-mediated chondrocyte differentiation of human mesenchymal stem cells. *Tissue Eng.* 2004 May-Jun;10(5-6):921-929.
- (24) Schumann D, Kujat R, Zellner J, Angele MK, Nerlich M, Mayr E, et al. Treatment of human mesenchymal stem cells with pulsed low intensity ultrasound enhances the chondrogenic phenotype in vitro. *Biorheology* 2006;43(3-4):431-443.
- (25) Torzilli PA, Grigiene R, Huang C, Friedman SM, Doty SB, Boskey AL, et al. Characterization of cartilage metabolic response to static and dynamic stress using a mechanical explant test system. *J. Biomech.* 1997 Jan;30(1):1-9.
- (26) Toyoda T, Seedhom BB, Kirkham J, Bonass WA. Upregulation of aggrecan and type II collagen mRNA expression in bovine chondrocytes by the application of hydrostatic pressure. *Biorheology* 2003;40(1-3):79-85.
- (27) Zhang ZJ, Huckle J, Francomano CA, Spencer RG. The effects of pulsed low-intensity ultrasound on chondrocyte viability, proliferation, gene expression and matrix production. *Ultrasound Med. Biol.* 2003 Nov;29(11):1645-1651.
- (28) Park SR, Choi BH, Min BH. Low-intensity ultrasound (LIUS) as an innovative tool for chondrogenesis of mesenchymal stem cells (MSCs). *Organog.* 2007 Oct;3(2):74-78.
- (29) Parvizi J, Wu CC, Lewallen DG, Greenleaf JF, Bolander ME. Low-intensity ultrasound stimulates proteoglycan synthesis in rat chondrocytes by increasing aggrecan gene expression. *J. Orthop. Res.* 1999 Jul;17(4):488-494.
- (30) Kokubu T, Matsui N, Fujioka H, Tsunoda M, Mizuno K. Low intensity pulsed ultrasound exposure increases prostaglandin E2 production via the induction of

cyclooxygenase-2 mRNA in mouse osteoblasts. *Biochem. Biophys. Res. Commun.* 1999 Mar 16;256(2):284-287.

(31) Mukai S, Ito H, Nakagawa Y, Akiyama H, Miyamoto M, Nakamura T. Transforming growth factor-beta1 mediates the effects of low-intensity pulsed ultrasound in chondrocytes. *Ultrasound Med. Biol.* 2005 Dec;31(12):1713-1721.

(32) Doan N, Reher P, Meghji S, Harris M. In vitro effects of therapeutic ultrasound on cell proliferation, protein synthesis, and cytokine production by human fibroblasts, osteoblasts, and monocytes. *J. Oral Maxillofac. Surg.* 1999 discussion 420; Apr;57(4):409-419.

(33) Mostafa, NZ, Uludag H, Dederich, DN, Doschak MR, El-Bialy TH. Anabolic effects of low intensity pulsed ultrasound on gingival fibroblasts. *Archives of Oral Biology* (in press).

A1

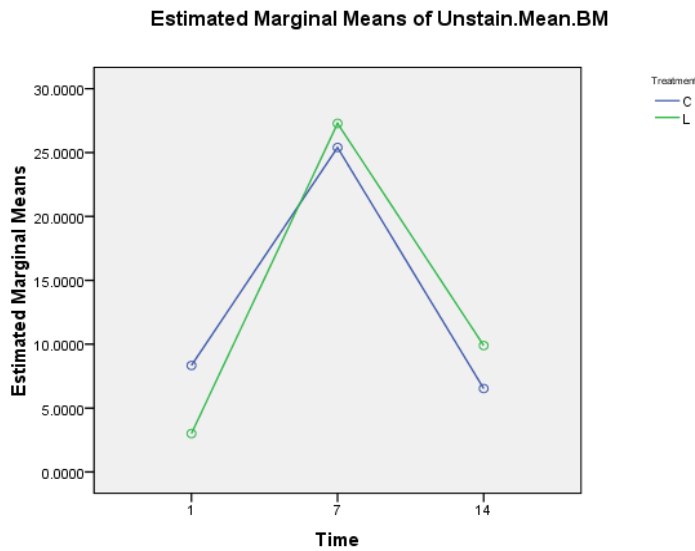


Figure A1.1. Unstained samples: mean differences of Isotype IgG between LIPUS (L) and control (C) in basic media on days 1, 7, and 14

Parameter Estimates

Dependent Variable: Unstain.Mean.BM

Parameter	B	Std. Error	t	Sig.	95% Confidence Interval	
					Lower Bound	Upper Bound
Intercept	9.897	3.260	3.036	.010	2.794	16.999
[Time=1]	-6.890	4.610	-1.495	.161	-16.935	3.155
[Time=7]	17.387	4.610	3.771	.003	7.342	27.431
[Time=14]	0 ^a
[Treatment=C]	-3.367	4.610	-.730	.479	-13.411	6.678
[Treatment=L]	0 ^a
[Time=1] * [Treatment=C]	8.697	6.520	1.334	.207	-5.509	22.902
[Time=1] * [Treatment=L]	0 ^a
[Time=7] * [Treatment=C]	1.480	6.520	.227	.824	-12.725	15.685
[Time=7] * [Treatment=L]	0 ^a
[Time=14] * [Treatment=C]	0 ^a
[Time=14] * [Treatment=L]	0 ^a

a. This parameter is set to zero because it is redundant.

Table A1.1. Mean \pm SD results of t-test of mean of unstained samples: isotype IgG; differences between LIPUS (L) and control (C) in basic media on days 1, 7, and 14

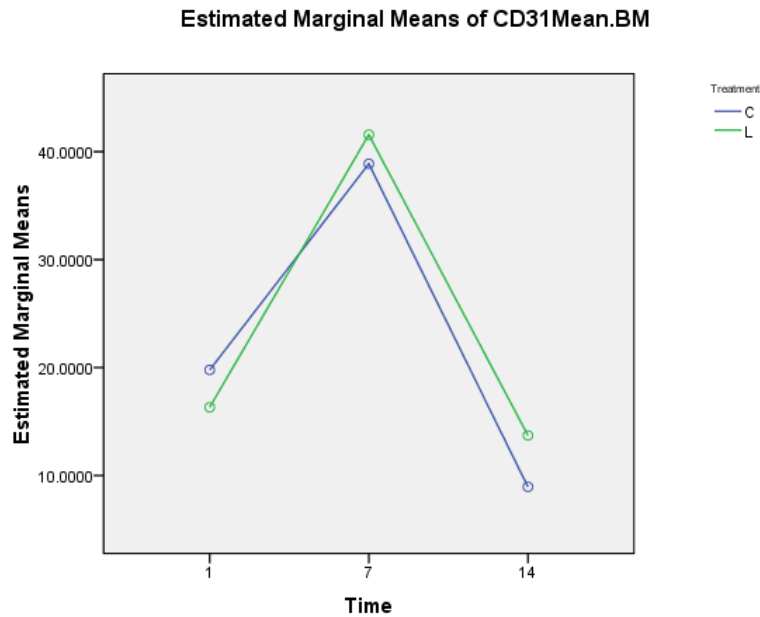


Figure A1.2. CD 31: mean differences between LIPUS (L) and control (C) in basic media on days 1, 7, and 14

Parameter Estimates

Dependent Variable: CD31Mean.BM

Parameter	B	Std. Error	t	Sig.	95% Confidence Interval	
					Lower Bound	Upper Bound
Intercept	13.710	5.483	2.500	.028	1.764	25.656
[Time=1]	2.603	7.754	.336	.743	-14.291	19.498
[Time=7]	27.860	7.754	3.593	.004	10.965	44.755
[Time=14]	0 ^a
[Treatment=C]	-4.760	7.754	-.614	.551	-21.655	12.135
[Treatment=L]	0 ^a
[Time=1] * [Treatment=C]	8.227	10.966	.750	.468	-15.666	32.119
[Time=1] * [Treatment=L]	0 ^a
[Time=7] * [Treatment=C]	2.070	10.966	.189	.853	-21.822	25.962
[Time=7] * [Treatment=L]	0 ^a
[Time=14] * [Treatment=C]	0 ^a
[Time=14] * [Treatment=L]	0 ^a

a. This parameter is set to zero because it is redundant.

Table A1.2. Mean \pm SD results of t-test of mean CD31 differences between LIPUS (L) and control (C) in basic media on days 1, 7, and 14

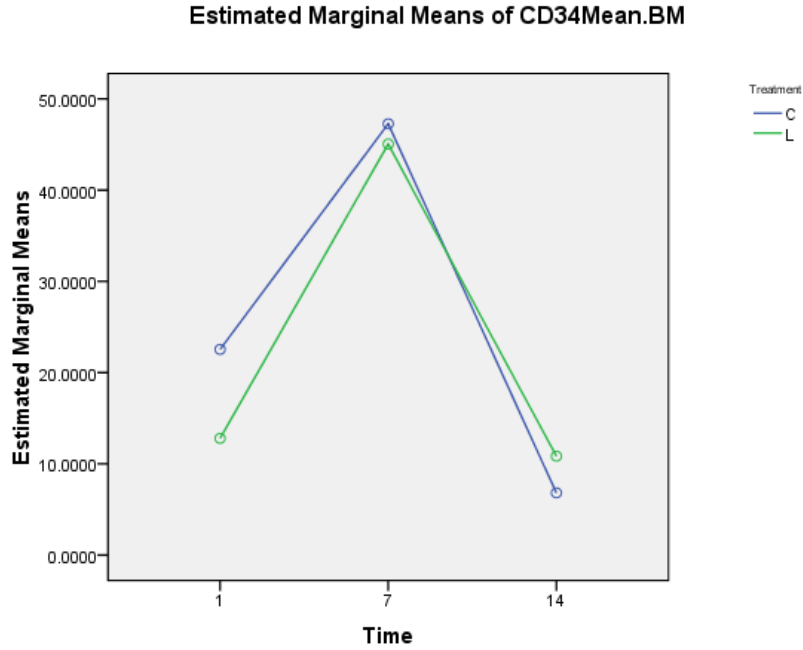


Figure A1.3. CD 34: mean differences between LIPUS (L) and control (C) in basic media on days 1, 7, and 14

Parameter Estimates

Dependent Variable: CD34Mean.BM

Parameter	B	Std. Error	t	Sig.	95% Confidence Interval	
					Lower Bound	Upper Bound
Intercept	10.840	10.038	1.080	.301	-11.031	32.711
[Time=1]	1.957	14.196	.138	.893	-28.973	32.886
[Time=7]	34.203	14.196	2.409	.033	3.274	65.133
[Time=14]	0 ^a
[Treatment=C]	-4.020	14.196	-.283	.782	-34.950	26.910
[Treatment=L]	0 ^a
[Time=1] * [Treatment=C]	13.767	20.076	.686	.506	-29.974	57.508
[Time=1] * [Treatment=L]	0 ^a
[Time=7] * [Treatment=C]	6.247	20.076	.311	.761	-37.494	49.988
[Time=7] * [Treatment=L]	0 ^a
[Time=14] * [Treatment=C]	0 ^a
[Time=14] * [Treatment=L]	0 ^a

a. This parameter is set to zero because it is redundant.

Table A1.3. Mean ± SD results of t-test of mean CD34 differences between LIPUS (L) and control (C) in basic media on days 1, 7, and 14

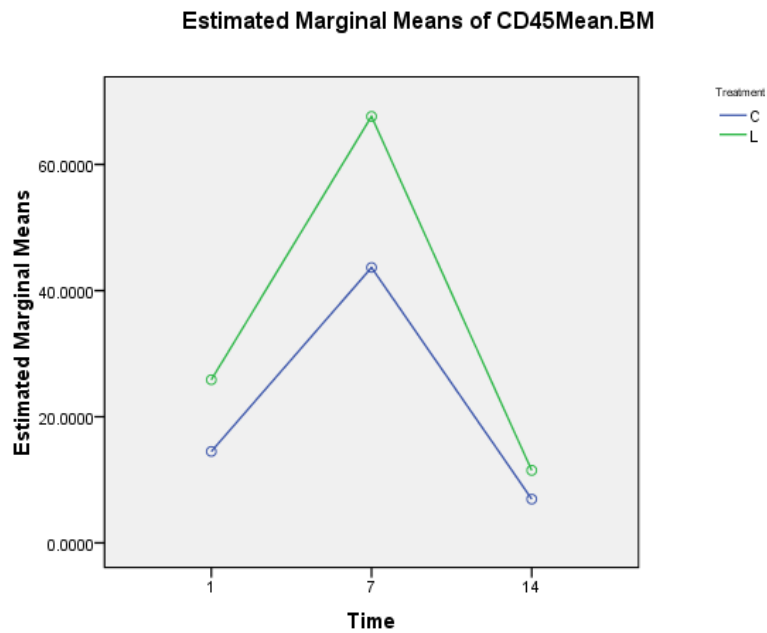


Figure A1.4. CD 45: mean differences between LIPUS (L) and control (C) in basic media on days 1, 7, and 14

Parameter Estimates

Dependent Variable: CD45Mean.BM

Parameter	B	Std. Error	t	Sig.	95% Confidence Interval	
					Lower Bound	Upper Bound
Intercept	11.503	17.012	.676	.512	-25.563	48.570
[Time=1]	14.360	24.059	.597	.562	-38.060	66.780
[Time=7]	56.103	24.059	2.332	.038	3.683	108.523
[Time=14]	0 ^a
[Treatment=C]	-4.557	24.059	-.189	.853	-56.977	47.863
[Treatment=L]	0 ^a
[Time=1] * [Treatment=C]	-6.807	34.024	-.200	.845	-80.940	67.326
[Time=1] * [Treatment=L]	0 ^a
[Time=7] * [Treatment=C]	-19.390	34.024	-.570	.579	-93.523	54.743
[Time=7] * [Treatment=L]	0 ^a
[Time=14] * [Treatment=C]	0 ^a
[Time=14] * [Treatment=L]	0 ^a

a. This parameter is set to zero because it is redundant.

Table A1.4: Mean \pm SD results of t-test of mean CD45 differences between LIPUS (L) and control (C) in basic media on days 1, 7, and 14

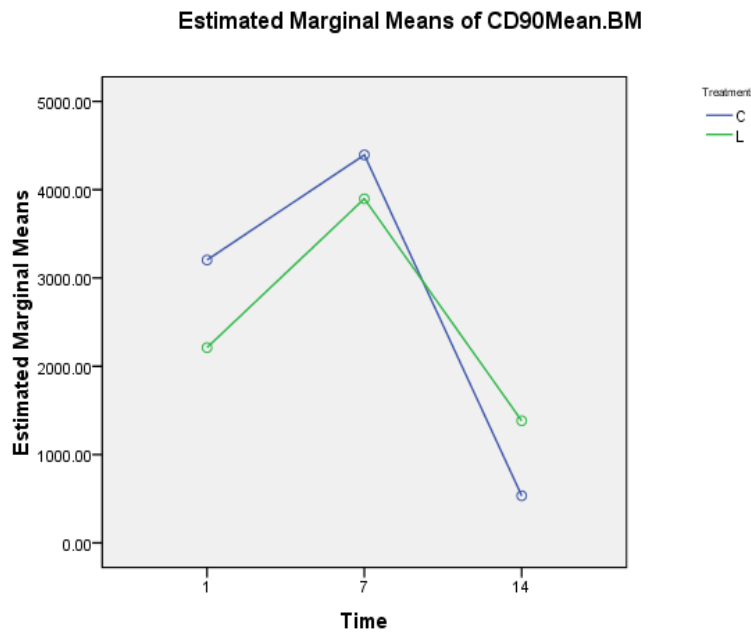


Figure A1.5. CD 90: mean differences between LIPUS (L) and control (C) in basic media on days 1, 7, and 14

Parameter Estimates

Dependent Variable: CD90Mean.BM

Parameter	B	Std. Error	t	Sig.	95% Confidence Interval	
					Lower Bound	Upper Bound
Intercept	1383.220	760.806	1.818	.094	-274.434	3040.874
[Time=1]	828.680	1075.942	.770	.456	-1515.596	3172.956
[Time=7]	2513.633	1075.942	2.336	.038	169.357	4857.910
[Time=14]	0 ^a
[Treatment=C]	-848.463	1075.942	-.789	.446	-3192.740	1495.813
[Treatment=L]	0 ^a
[Time=1] * [Treatment=C]	1840.577	1521.612	1.210	.250	-1474.731	5155.884
[Time=1] * [Treatment=L]	0 ^a
[Time=7] * [Treatment=C]	1345.797	1521.612	.884	.394	-1969.511	4661.104
[Time=7] * [Treatment=L]	0 ^a
[Time=14] * [Treatment=C]	0 ^a
[Time=14] * [Treatment=L]	0 ^a

a. This parameter is set to zero because it is redundant.

Table A1.5: Mean \pm SD results of t-test of mean CD90 differences between LIPUS (L) and control (C) in basic media on days 1, 7, and 14

Estimated Marginal Means of MHC.I.Mean.BM

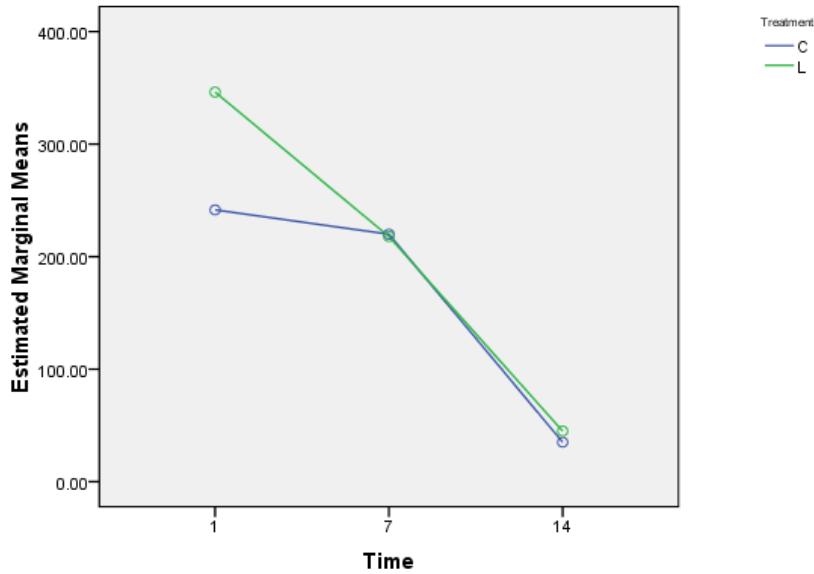


Figure A1.6. MHC.I: mean differences between LIPUS (L) and control (C) in basic media on days 1, 7, and 14

Parameter Estimates

Dependent Variable: MHC.I.Mean.BM

Parameter	B	Std. Error	t	Sig.	95% Confidence Interval	
					Lower Bound	Upper Bound
Intercept	44.973	23.481	1.915	.080	-6.188	96.135
[Time=1]	301.243	33.208	9.072	.000	228.890	373.597
[Time=7]	172.923	33.208	5.207	.000	100.570	245.277
[Time=14]	0 ^a
[Treatment=C]	-9.887	33.208	-.298	.771	-82.240	62.467
[Treatment=L]	0 ^a
[Time=1] * [Treatment=C]	-94.830	46.963	-2.019	.066	-197.153	7.493
[Time=1] * [Treatment=L]	0 ^a
[Time=7] * [Treatment=C]	11.893	46.963	.253	.804	-90.430	114.216
[Time=7] * [Treatment=L]	0 ^a
[Time=14] * [Treatment=C]	0 ^a
[Time=14] * [Treatment=L]	0 ^a

a. This parameter is set to zero because it is redundant.

Table A1.6: Mean ± SD results of t-test of mean MHC.I differences between LIPUS (L) and control (C) in basic media on days 1, 7, and 14

Estimated Marginal Means of MHC.II.Mean.BM

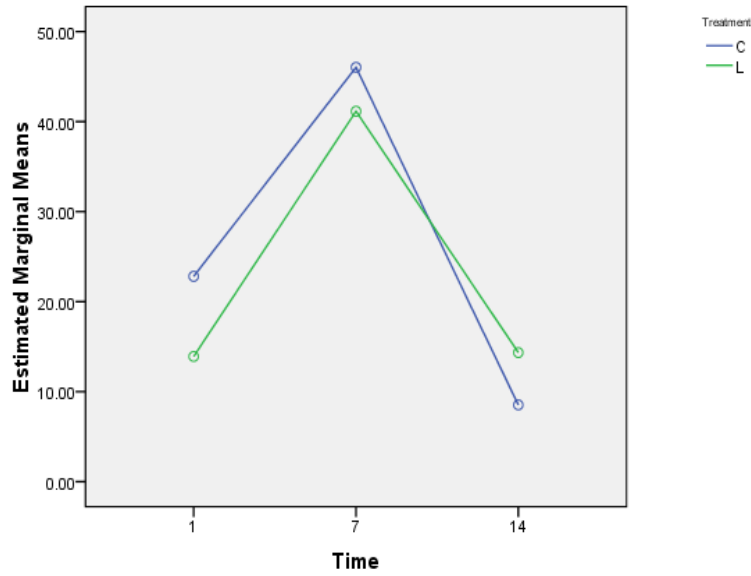


Figure A1.7. MHCII: mean differences between LIPUS (L) and control (C) in basic media on days 1, 7, and 14

Parameter Estimates

Dependent Variable: MHC.II.Mean.BM

Parameter	B	Std. Error	t	Sig.	95% Confidence Interval	
					Lower Bound	Upper Bound
Intercept	14.343	8.726	1.644	.126	-4.670	33.356
[Time=1]	-.433	12.341	-.035	.973	-27.322	26.455
[Time=7]	26.800	12.341	2.172	.051	-.088	53.688
[Time=14]	0 ^a
[Treatment=C]	-5.817	12.341	-.471	.646	-32.705	21.072
[Treatment=L]	0 ^a
[Time=1] * [Treatment=C]	14.717	17.453	.843	.416	-23.309	52.743
[Time=1] * [Treatment=L]	0 ^a
[Time=7] * [Treatment=C]	10.707	17.453	.613	.551	-27.319	48.733
[Time=7] * [Treatment=L]	0 ^a
[Time=14] * [Treatment=C]	0 ^a
[Time=14] * [Treatment=L]	0 ^a

a. This parameter is set to zero because it is redundant.

Table A1.7. Mean ± SD results of t-test of mean MHCII differences between LIPUS (L) and control (C) in basic media on days 1, 7, and 14

Experiment Design

(4.5) LIPUS Treated Plates

(4.5) Control Plates

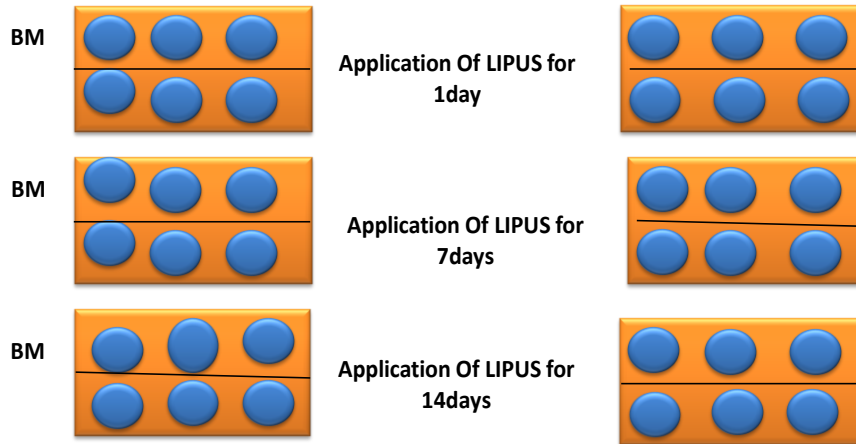


Figure A1.8. Schematic diagram that explains the experimental design; basic media, LIPUS = low intensity pulsed ultrasound

Parameter Estimates

Dependent Variable	Parameter	B	Std. Error	t	Sig.	95% Confidence Interval	
						Lower Bound	Upper Bound
Cellcount	Intercept	346834.000	108562.409	3.195	.008	110296.831	583371.169
	[Time=1]	-287917.333	153530.431	-1.875	.085	-622431.405	46596.738
	[Time=7]	-206848.000	153530.431	-1.347	.203	-541362.072	127666.072
	[Time=14]	0 ^a
	[Treatment=C]	-2693.333	153530.431	-.018	.986	-337207.405	331820.738
	[Treatment=L]	0 ^a
	[Time=1] * [Treatment=C]	13938.000	217124.817	.064	.950	-459136.337	487012.337
	[Time=1] * [Treatment=L]	0 ^a
	[Time=7] * [Treatment=C]	-14379.333	217124.817	-.066	.948	-487453.670	458695.004
	[Time=7] * [Treatment=L]	0 ^a
	[Time=14] * [Treatment=C]	0 ^a
[Time=14] * [Treatment=L]	0 ^a	
DNA	Intercept	12.018	1.527	7.872	.000	8.692	15.345
	[Time=1]	-4.785	2.159	-2.216	.047	-9.489	-.081
	[Time=7]	-1.284	2.159	-.595	.563	-5.988	3.420
	[Time=14]	0 ^a
	[Treatment=C]	-.997	2.159	-.462	.653	-5.701	3.707
	[Treatment=L]	0 ^a
	[Time=1] * [Treatment=C]	1.309	3.053	.429	.676	-5.343	7.962
	[Time=1] * [Treatment=L]	0 ^a
	[Time=7] * [Treatment=C]	-.388	3.053	-.127	.901	-7.040	6.265
	[Time=7] * [Treatment=L]	0 ^a
	[Time=14] * [Treatment=C]	0 ^a
[Time=14] * [Treatment=L]	0 ^a	
ALP	Intercept	.217	.014	15.917	.000	.187	.247
	[Time=1]	-.088	.019	-4.539	.001	-.130	-.046
	[Time=7]	-.094	.019	-4.874	.000	-.136	-.052
	[Time=14]	0 ^a
	[Treatment=C]	-.053	.019	-2.728	.018	-.095	-.011
	[Treatment=L]	0 ^a
	[Time=1] * [Treatment=C]	.040	.027	1.476	.166	-.019	.100
	[Time=1] * [Treatment=L]	0 ^a
	[Time=7] * [Treatment=C]	.060	.027	2.197	.048	.000	.119
	[Time=7] * [Treatment=L]	0 ^a
	[Time=14] * [Treatment=C]	0 ^a
[Time=14] * [Treatment=L]	0 ^a	
ALP.DNA	Intercept	.020	.003	5.843	.000	.013	.028
	[Time=1]	-.002	.005	-.384	.708	-.013	.009
	[Time=7]	-.008	.005	-1.574	.142	-.018	.003
	[Time=14]	0 ^a
	[Treatment=C]	-.005	.005	-.938	.367	-.015	.006
	[Treatment=L]	0 ^a
	[Time=1] * [Treatment=C]	.003	.007	.407	.691	-.012	.018
	[Time=1] * [Treatment=L]	0 ^a
	[Time=7] * [Treatment=C]	.006	.007	.882	.395	-.009	.021
	[Time=7] * [Treatment=L]	0 ^a
	[Time=14] * [Treatment=C]	0 ^a
[Time=14] * [Treatment=L]	0 ^a	

a. This parameter is set to zero because it is redundant.

Table A1.8. Comparison of the mean \pm SD of t-test of cell count, ALP, DNA, ALP normalized to DNA levels between LIPUS (L) and control (C) on days 1, 7, and 14 in basic media

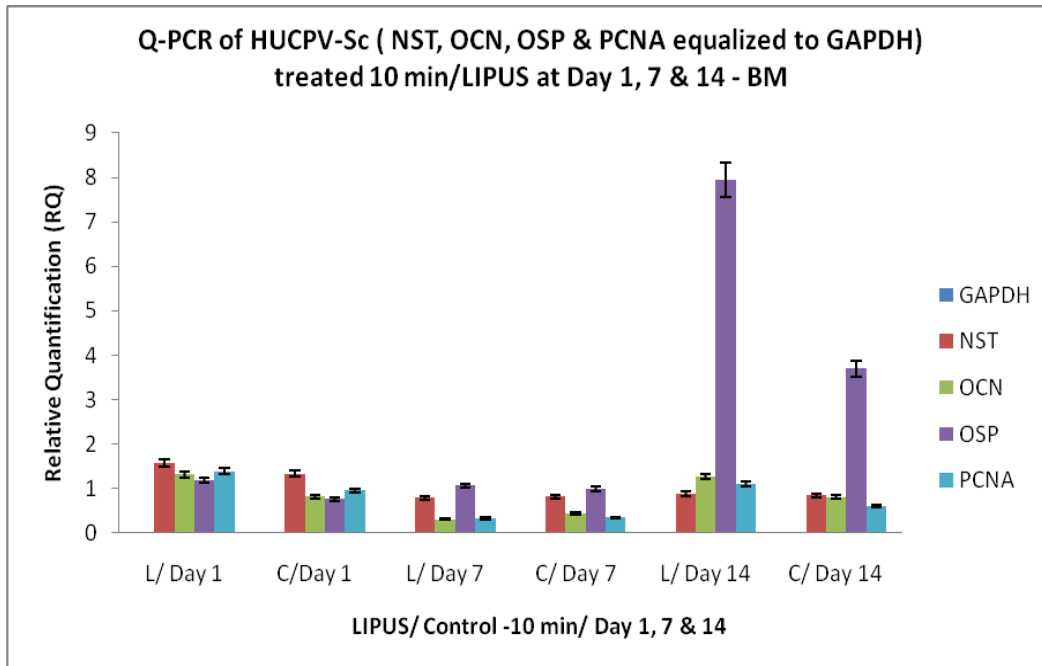


Figure A1.9. qPCR comparison of levels of nucleostemin, osteocalcin, osteopontin, and PCNA after their equalization to the endogenous control gene (GAPDH) between LIPUS (L) and control (C) on days 1, 7, and 14 in basic media

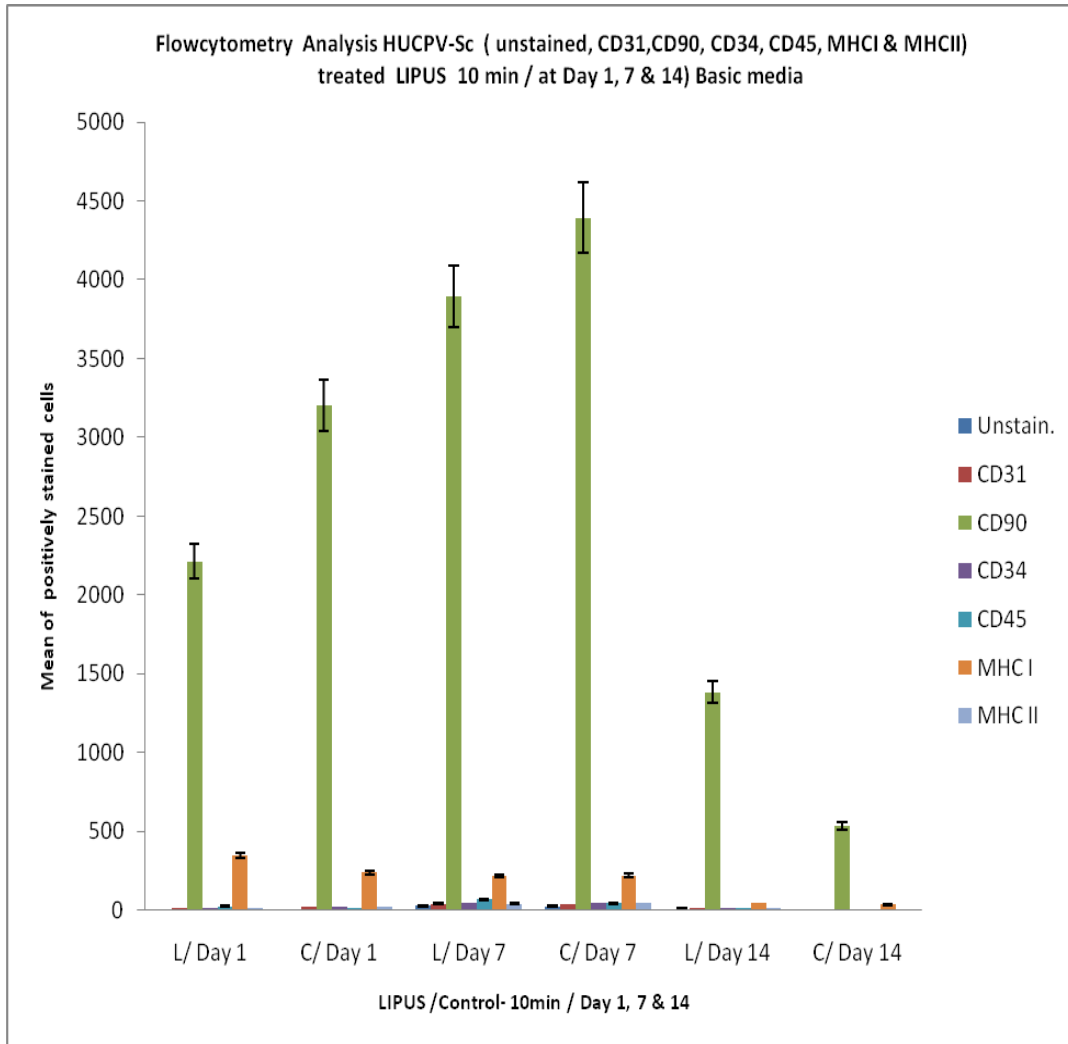


Figure A1.10. Flow-cytometry of HUCPV-SC (isotype IgG, CD31, CD90, CD34, CD45, MHC I, and MHCII) treated with LIPUS 10 min/day on days 1, 7, and 14 in basic media; differences between LIPUS (L) and control (C)

Target	Treatment Day 1	Mean	Std. Deviation
GAPDH	C	.00	.00
	L	.00	.00
NST	C	1.33	.32
	L	1.58	.44
OCN	C	.82	.33
	L	1.32	.27
OPN	C	.76	.21
	L	1.18	.37
PCNA	C	.96	.28
	L	1.38	.24

Table A1.9. qPCR comparison of the mean \pm SD of nucleostemin, osteocalcin, osteopontin, and PCNA after their equalization to the endogenous control gene (GAPDH) between LIPUS (L) and control (C) on day 1 in basic media

Target	Treatment Day 7	Mean	Std. Deviation
GAPDH	C	.00	.00
	L	.00	.00
NST	C	.81	.15
	L	.79	.03
OCN	C	.43	.11
	L	.30	.04
OPN	C	.99	.48
	L	1.06	.12
PCNA	C	.35	.17
	L	.32	.09

Table A1.10. qPCR comparison of the mean \pm SD of nucleostemin, osteocalcin, osteopontin, and PCNA after their equalization to the endogenous control gene (GAPDH) between LIPUS (L) and control (C) on day 7 in basic media

Target	Treatment Day 14	Mean	Std. Deviation
GAPDH	C	.00	.00
	L	.00	.00
NST	C	.85	.16
	L	.88	.16
OCN	C	.81	.22
	L	1.26	.29
OPN	C	3.69	2.26
	L	7.95	6.20
PCNA	C	.61	.29
	L	1.09	.49

Table A1.11. qPCR comparison of the mean \pm SD of nucleostemin, osteocalcin, osteopontin, and PCNA after their equalization to the endogenous control gene (GAPDH) between LIPUS (L) and control (C) on day 14 in basic media

Parameter Estimates

Dependent Variable: Relative Quantif.RQ

Parameter	B	Std. Error	t	Sig.	95% Confidence Interval	
					Lower Bound	Upper Bound
Intercept	1.380	.099	13.986	.000	1.183	1.577
[Targret=GAPDH]	-1.380	.136	-10.177	.000	-1.651	-1.110
[Targret=NST]	.198	.136	1.462	.148	-.072	.469
[Targret=OCN]	-.065	.144	-.447	.656	-.353	.224
[Targret=OSP]	-.198	.140	-1.420	.160	-.477	.080
[Targret=PCNA]	0 ^a
[Treatment=C]	-.424	.144	-2.933	.005	-.712	-.135
[Treatment=L]	0 ^a
[Targret=GAPDH] * [Treatment=C]	.424	.195	2.168	.034	.034	.814
[Targret=GAPDH] * [Treatment=L]	0 ^a
[Targret=NST] * [Treatment=C]	.178	.202	.881	.382	-.225	.580
[Targret=NST] * [Treatment=L]	0 ^a
[Targret=OCN] * [Treatment=C]	-.077	.212	-.361	.719	-.500	.347
[Targret=OCN] * [Treatment=L]	0 ^a
[Targret=OSP] * [Treatment=C]	.002	.201	.010	.992	-.399	.403
[Targret=OSP] * [Treatment=L]	0 ^a
[Targret=PCNA] * [Treatment=C]	0 ^a
[Targret=PCNA] * [Treatment=L]	0 ^a

a. This parameter is set to zero because it is redundant.

Table A1.12. t-test of qPCR comparing the mean \pm SD of nucleostemin, osteocalcin, osteopontin, and PCNA after their equalization to the endogenous control gene (GAPDH) between LIPUS (L) and control (C) on day 1 in basic media

Parameter Estimates

Dependent Variable: Relative Quantif.RQ

Parameter	B	Std. Error	t	Sig.	95% Confidence Interval	
					Lower Bound	Upper Bound
Intercept	.326	.060	5.471	.000	.208	.445
[Targret=GAPDH]	-.326	.084	-3.869	.000	-.494	-.158
[Targret=NST]	.467	.084	5.539	.000	.299	.635
[Targret=OCN]	-.024	.084	-.289	.773	-.192	.143
[Targret=OSP]	.736	.084	8.722	.000	.568	.904
[Targret=PCNA]	0 ^a					
[Tretment=C]	.019	.084	.222	.825	-.149	.187
[Tretment=L]	0 ^a					
[Targret=GAPDH] * [Tretment=C]	-.019	.119	-.157	.875	-.256	.219
[Targret=GAPDH] * [Tretment=L]	0 ^a					
[Targret=NST] * [Tretment=C]	.001	.119	.004	.997	-.237	.238
[Targret=NST] * [Tretment=L]	0 ^a					
[Targret=OCN] * [Tretment=C]	.114	.119	.957	.341	-.123	.352
[Targret=OCN] * [Tretment=L]	0 ^a					
[Targret=OSP] * [Tretment=C]	-.088	.119	-.741	.461	-.326	.149
[Targret=OSP] * [Tretment=L]	0 ^a					
[Targret=PCNA] * [Tretment=C]	0 ^a					
[Targret=PCNA] * [Tretment=L]	0 ^a					

a. This parameter is set to zero because it is redundant.

Table A1.13. t-test of qPCR comparing the mean \pm SD of nucleostemin, osteocalcin, osteopontin, and PCNA after their equalization to the endogenous control gene (GAPDH) between LIPUS (L) and control (C) on day 7 in basic media

Parameter Estimates

Dependent Variable: Relative Quantif.RQ

Parameter	B	Std. Error	t	Sig.	95% Confidence Interval	
					Lower Bound	Upper Bound
Intercept	1.099	.700	1.570	.120	-.294	2.491
[Targret=GAPDH]	-1.099	.990	-1.110	.270	-3.068	.871
[Targret=NST]	-.216	.990	-.218	.828	-2.185	1.754
[Targret=OCN]	.165	.990	.167	.868	-1.804	2.134
[Targret=OSP]	6.850	.990	6.921	.000	4.880	8.819
[Targret=PCNA]	0 ^a
[Tretment=C]	-.487	.990	-.492	.624	-2.457	1.482
[Tretment=L]	0 ^a
[Targret=GAPDH] * [Tretment=C]	.487	1.400	.348	.729	-2.298	3.272
[Targret=GAPDH] * [Tretment=L]	0 ^a
[Targret=NST] * [Tretment=C]	.454	1.400	.324	.747	-2.331	3.239
[Targret=NST] * [Tretment=L]	0 ^a
[Targret=OCN] * [Tretment=C]	.033	1.400	.024	.981	-2.752	2.818
[Targret=OCN] * [Tretment=L]	0 ^a
[Targret=OSP] * [Tretment=C]	-3.766	1.400	-2.691	.009	-6.551	-.981
[Targret=OSP] * [Tretment=L]	0 ^a
[Targret=PCNA] * [Tretment=C]	0 ^a
[Targret=PCNA] * [Tretment=L]	0 ^a

a. This parameter is set to zero because it is redundant.

Table A1.14. t-test of qPCR comparing the mean ± SD of nucleostemin, osteocalcin, osteopontin, and PCNA after their equalization to the endogenous control gene (GAPDH) between LIPUS (L) and control (C) on day 14 in basic media

A2

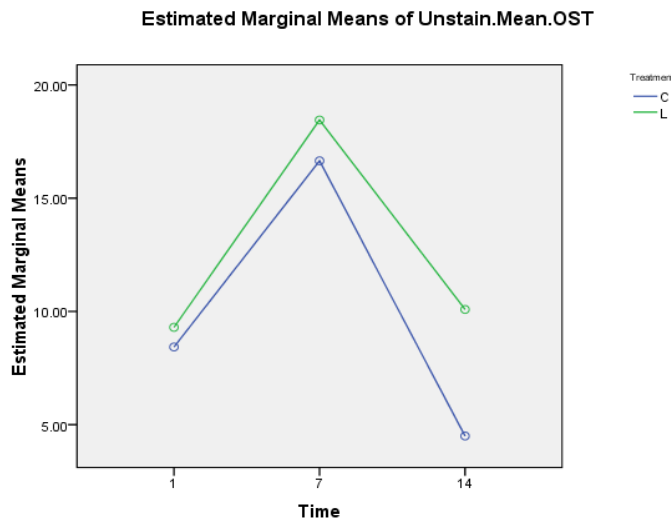


Figure A2.1. Unstained samples: mean differences of isotype IgG between LIPUS (L) and control (C) in OST on days 1, 7, and 14

Parameter Estimates

Dependent Variable: Unstain.Mean.OST

Parameter	B	Std. Error	t	Sig.	95% Confidence Interval	
					Lower Bound	Upper Bound
Intercept	10.087	3.509	2.874	.014	2.441	17.732
[Time=1]	-.787	4.963	-.159	.877	-11.599	10.026
[Time=7]	8.363	4.963	1.685	.118	-2.449	19.176
[Time=14]	0 ^a
[Treatment=C]	-5.587	4.963	-1.126	.282	-16.399	5.226
[Treatment=L]	0 ^a
[Time=1] * [Treatment=C]	4.717	7.018	.672	.514	-10.575	20.008
[Time=1] * [Treatment=L]	0 ^a
[Time=7] * [Treatment=C]	3.787	7.018	.540	.599	-11.505	19.078
[Time=7] * [Treatment=L]	0 ^a
[Time=14] * [Treatment=C]	0 ^a
[Time=14] * [Treatment=L]	0 ^a

a. This parameter is set to zero because it is redundant.

Table A2.1. Mean \pm SD results of t-test of mean unstained samples isotype IgG differences between LIPUS (L) and control (C) in OST on days 1, 7, and 14

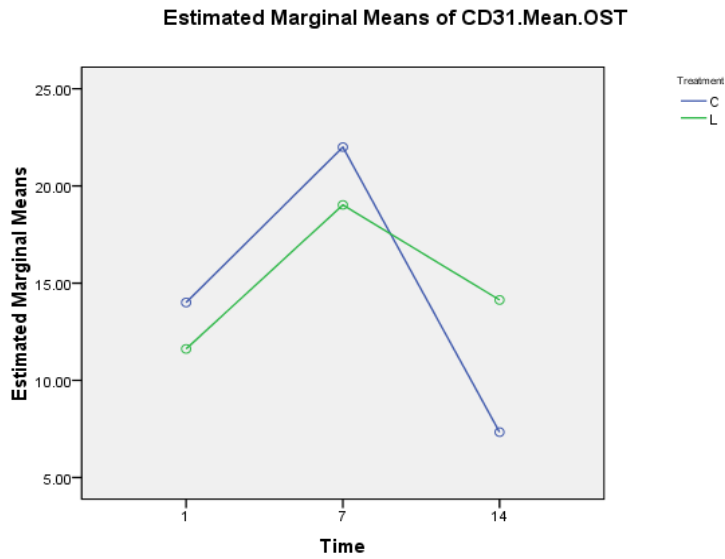


Figure A2.2. CD 31: mean differences between LIPUS (L) and control (C) in OST on days 1, 7, and 14

Parameter Estimates

Dependent Variable: CD31.Mean.OST

Parameter	B	Std. Error	t	Sig.	95% Confidence Interval	
					Lower Bound	Upper Bound
Intercept	14.133	4.090	3.456	.005	5.223	23.044
[Time=1]	-2.517	5.784	-.435	.671	-15.118	10.085
[Time=7]	4.890	5.784	.845	.414	-7.712	17.492
[Time=14]	0 ^a
[Treatment=C]	-6.797	5.784	-1.175	.263	-19.398	5.805
[Treatment=L]	0 ^a
[Time=1] * [Treatment=C]	9.183	8.179	1.123	.284	-8.638	27.005
[Time=1] * [Treatment=L]	0 ^a
[Time=7] * [Treatment=C]	9.770	8.179	1.194	.255	-8.051	27.591
[Time=7] * [Treatment=L]	0 ^a
[Time=14] * [Treatment=C]	0 ^a
[Time=14] * [Treatment=L]	0 ^a

a. This parameter is set to zero because it is redundant.

Table A2.2. Mean \pm SD results of t-test of mean CD31 differences between LIPUS (L) and control (C) in OST on days 1, 7, and 14

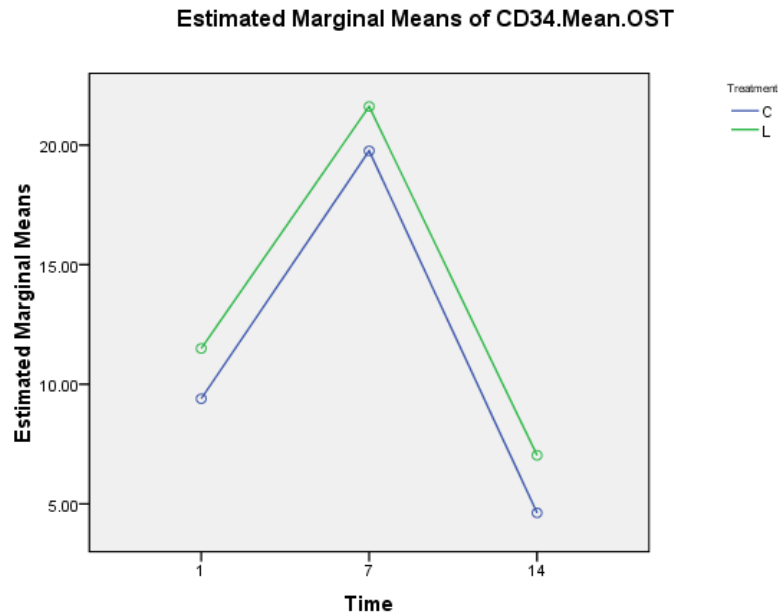


Figure A2.3. CD 34: mean differences between LIPUS (L) and control (C) in OST on days 1, 7, and 14

Parameter Estimates

Dependent Variable: CD34.Mean.OST

Parameter	B	Std. Error	t	Sig.	95% Confidence Interval	
					Lower Bound	Upper Bound
Intercept	7.030	4.351	1.616	.132	-2.450	16.510
[Time=1]	4.467	6.153	.726	.482	-8.941	17.874
[Time=7]	14.583	6.153	2.370	.035	1.176	27.991
[Time=14]	0 ^a
[Treatment=C]	-2.407	6.153	-.391	.703	-15.814	11.001
[Treatment=L]	0 ^a
[Time=1] * [Treatment=C]	.307	8.702	.035	.972	-18.654	19.267
[Time=1] * [Treatment=L]	0 ^a
[Time=7] * [Treatment=C]	.553	8.702	.064	.950	-18.407	19.514
[Time=7] * [Treatment=L]	0 ^a
[Time=14] * [Treatment=C]	0 ^a
[Time=14] * [Treatment=L]	0 ^a

a. This parameter is set to zero because it is redundant.

Table A2.3. Mean \pm SD results of t-test of mean CD34 differences between LIPUS (L) and control (C) in OST on days 1, 7, and 14

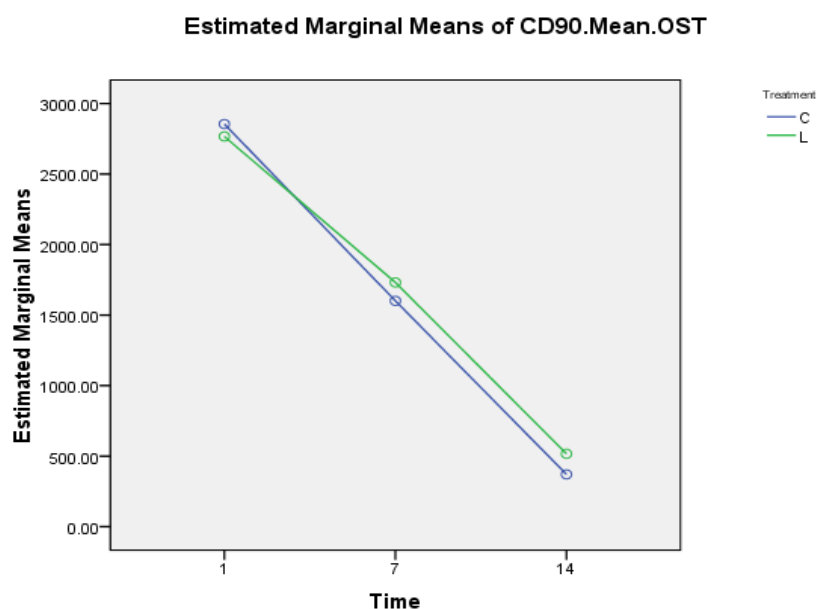


Figure A2.4. CD 90: mean differences between LIPUS (L) and control (C) in OST on days 1, 7, and 14

Parameter Estimates

Dependent Variable: CD90.Mean.OST

Parameter	B	Std. Error	t	Sig.	95% Confidence Interval	
					Lower Bound	Upper Bound
Intercept	516.700	295.396	1.749	.106	-126.912	1160.312
[Time=1]	2249.963	417.753	5.386	.000	1339.758	3160.168
[Time=7]	1214.557	417.753	2.907	.013	304.352	2124.762
[Time=14]	0 ^a
[Treatment=C]	-145.987	417.753	-.349	.733	-1056.192	764.218
[Treatment=L]	0 ^a
[Time=1] * [Treatment=C]	233.783	590.792	.396	.699	-1053.441	1521.008
[Time=1] * [Treatment=L]	0 ^a
[Time=7] * [Treatment=C]	15.873	590.792	.027	.979	-1271.351	1303.098
[Time=7] * [Treatment=L]	0 ^a
[Time=14] * [Treatment=C]	0 ^a
[Time=14] * [Treatment=L]	0 ^a

a. This parameter is set to zero because it is redundant.

Table A2.4. Mean ± SD results of t-test of mean CD90 differences between LIPUS (L) and control (C) in OST on days 1, 7, and 14

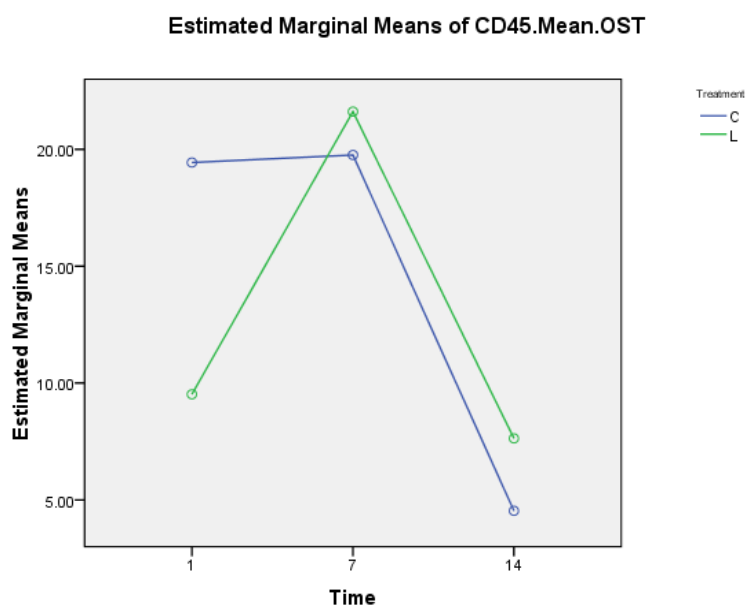


Figure A2.5. CD 45: mean differences between LIPUS (L) and control (C) in OST on days 1, 7, and 14

Parameter Estimates

Dependent Variable: CD45.Mean.OST

Parameter	B	Std. Error	t	Sig.	95% Confidence Interval	
					Lower Bound	Upper Bound
Intercept	7.633	5.516	1.384	.192	-4.385	19.652
[Time=1]	1.887	7.801	.242	.813	-15.110	18.883
[Time=7]	13.980	7.801	1.792	.098	-3.017	30.977
[Time=14]	0 ^a
[Treatment=C]	-3.100	7.801	-.397	.698	-20.097	13.897
[Treatment=L]	0 ^a
[Time=1] * [Treatment=C]	13.017	11.032	1.180	.261	-11.020	37.054
[Time=1] * [Treatment=L]	0 ^a
[Time=7] * [Treatment=C]	1.247	11.032	.113	.912	-22.790	25.284
[Time=7] * [Treatment=L]	0 ^a
[Time=14] * [Treatment=C]	0 ^a
[Time=14] * [Treatment=L]	0 ^a

a. This parameter is set to zero because it is redundant.

Table A2.5. Mean ± SD results of t-test of mean CD45 differences between LIPUS (L) and control (C) in OST on days 1, 7, and 14

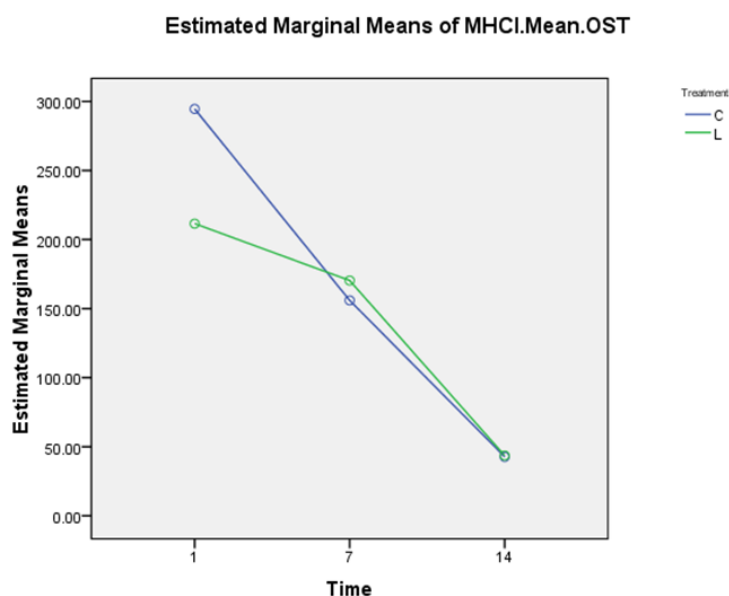


Figure A2.6. MHCI: mean differences between LIPUS (L) and control (C) in OST on days 1, 7, and 14

Parameter Estimates

Dependent Variable: MHCI Mean OST

Parameter	B	Std. Error	t	Sig.	95% Confidence Interval	
					Lower Bound	Upper Bound
Intercept	43.600	70.353	.620	.547	-109.685	196.885
[Time=1]	167.903	99.494	1.688	.117	-48.874	384.681
[Time=7]	126.747	99.494	1.274	.227	-90.031	343.524
[Time=14]	0 ^a
[Treatment=C]	-.857	99.494	-.009	.993	-217.634	215.921
[Treatment=L]	0 ^a
[Time=1] * [Treatment=C]	83.900	140.705	.596	.562	-222.670	390.470
[Time=1] * [Treatment=L]	0 ^a
[Time=7] * [Treatment=C]	-13.543	140.705	-.096	.925	-320.113	293.027
[Time=7] * [Treatment=L]	0 ^a
[Time=14] * [Treatment=C]	0 ^a
[Time=14] * [Treatment=L]	0 ^a

a. This parameter is set to zero because it is redundant.

Table A2.6. Mean ± SD results of t-test of mean MHCI differences between LIPUS (L) and control (C) in OST on days 1, 7, and 14

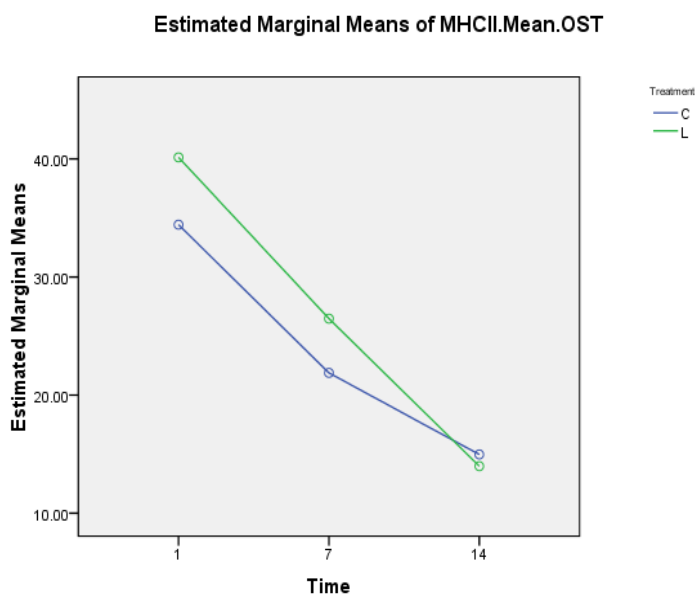


Figure A2.7. MHCII: mean differences between LIPUS (L) and control (C) in OST on days 1, 7, and 14

Parameter Estimates

Dependent Variable: MHCII.Mean.OST

Parameter	B	Std. Error	t	Sig.	95% Confidence Interval	
					Lower Bound	Upper Bound
Intercept	13.983	9.964	1.403	.186	-7.727	35.694
[Time=1]	26.150	14.092	1.856	.088	-4.553	56.853
[Time=7]	12.493	14.092	.887	.393	-18.210	43.197
[Time=14]	0 ^a
[Treatment=C]	.990	14.092	.070	.945	-29.713	31.693
[Treatment=L]	0 ^a
[Time=1] * [Treatment=C]	-6.693	19.929	-.336	.743	-50.114	36.728
[Time=1] * [Treatment=L]	0 ^a
[Time=7] * [Treatment=C]	-5.587	19.929	-.280	.784	-49.008	37.834
[Time=7] * [Treatment=L]	0 ^a
[Time=14] * [Treatment=C]	0 ^a
[Time=14] * [Treatment=L]	0 ^a

a. This parameter is set to zero because it is redundant.

Table A2.7. Mean \pm SD results of t-test of mean MHCII differences between LIPUS (L) and control (C) in OST on days 1, 7, and 14

Experiment Design

(4.5) LIPUS Treated Plates

(4.5) Control Plates

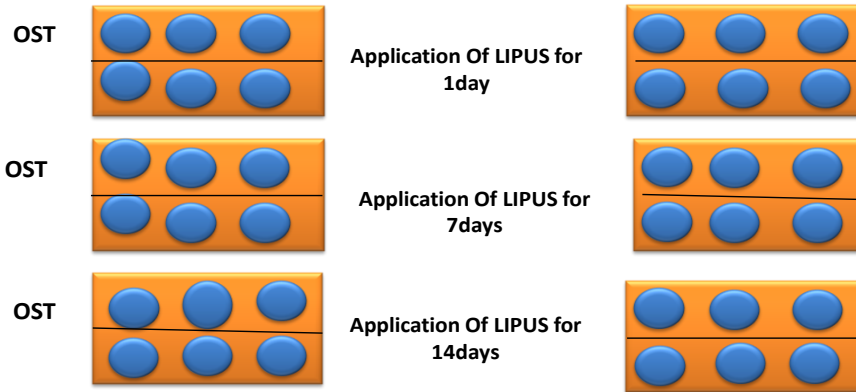


Figure A2.8. Schematic diagram that explains the experimental design: OST, LIPUS (low intensity pulsed ultrasound)

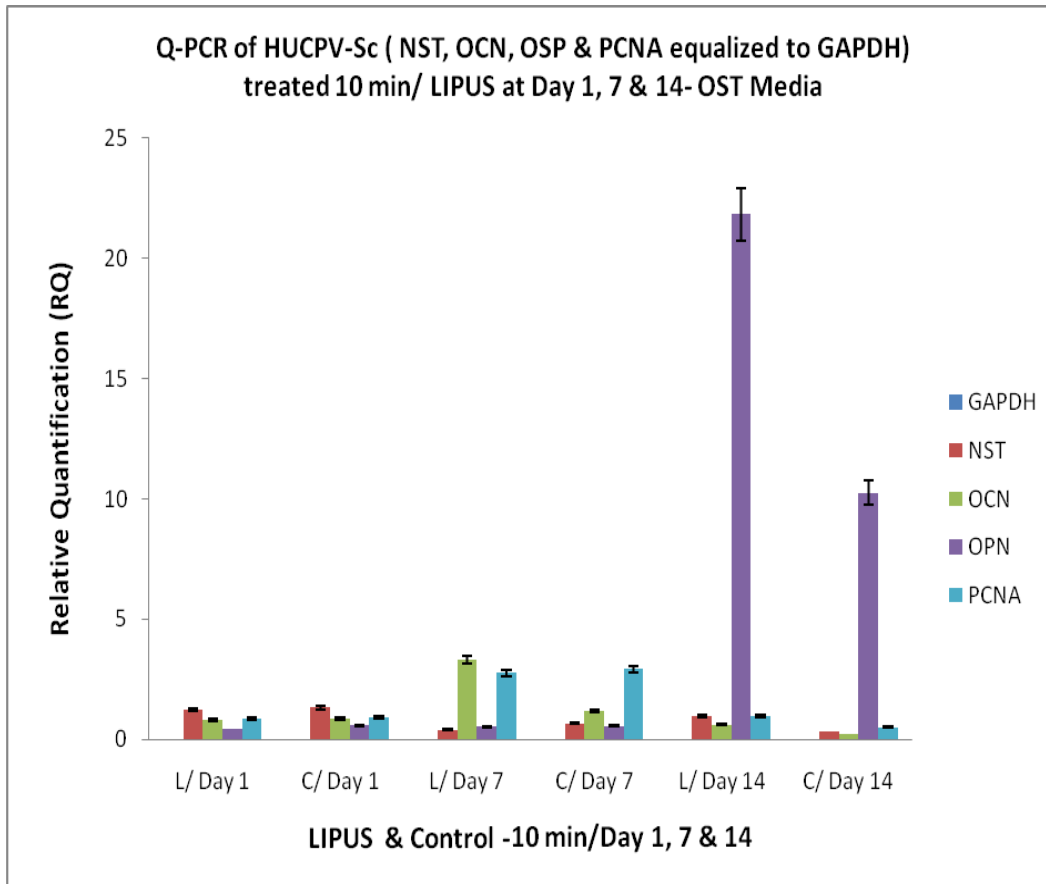


Figure A2.9. qPCR comparison of levels of nucleostemin, osteocalcin, osteopontin, and PCNA after their equalization to the endogenous control gene (GAPDH) between LIPUS (L) and control (C) on days 1, 7, and 14 (OST)

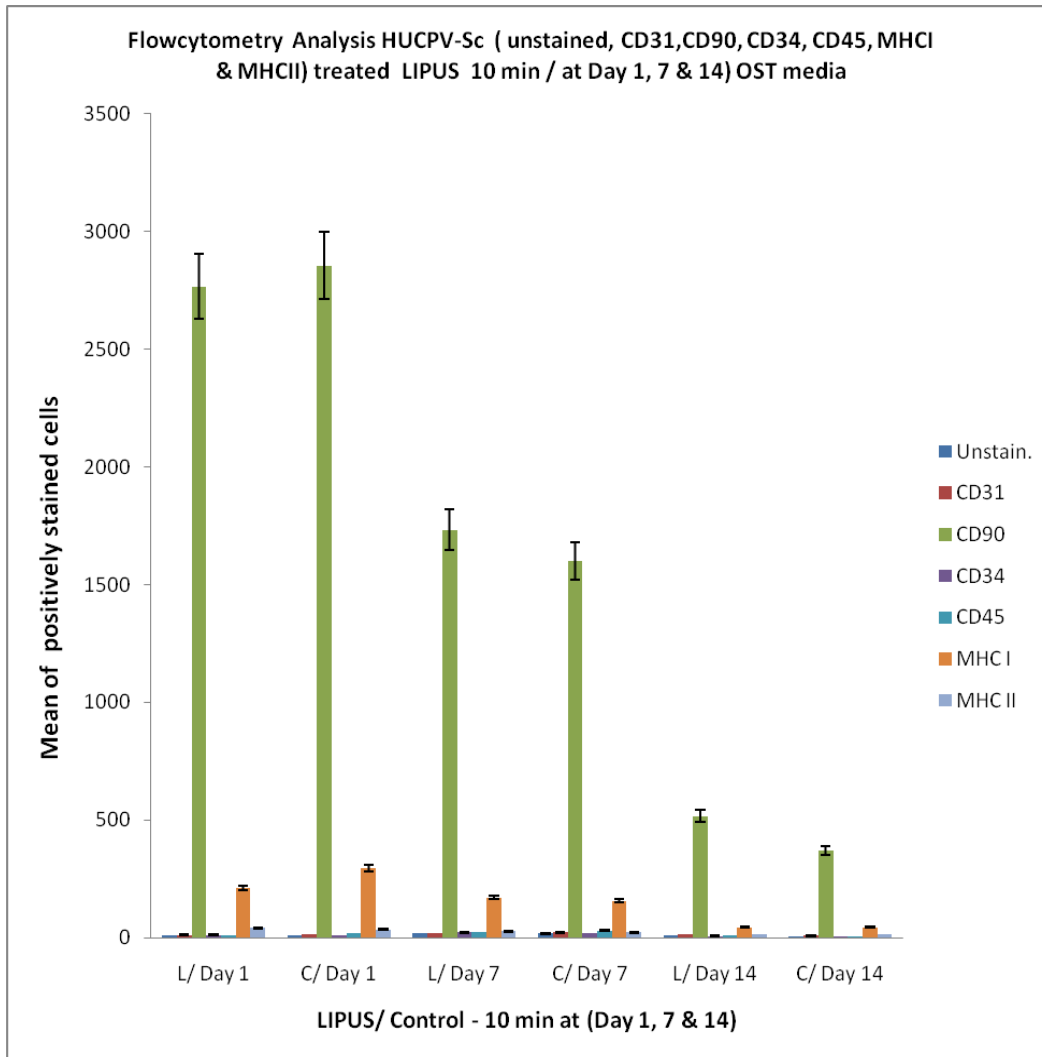


Figure A2.10. Flow-cytometry of HUCPV-SC (isotype IgG, CD31, CD90, CD34, CD45, MHC I, and MHCII) treated with LIPUS 10 min/day on days 1, 7, and 14 in OST; difference between LIPUS (L) and control (C)

Parameter Estimates

Dependent Variable	Parameter	B	Std. Error	t	Sig.	95% Confidence Interval	
						Lower Bound	Upper Bound
Cell.count	Intercept	244756.667	83938.546	2.916	.013	61870.285	427643.048
	[Time=1]	-209743.333	118707.031	-1.767	.103	-468383.735	48897.068
	[Time=7]	-99114.667	118707.031	-.835	.420	-357755.068	159525.735
	[Time=14]	0 ^a
	[Treatment=C]	84166.667	118707.031	.709	.492	-174473.735	342807.068
	[Treatment=L]	0 ^a
	[Time=1] * [Treatment=C]	-68882.000	167877.093	-.410	.689	-434654.764	296890.764
	[Time=1] * [Treatment=L]	0 ^a
	[Time=7] * [Treatment=C]	-104097.333	167877.093	-.620	.547	-469870.097	261675.430
	[Time=7] * [Treatment=L]	0 ^a
[Time=14] * [Treatment=C]	0 ^a	
[Time=14] * [Treatment=L]	0 ^a	
DNA	Intercept	11.348	1.605	7.073	.000	7.852	14.845
	[Time=1]	-4.086	2.269	-1.801	.097	-9.030	.858
	[Time=7]	-.960	2.269	-.423	.680	-5.904	3.984
	[Time=14]	0 ^a
	[Treatment=C]	-1.313	2.269	-.579	.574	-6.257	3.631
	[Treatment=L]	0 ^a
	[Time=1] * [Treatment=C]	1.190	3.209	.371	.717	-5.802	8.182
	[Time=1] * [Treatment=L]	0 ^a
	[Time=7] * [Treatment=C]	1.820	3.209	.567	.581	-5.172	8.812
	[Time=7] * [Treatment=L]	0 ^a
[Time=14] * [Treatment=C]	0 ^a	
[Time=14] * [Treatment=L]	0 ^a	
ALP	Intercept	.161	.018	8.833	.000	.121	.200
	[Time=1]	-.031	.026	-1.216	.247	-.087	.025
	[Time=7]	.022	.026	.854	.410	-.034	.078
	[Time=14]	0 ^a
	[Treatment=C]	.011	.026	.441	.667	-.045	.067
	[Treatment=L]	0 ^a
	[Time=1] * [Treatment=C]	-8.333E-5	.036	-.002	.998	-.079	.079
	[Time=1] * [Treatment=L]	0 ^a
	[Time=7] * [Treatment=C]	-.068	.036	-1.862	.087	-.147	.012
	[Time=7] * [Treatment=L]	0 ^a
[Time=14] * [Treatment=C]	0 ^a	
[Time=14] * [Treatment=L]	0 ^a	
ALP.DNA	Intercept	.015	.003	4.797	.000	.008	.022
	[Time=1]	.003	.005	.571	.578	-.007	.012
	[Time=7]	.003	.005	.585	.569	-.007	.013
	[Time=14]	0 ^a
	[Treatment=C]	.003	.005	.701	.497	-.007	.013
	[Treatment=L]	0 ^a
	[Time=1] * [Treatment=C]	.000	.006	-.154	.880	-.015	.013
	[Time=1] * [Treatment=L]	0 ^a
	[Time=7] * [Treatment=C]	-.009	.006	-1.393	.189	-.023	.005
	[Time=7] * [Treatment=L]	0 ^a
[Time=14] * [Treatment=C]	0 ^a	
[Time=14] * [Treatment=L]	0 ^a	

a. This parameter is set to zero because it is redundant.

Table A2.8. Comparison of the mean \pm SD of t-test of cell count, ALP, DNA, ALP normalized to DNA levels, between LIPUS (L) and control (C) on days 1, 7, and 14 in OST

Target	Treatment/Day 1	Mean	Std. Deviation
GAPDH	C	.00	.00
	L	.00	.00
NST	C	1.32	.19
	L	1.23	.16
OCN	C	.87	.12
	L	.79	.19
OPN	C	.57	.42
	L	.43	.21
PCNA	C	.91	.04
	L	.87	.15

Table A2.9. qPCR comparison of the mean \pm SD of nucleostemin, osteocalcin, osteopontin, and PCNA after their equalization to the endogenous control gene (GAPDH) between LIPUS (L) and control (C) on day 1 in OST

Target	Treatment/Day 7	Mean	Std. Deviation
GAPDH	C	.00	.00
	L	.00	.00
NST	C	.66	.57
	L	.39	.42
OCN	C	1.18	1.39
	L	3.33	3.54
OPN	C	.56	.65
	L	.54	.40
PCNA	C	2.92	3.62
	L	2.76	2.01

Table A2.10. qPCR comparison of the mean \pm SD of nucleostemin, osteocalcin, osteopontin, and PCNA after their equalization to the endogenous control gene (GAPDH) between LIPUS (L) and control (C) on day 7 in OST

Target	Treatment/Day 14	Mean	Std. Deviation
GAPDH	C	.00	.00
	L	.00	.00
NST	C	.33	.05
	L	.95	.10
OCN	C	.22	.07
	L	.62	.29
OPN	C	10.25	3.61
	L	21.84	15.64
PCNA	C	.51	.05
	L	.98	.10

Table A2.11. qPCR comparison of the mean \pm SD of nucleostemin, osteocalcin, osteopontin, and PCNA after their equalization to the endogenous control gene (GAPDH) between LIPUS (L) and control (C) on day 14 in OST

Parameter Estimates

Dependent Variable: Relative Quantif.RQ

Parameter	B	Std. Error	t	Sig.	95% Confidence Interval	
					Lower Bound	Upper Bound
Intercept	.874	.063	13.856	.000	.748	1.000
[Targret=GAPDH]	-.874	.089	-9.798	.000	-1.052	-.696
[Targret=NST]	.354	.089	3.966	.000	.176	.531
[Targret=OCN]	-.080	.089	-.897	.373	-.257	.098
[Targret=OSP]	-.440	.089	-4.929	.000	-.617	-.262
[Targret=PCNA]	0 ^a
[Treatment=C]	.031	.089	.350	.728	-.146	.209
[Treatment=L]	0 ^a
[Targret=GAPDH] * [Treatment=C]	-.031	.126	-.247	.805	-.282	.220
[Targret=GAPDH] * [Treatment=L]	0 ^a
[Targret=NST] * [Treatment=C]	.064	.126	.505	.615	-.187	.315
[Targret=NST] * [Treatment=L]	0 ^a
[Targret=OCN] * [Treatment=C]	.041	.126	.326	.745	-.210	.292
[Targret=OCN] * [Treatment=L]	0 ^a
[Targret=OSP] * [Treatment=C]	.106	.126	.839	.404	-.145	.357
[Targret=OSP] * [Treatment=L]	0 ^a
[Targret=PCNA] * [Treatment=C]	0 ^a
[Targret=PCNA] * [Treatment=L]	0 ^a

a. This parameter is set to zero because it is redundant.

Table A2.12. t-test of qPCR comparing the mean \pm SD of nucleostemin, osteocalcin, osteopontin, and PCNA after their equalization to the endogenous control gene (GAPDH) between LIPUS (L) and control (C) on day 1 in OST

Parameter Estimates

Dependent Variable: Relative Quantif.RQ

Parameter	B	Std. Error	t	Sig.	95% Confidence Interval	
					Lower Bound	Upper Bound
Intercept	2.757	.666	4.140	.000	1.429	4.085
[Targret=GAPDH]	-2.757	.915	-3.012	.004	-4.582	-.932
[Targret=NST]	-2.360	.975	-2.421	.018	-4.303	-.416
[Targret=OCN]	.572	.915	.625	.534	-1.253	2.397
[Targret=OSP]	-2.220	.942	-2.357	.021	-4.098	-.342
[Targret=PCNA]	0 ^a
[Tretment=C]	.166	.915	.181	.857	-1.659	1.991
[Tretment=L]	0 ^a
[Targret=GAPDH] * [Tretment=C]	-.166	1.275	-.130	.897	-2.708	2.377
[Targret=GAPDH] * [Tretment=L]	0 ^a
[Targret=NST] * [Tretment=C]	.097	1.337	.073	.942	-2.569	2.764
[Targret=NST] * [Tretment=L]	0 ^a
[Targret=OCN] * [Tretment=C]	-2.315	1.319	-1.756	.083	-4.944	.314
[Targret=OCN] * [Tretment=L]	0 ^a
[Targret=OSP] * [Tretment=C]	-.146	1.337	-.109	.913	-2.813	2.520
[Targret=OSP] * [Tretment=L]	0 ^a
[Targret=PCNA] * [Tretment=C]	0 ^a
[Targret=PCNA] * [Tretment=L]	0 ^a

a. This parameter is set to zero because it is redundant.

Table A2.13. t-test of qPCR comparing the mean ± SD of nucleostemin, osteocalcin, osteopontin, and PCNA after their equalization to the endogenous control gene (GAPDH) between LIPUS (L) and control (C) on day 7 in OST

Parameter Estimates

Dependent Variable: Relative Quantif.RQ

Parameter	B	Std. Error	t	Sig.	95% Confidence Interval	
					Lower Bound	Upper Bound
Intercept	.975	1.692	.576	.566	-2.393	4.343
[Targret=GAPDH]	-.975	2.393	-.407	.685	-5.738	3.788
[Targret=NST]	-.029	2.393	-.012	.991	-4.791	4.734
[Targret=OCN]	-.358	2.393	-.150	.881	-5.121	4.405
[Targret=OSP]	20.867	2.393	8.719	.000	16.104	25.630
[Targret=PCNA]	0 ^a
[Treatment=C]	-.465	2.393	-.194	.846	-5.228	4.297
[Treatment=L]	0 ^a
[Targret=GAPDH] * [Treatment=C]	.465	3.385	.138	.891	-6.270	7.201
[Targret=GAPDH] * [Treatment=L]	0 ^a
[Targret=NST] * [Treatment=C]	-.154	3.385	-.045	.964	-6.889	6.582
[Targret=NST] * [Treatment=L]	0 ^a
[Targret=OCN] * [Treatment=C]	.067	3.385	.020	.984	-6.669	6.802
[Targret=OCN] * [Treatment=L]	0 ^a
[Targret=OSP] * [Treatment=C]	-11.130	3.385	-3.288	.001	-17.865	-4.394
[Targret=OSP] * [Treatment=L]	0 ^a
[Targret=PCNA] * [Treatment=C]	0 ^a
[Targret=PCNA] * [Treatment=L]	0 ^a

a. This parameter is set to zero because it is redundant.

Table A2.14. t-test of qPCR comparing the mean \pm SD of nucleostemin, osteocalcin, osteopontin, and PCNA after their equalization to the endogenous control gene (GAPDH) between LIPUS (L) and control (C) on day 14 in OST